

Marine Geology

Relict and contemporary influences on the postglacial geomorphology and evolution of a current swept shelf: the Eastern Cape Coast, South Africa --Manuscript Draft--

Manuscript Number:	MARGO_2019_128R2
Article Type:	Research Paper
Keywords:	Barriers; current-dominated shelf; palaeo-shorelines; Agulhas Current; melt water pulse
Corresponding Author:	Andrew Green University of Kwazulu-Natal Westville, South Africa
First Author:	Andrew Green
Order of Authors:	Andrew Green Andrew Cooper Nontuthuzo Dlamini Nonkululeko Dladla Denham Parker Sven Kerwath
Abstract:	<p>Few stratigraphic models of continental shelves incorporate the process of geostrophic current-sweeping, consequently its role in the stratigraphic record is often overlooked. We examine the narrow, current-swept Eastern Cape shelf of South Africa using a combination of geophysical techniques, seafloor sampling and video observations and interpret the role of current action on the transgressive stratigraphy of this steep subtropical shelf. During the Last Glacial Maximum, fluvial valleys incised the acoustic basement rocks. During the subsequent transgression, two distinct shorelines were formed and preserved at -105 m and -60 m. Their development and preservation is linked to (i) high sediment supply from adjacent fluvial sources, (ii) early diagenesis and (iii) alternating sea-level stillstands and periods of rapid sea-level rise during melt water pulses 1A and 1B, respectively. The deeper shoreline formed in a sandy, wide coastal plain setting with limited bedrock influence, whereas the shallower shoreline comprised alternating rock headlands and embayments like the contemporary coast. Differences in antecedent topography and geology are responsible for the temporal variability in shoreline type.</p> <p>Between the two shoreline complexes, in the mid-shelf, the transgressive stratigraphy records initial valley infill by progradation of coast-parallel sandy spits. These are capped by a stiff lagoonal mud deposited as ongoing sea-level rise overspilled the valley interfluvies, overlapping the adjacent aeolianites. The uppermost stratigraphy comprises mounds of rhodoliths which interfinger with a sandy inner to middle shelf highstand wedge.</p> <p>After sea-level reached its present position ca 7.4 ka yr BP, the shelf became subject to reworking by the high-energy, geostrophic Agulhas Current. This has had the following major effects on the shelf stratigraphy: 1. the topographic relief of the cemented palaeo-shorelines has been emphasised by removal of the post-transgressive cover; and 2. The shelf no longer acts as a depocenter; instead, the seabed consists of rhodoliths, gravel streamers, bedrock or gravel hash of the wave ravinement surface. Given the necessary antecedent conditions such as accommodation, sediment supply and favourable diagenetic climate, prominent shorelines can form and be preserved on the shelf. Strong current sweeping emphasises these morphological features on subtropical shelves.</p>
Suggested Reviewers:	Scott Nichol scott.nichol@ga.gov.au Likewise, has worked on submerged shorelines similar to these

	<p>Andy Plater gg07@liverpool.ac.uk Prof. Plater has been publishing much on similar processes of barrier overstepping on shelves</p>
	<p>Robin Beaman robin.beaman@jcu.edu.au Again, has worked on a variety of submerged shorelines</p>
	<p>Julian orford j.orford@qub.ac.uk Prof. Orford has much experience on barriers being overstepped</p>
	<p>Brendan Brooke Brendan.Brooke@ga.gov.au Expertise in submerged shorelines</p>
	<p>Francesco Chiocci francesco.chiocci@uniroma1.it Prof. Chiocci has wokred on numerous systems in the Mediterranean, including submerged beachrocks and shorelines</p>
	<p>Edward Anthony anthony@cerege.fr Prof. Anthony has much experience in coastal evolution which is what we deal with here</p>
Response to Reviewers:	

1 Relict and contemporary influences on the postglacial geomorphology and evolution of a
2 current swept shelf: the Eastern Cape Coast, South Africa

3 Green, A.N.¹, Cooper, J.A.G.^{1,2}, Dlamini, N.P.¹, Dladla, N.N.¹, Parker, D.³, Kerwath, S.E.^{3,4}

4 ¹Geological Sciences, University of KwaZulu-Natal, Westville, Private Bag X54001, South
5 Africa

6 ²School of Geography & Environmental Sciences, University of Ulster, Cromore Road,
7 Coleraine, Northern Ireland, UK

8 ³Department of Agriculture, Forestry and Fisheries, Vlaeberg 8018, Cape Town, South Africa

9 ⁴Biological Sciences, University of Cape Town, Rondebosch 7700, South Africa

10

11 Abstract

12 ~~Few studies incorporate current sweeping into the~~Few stratigraphic models of continental
13 shelves incorporate the process of geostrophic current-sweeping, consequently ~~their~~
14 ~~representation~~its role in the stratigraphic record is ~~poorly understood, often overlooked~~. We
15 examine the narrow, current-swept Eastern Cape shelf of South Africa using a combination of
16 geophysical techniques, seafloor sampling and video observations. ~~A steeply seaward dipping~~
17 ~~acoustic basement is incised by valleys~~ and interpret the role of current action on the
18 transgressive stratigraphy of this steep subtropical shelf. During the Last Glacial Maximum
19 ~~that abut aeolianite pinnacles. A series of~~, fluvial valleys incised the acoustic basement rocks.
20 During the subsequent transgression, two distinct shorelines were formed and preserved at -
21 105 m and -60 m. Their development and preservation is linked to (i) high sediment supply
22 from adjacent fluvial sources, (ii) early diagenesis and (iii) alternating sea-level stillstands and

23 periods of rapid sea-level rise during melt water pulses 1A and 1B, respectively. The deeper
24 shoreline formed in a sandy, wide coastal plain setting with limited bedrock influence, whereas
25 the shallower shoreline comprised alternating rock headlands and embayments like the
26 contemporary coast. Differences in antecedent topography and geology are responsible for
27 the temporal variability in shoreline type.

28
29 Between the two shoreline complexes, in the mid-shelf, the transgressive stratigraphy records
30 initial valley infill by progradation of coast-parallel sandy spits prograde into the valleys in the
31 middle shelf. These are capped by a stiff lagoonal mud ~~that~~deposited as ongoing sea-level rise
32 overspilled the valley interfluves, onlapping the adjacent aeolianites. The uppermost
33 stratigraphy comprises mounds of rhodoliths which interfinger with a sandy inner to middle
34 shelf highstand wedge. ~~Multibeam and side-scan sonar data reveal the aeolianite pinnacles to~~
35 ~~form a variety of planform equilibrium palaeo-shorelines at 105 m and at 60 m. These, along~~
36 ~~with the adjacent middle to outer shelf are current swept, with rhodoliths, gravel streamers,~~
37 ~~exposed bedrock or gravel hash of the wave ravinement exposed throughout.~~

38 ~~The deeper shoreline formed in a sandy, wide coastal plain setting, whereas the shallower~~
39 ~~shoreline was constrained to rock embayments like the contemporary coast. The 105 m and~~
40 ~~60 m shorelines were formed and preserved during stillstands and melt water pulses 1A and~~
41 ~~1B, respectively, aided by subtropical diagenesis.~~

42 ~~By ~7000 yr BP, the ensuing transgression had exposed the shelf to the effects of the Agulhas~~
43 ~~Current, and post-transgressive cover was removed by current whittling to expose the palaeo-~~
44 ~~shorelines.~~

45 After sea-level reached its present position ca 7.4 ka yr BP, the shelf became subject to
46 reworking by the high-energy, geostrophic Agulhas Current. This has had the following major
47 effects on the shelf stratigraphy: 1. the topographic relief of the cemented palaeo-shorelines

48 has been emphasised by removal of the post-transgressive cover; and 2. The shelf no longer
49 acts as a depocenter; instead, the seabed consists of rhodoliths, gravel streamers, bedrock or
50 gravel hash of the wave ravinement surface.

51

52 Given the necessary antecedent conditions such as accommodation, sediment supply and
53 favourable diagenetic climate, prominent shorelines can form. ~~When coupled to rapid rates of~~
54 ~~sea-level rise~~ and be preserved on the shelf. Strong current sweeping, ~~they are preserved as~~
55 ~~persistent~~ emphasises these morphological features ~~of current swept on~~ subtropical shelves.

56

57 Key words: palaeo-shorelines, barrier islands, melt water pulse, current-dominated shelf,
58 Agulhas Current

59

60 1. Introduction

61 The southeastern shelf of South Africa, off the rocky and high-energy “Wild Coast” of the
62 Eastern Cape Province, is little known in comparison to the adjacent shelves of KwaZulu-Natal
63 (Green et al. 2018; Pretorius et al., 2019) to the north and the Southern Cape to the south
64 (Cawthra et al., 2016; Flemming and Martin, 2018). The combination of a narrow and shallow
65 shelf with the south-westward-flowing Agulhas Current, one of the fastest flowing boundary
66 currents on the globe, results in a shelf that is strongly modified by current activity. To date,
67 there are few studies that incorporate current sweeping into models of shelf stratigraphy and
68 morphology (cf. Cawthra et al., 2012) and little is known of the processes that control the
69 development and preservation of such features in the stratigraphic record. A key gap in
70 knowledge is how coastal evolution is influenced by shelf-sweeping, coupled to sea-level rise,
71 i.e. how does a coastline evolve as the shelf is drowned and becomes increasingly swept by
72 oceanic currents?

73 The morphology and Quaternary/Holocene evolution of the Eastern Cape shelf is poorly
74 studied, and little attention has been paid to shelf geomorphology and stratigraphy despite
75 ~~Flemming (1980) first recognising~~ the current-swept nature of the area. having been long
76 identified (Flemming, 1980). Martin and Flemming (1987) notably documented a series of
77 prominent outcropping palaeo-shorelines in the area, which along adjacent shelves, have since
78 been more closely examined and recognised as exceptionally well-preserved and
79 geomorphologically complex shoreline features (Green et al., 2018). These features provide
80 abundant opportunities to examine shoreline changes in both time and space and importantly
81 provide insight into long-term shoreline behaviour over ~~centurial~~centennial to millennial scales
82 (Cooper et al., ~~2018~~2018a; Mellet and Plater, 2018). Such insights are often lacking from
83 current-swept areas where sediment retention is limited by erosion.

84 Current-swept shelves ~~may~~typically comprise thin veneers of sandy/gravelly sediments (the
85 palimpsest sediments of Swift, 1974), which mantle a relatively flat and low-relief bedrock
86 outcrop (Shideler and Swift, 1972; Toscano and Sorgente, 2002; Coffey and Read, 2004; Green
87 and Garlick, 2011; Flemming and Martin, 2018). However, under certain circumstances, e.g.
88 sufficient antecedent accommodation and sediment supply, rapid sea-level rise and a climate
89 that fosters rapid carbonate diagenesis, large-scale submerged shorelines may be preserved and
90 exposed as spectacular seafloor features by the current action. Notable examples include the
91 Loop Current-exposed Pulley Ridge of SW Florida (e.g. Locker et al., 1996; Jarrett et al.,
92 2005), the Bass Cascade and Bass Strait-influenced Gippsland Shelf of SE Australia (Brooke
93 et al., 2017), the Leeuwin Current-influenced Carnarvon (Nichol and Brooke, 2011) and
94 Rottnest shelves of Western Australia (Brooke et al., 2017) and the Agulhas Current-dominated
95 KwaZulu-Natal shelf of SE Africa (Green et al., 2013a; Green et al., 2014). In these instances,
96 several drivers operate to define the shelf stratigraphy and geomorphology and may include
97 longer-term allocyclic processes such as rate of sea-level fluctuation (Locker et al., 1996;

98 Salzmann et al., 2013), shorter term or near instantaneous allocyclic processes such as
99 oceanographic forcing (Flemming, 1980; 1981), and long-term autocyclic conditioning of shelf
100 gradient and palaeo-topography (e.g. Green et al., 2018; Kirkpatrick et al., 2019).

101 The broad aim of this paper is to investigate the morphological and stratigraphic evolution of
102 a typical current-swept shelf, with focus on the Eastern Cape shelf of South Africa (Fig. 1). We
103 examine the fundamental drivers of shelf evolution ~~such as~~including (i) sea-level changes
104 during the last glacial cycle and (ii) contemporary ocean dynamics ~~with an.~~ Thereby we aim
105 to (1) describe the shelf stratigraphy and surface morphology; (2) identify modern and relict
106 seafloor features (3) interpret the origin and genesis of seafloor features; and (4) present a
107 model for current-swept shelf evolution driven by relict and modern forcing agents. This is
108 ~~linked with~~compared to other similar shelves around the globe.

109

110 2. Regional setting

111 The southeast African continental margin is a sheared passive margin along which South
112 America separated from southern Africa during the initial opening of the South Atlantic
113 (Scrutton and Du Plessis, 1973). Regionally, it is exceptionally straight and narrow, but on a
114 local scale, there are extensive variations in morphology, especially in the distribution of
115 canyons and other irregularities on the continental slope (Flemming, 1981; Dingle et al., 1983).
116 The East London shelf break occurs between 110 m and 120 m depth (Fig. 1), with a shelf
117 width that varies between 19 km to 23 km, making it narrower and slightly shallower than the
118 world average of 75 km and 130 m, respectively (Flemming, 1981). The shelf gradient varies,
119 with a shallower gradient ca. 1.4° in the outer shelf, steepening up to 2.9° in the inner to middle
120 shelf (Dlamini, 2018). The adjoining coastline is fragmented by a series of zeta (half-moon)

121 bays of which their origin is related to the brittle deformation phases associated with the break-
122 up of Gondwana (Watkeys, 2006).

123 The continental margin of southeast Africa is a high-energy environment dominated by south-
124 westerly swells. The entire coast is subject to high-energy swells (Hs 2.1 m; T 11 s; HRU
125 1968), where the significant wave heights for 1, 0.1, and 0.01% exceedance are around 3.9 m,
126 5.0 m, and 6.0 m, respectively (Rossouw 1984). Swell heights commonly range between 1 and
127 2 m, with the largest recorded swell (12–13 June 1997) in the last 22 years having a significant
128 wave height (Hs) of 9.3 m (Dixon et al., 2015). Spring tidal range is between 1.8 and 2.0 m,
129 and neap tidal range is 0.6 to 0.8 m (HRU 1968). The mid-outer shelf is dominated by the
130 Agulhas Current, a fast poleward-flowing geostrophic current that can reach surface velocities
131 of >2.5 m/sec (Pearce et al., 1978). ~~The formation of giant waves~~ Along the shelf margin giant
132 waves may be formed by the propagation of high swells into the current (Mallory, 1974; Smith,
133 1976).

134 The study area comprises Gondwana-age sedimentary rocks of the Karoo Supergroup that are
135 overlapped by Cretaceous through to Quaternary age sedimentary rocks. Sandstones and shales
136 of the Karoo Supergroup crop out along the coastline and are overlain by limestones of the
137 Cretaceous Igoda Formation (Dingle et al., 1983). Calcareous sandstones of the Neogene
138 Nanaga Formation occur locally, together with shelly sands, soils and middens of the
139 Pleistocene-age Schelmuhoek Formation (Roberts et al., 2006).

140 Along the coast and on the shelf, a variety of Pleistocene to Holocene age beachrocks and
141 aeolianites are found (Roberts et al., 2006). These aeolianites comprise the Nahoon Formation,
142 a former parabolic dune complex deposited at ~200 ka (Le Roux, 1989) and since bevelled into
143 a series of raised shore platforms that occur at 4 to 5 m above mean sea level and mean sea
144 level, respectively. The upper platform is mantled by a coquina of assumed Marine Isotope

145 Stage (MIS) 5e age (Roberts et al., 2006). Unconsolidated sediment mantles these in places
146 and occurs as a narrow wedge of shelf sediment that forms the contemporary shoreface
147 (Flemming, 1981).

148 Sediment is supplied to the coast via three main river drainage systems, the Kei, Mzimvubu
149 and Great Fish Rivers (Table 1). The Great Fish and Kei River catchments supply 11.48×10^6
150 m^3 and $11.134 \times 10^6 m^3$ of sediment to the coast respectively (Table 1) (Flemming, 1981). The
151 Mzimvubu River debouches to the north and when combined with the Mbashe River, provides
152 a further $10.458 \times 10^6 m^3$ of fluvial sediment per year. The zone between the Great Fish and
153 Mzimvubu Rivers was identified by Flemming (1981) as a discrete sediment compartment
154 supplied by the above rivers and mostly dominated by current sweeping of the adjacent shelf.
155 According to Rooseboom (1978), this entire coastal strip is characterised by annual sediment
156 yields that range from $150 t/km^2$ up to $800 t/km^2$ per year.

157 Martin and Flemming (1987) identified a series of palaeo-coastlines on the shelf at a depth of
158 60-70 m, and at the shelf edge (-100-105 m). These shorelines extend for over 600 km to the
159 north of the study area (Green et al., 2014) and are thought to have formed when sea levels
160 occupied depths of 100 m ~ 14 600 yr BP (Green et al., 2014) and ~ 60 m between 13 000 and
161 12 500 cal yr BP (Cooper et al., [2018](#)[2018b](#)).

162

163 3. Methods

164 Ultra-high-resolution seismic data were collected aboard the RV Meteor cruise M123 in
165 February 2016. The data were acquired with an Atlas PARASOUND parametric echosounder
166 using a primary low frequency of 4 kHz. Navigation was provided by a differential GPS
167 (DGPS) capable of ~ 1 m accuracy in the X and Y domains.

168 The data were processed with Atlas PARASTORE, where the sea bottom was tracked, the data
169 match-filtered and swell corrected, time varied gains were applied, and the processed data
170 exported in SEGY format. All data were then interpreted in IHS Kingdom Suite or Hypack
171 SBP utility. Sound velocity estimates of $1\,500\text{ ms}^{-1}$ in water and $1\,600\text{ ms}^{-1}$ in sediment were
172 applied for all time-depth conversions.

173 Seismic units were defined by reflector packages, bound by distinct unconformity surfaces
174 where the internal reflectors were either truncated, or where they downlapped, toplapped and
175 onlapped the unconformities (see Mitchum et al., 1977). The units were described according
176 to the internal reflector amplitudes, geometries and continuity and designated a unit name from
177 Unit 1 to 4.

178 Multibeam data were collected using two different systems. Data offshore Morgan Bay, East
179 London shelf edge and the Mazeppa Bay area were collected using a Reson 7125 multibeam
180 echosounder coupled to a DGPS and Applanix POS-MV motion reference unit. The data were
181 collected and processed by Marine Geosolutions Pty Ltd., and resolve to a $1\text{ x }1\text{ m}$ grid, with a
182 depth resolution of $\sim 30\text{ cm}$. Backscatter data were collected simultaneously with a Klein 3000
183 side scan sonar system with a scan range of 75 m using the 500 kHz channel. The data were
184 processed using the Klein SonarPro software, where the bottom was manually tracked, the data
185 were filtered, time varied gains applied, the channels colour balanced and the nadir zone
186 removed for seamless mosaicking. The final data set resolve to a mosaic pixel approximating
187 $1\text{ x }1\text{ m}$.

188 The second set of multibeam data were collected aboard the RV Ellen Khuzwayo, voyage 159,
189 using a Reson 7101 ER multibeam system, coupled to a DGPS and a SBG Systems Ekinox-D
190 INS motion reference unit. All soundings were reduced to mean sea level during processing.
191 The final data were output as a $5\text{ x }5\text{ m}$ resolution grid, with a depth resolution of $\sim 50\text{ cm}$. Co-

192 registered pseudo-side scan sonar data were collected as Snippets for backscatter mapping, the
193 final output of these on the same horizontal scale as the bathymetry data.

194 Seafloor materials were sampled using a benthic sled, a Shipek grab and a dredge, depending
195 on the substrate; rocky substrate necessitated a dredge as opposed to the less consolidated
196 materials such as mud and sandy material/gravels. Sampling was mainly done for biological
197 purposes and as such, not all the bathymetric and backscatter features observed were sampled.

198 An intact rhodolith was selected for ^{14}C dating using accelerator mass spectrometry (AMS).
199 Two samples, one from the centre of the rhodolith, the other from the exterior were analysed.
200 Calibrated ages were calculated using the Southern Hemisphere atmospheric curve SHCal13
201 (Hogg et al., 2013). A reservoir correction (DeltaR) of 161 +/- 30 was applied to coralline
202 material. Analyses were performed by Beta Analytic in their Florida radiocarbon facilities.

203

204 4. Results

205 4.1. Seismic stratigraphy

206 The seismic stratigraphy of the study area is shown in figure 2 (a-d). The acoustic basement
207 comprises a series of moderate to high amplitude, inclined parallel reflectors. These dip
208 seawards at $\sim 2^\circ$ and are truncated by an erosional surface, S1, marked by incised valleys up to
209 20 m deep in the middle shelf (Fig. 2c and d). These valleys abut a series of pinnacles and
210 ridges of acoustically opaque material (Unit 1) that span the middle shelf to shelf edge, the
211 bases of which occur at depths of 105 m. To seaward of the most landward ridge, a tangential
212 oblique-prograding wedge of material onlaps the ridges (Unit 2) (Fig. 2a; c and d) and
213 progrades into the valleys (Fig. 2d). In some areas, this wedge ~~may appear~~appears acoustically

214 transparent (Fig. 2b). A thin (<2 m) body of discontinuous, wavy to horizontal, low amplitude
215 reflectors (Unit 3) locally onlaps Unit 2 and interfingers with the overlying units (Fig. 2a and
216 b).

217 Units 1, 2 and 3 are all in turn onlapped by a finely layered, low amplitude set of reflectors
218 (Unit 4) that spill out of the middle shelf incised valleys (Fig. 3) and terminate behind the main
219 ridges that comprise Unit 1 (Fig. 2b-d). This forms a meter-thick package, that is exposed at
220 the seafloor (Fig. 2b-d; 3). In the middle shelf, this forms an acoustically transparent, landward
221 pinching wedge of material that onlaps the ridge on its landward side and overlies the incised
222 valleys in the more proximal middle shelf regions (Fig. 2d).

223 Overlying Unit 4 in the middle to outer shelf is an internally complex mound ~~of~~ characterised
224 by chaotic and discontinuous, landward and seaward dipping reflectors (Unit 5) (Fig. 2). These
225 interfinger to landward with moderate amplitude, sigmoidal prograding reflectors of Unit 6.
226 Along coastal strike, Unit 6 forms a coast-parallel prograding body of sediment. These units
227 are separated from the underlying units by a high amplitude erosional reflector, S2, that
228 truncates the lower units (Units 1-4) (Fig. 2 and 3). S2 is exposed along the seafloor from the
229 middle shelf to outer shelf.

230

231 4.2. Seafloor morphology

232 The spatial attributes of the main seafloor morphological features are described in table 2.
233 Where Unit 1 crops out, (see Figure 2 for example), the seafloor morphology comprises a
234 variety of ridges that exhibit distinct plan forms/morphologies (Fig. 4). The shallowest
235 areas are characterised by a series of parabolic-shaped ridges and depressions (Fig. Figs 2, 3
236 and 4a) that crop out at their seaward edge at ~ 60 m depth. The ridge reliefs vary between 1

237 to 7 m, with the parabolic forms spaced ~ 500 m apart (Table 2). Along strike and at similar
238 depths, Unit 1 takes the form of narrow (≤ 80 m) crenulate ridges 0.5 to 2 m in relief,
239 superimposed on basement rocks that crop out as strongly SE-NW orientated, blocky seafloor
240 (Fig. 4b).

241 In the middle shelf areas, between 60 and 80 m depth, the parabolic ridges and depressions of
242 Unit 1 form cusped features that separate semi-circular seafloor depressions, > 2 km-wide and
243 up to 6 m in vertical relief (Fig. 4c and d; Table 2). The edges of these depressions are
244 characterised by multiple, prograding arcuate ridges, up to 4 m in relief and spaced ~ 200 m
245 apart (Fig. 4c).

246 The outer shelf is mostly characterised by subdued relief seafloor between 80 and 90 m deep.
247 A large, coast parallel ridge of Unit 1 occurs throughout the study area, the seaward fringe of
248 which occurs at -100 m (Fig. 4e and f; Table 2). In some areas, this ridge forms a feature with
249 up to 15 m relief, with multiple recurved ridges attached to its landward flank (Fig. 4e). The
250 recurved ridges are ~ 250 to 350 m-wide, with relief of up to 4 m. Depressions up to 2 m are
251 evident in the ridge (Fig. 4e and f), forming low-lying areas on the seafloor in which smaller,
252 prograded ridges of ~ 0.5 m relief and 40 m spacing occur (Fig. 4e). In other areas, cusped,
253 landward-narrowing ridges occur along the main ridge line (~~Fig. 4f, forming triangular seafloor~~
254 features 300 to 500 m long (Fig. 4f; Table 2).

255 The inner shelf ~~areas are~~ marked by ~~the surface expression of these~~ several underfilled valleys
256 ~~identified~~ manifest as elongate seafloor depressions. These are correlated in seismic profile ~~as~~
257 the incisions associated with surface S1. These palaeo-valleys form topographic lows on the
258 inner shelf where Unit 4 crops out. These areas are also characterised by the presence of
259 mounds of Unit 5, where they form in some of the depressions. The palaeo-valleys extend into

260 the semi-circular seafloor depressions and into the low-relief and deeper seafloor landward of
261 the -100 m ridge (Fig. 4).

262

263 4.3. Seafloor backscatter and sediment characteristics

264 The more proximal middle shelf comprises even-toned high backscatter seafloor, confined to
265 the topographic low of the underfilled incised valley (Fig. 5a). This merges with moderate and
266 irregular backscatter where the valley widens towards the semi-circular depressions (Fig. 5a).
267 On either side of the valley, high relief, irregular and alternating moderate to high backscatter
268 seafloor marks the parabolic ridges and depressions of Unit 1, respectively. This seafloor
269 texture ~~extends all the way~~ to the outer shelf. ~~Where~~ The lower relief areas of the semi-circular
270 depressions ~~are encountered, these~~ are characterised by moderate, even toned backscatter.

271 Several coast-parallel elongate furrows are evident ~~from~~on the middle to outer shelf (Fig. 3b
272 and 4b). These form linear depressions up to 30 cm deep and are associated with linear patches
273 of high backscatter (Fig. 5). These overprint the low relief sea floor features and mark the
274 surface exposure of S2. Throughout the study area, isolated patches of rippled, alternating high
275 to low backscatter seafloor are apparent.

276 Seafloor inspections reveal the even-toned high backscatter areas to comprise weakly
277 laminated, stiff, muddy deposits (Fig. 5; 6a). In the proximal underfilled incised valley, this is
278 mantled by sandy material with mud cropping out in the depressions of current ripples (Fig. 1;
279 6b) The adjoining moderate and irregular backscatter seafloor is paved by a thin cover of
280 rhodoliths (Fig. 5; 6c). In contrast, on the middle to outer shelf, the mounds of Unit 5 comprise
281 stacked accumulations of rhodoliths (Fig. 2; 6c). AMS ¹⁴C dates of the interior of the rhodoliths

282 ranged from 7406 - 7225 cal yr BP, with their surface material dating to present day (150 cal
283 yr BP to Post-Bomb).

284 The high relief, alternating high and moderate backscatter ridges and depressions correspond
285 with aeolianites cropping out along the seafloor (Fig. 6d). The lower relief seafloor marks
286 outcrop of subdued relief rocky material. The interleaving seafloor where S2 crops out is
287 marked by pebbles and cobbles of reworked aeolianite, together with finer bioclastic material
288 (Fig. 6e). The linear depressions of high backscatter are likewise lined by similar material (Fig.
289 6f). The isolated areas of rippled, alternating high to low backscatter represent isolated patches
290 of rippled bioclastic material interspersed with quartzose sand.

291

292 5. Discussion

293 5.1. Seismic stratigraphic interpretation

294 Aeolianites of Unit 1 at -105 m and shallower abut and overlie S1, the last glacial maximum
295 (LGM)-age subaerial unconformity that is commonly recognised across the SE African shelf
296 (Green et al., 2013a). We refer to these as the -100 m and -60 m shorelines based on these
297 previous works. Incised valleys formed in S1 relate to the LGM lowstand and constrain the age
298 of the aeolianite sequences to the most recent postglacial period (Pretorius et al., 2016; Cooper
299 et al., [2018](#)[2018b](#); Pretorius et al., 2019).

300 The tangential oblique-prograding wedge of Unit 2 that onlaps the aeolianites and enters the
301 incised valleys is architecturally similar to spit systems recognised from multiple large incised
302 valley systems, lagoons and lakes of the east coast of South Africa (Wright et al., 2000;
303 Benallack et al., 2016) and from shelf to lake environments elsewhere around the world (Novak

304 and Pederson, 2000; Raynal et al., 2009; Nutz et al., 2015). In keeping with this interpretation,
305 the chaotic and discontinuous reflectors of Unit 3 are similar to features identified elsewhere
306 as small-scale slump or mass wasting packages in waterbodies characterised by active spit
307 progradation (Wright et al., 2000; Rucińska-Zjadacz and Wróblewski, 2018).

308 Seafloor sampling and observations reveal Unit 4 to comprise stiff muddy materials. The
309 stratigraphic position as a capping and overspilling unit of the incised valleys points to
310 deposition in a lagoonal environment that overtopped the interfluves and ponded along the
311 shelf behind the barrier systems of Unit 1 (e.g. Green et al., 2013b; Benallack et al., 2016).

312 The intercalating upper units 5 and 6 represent the contemporary Holocene shelf sediment
313 prism which interfingers with the rhodolith mounds indicating that the two were deposited and
314 evolved contemporaneously. Studies of the Holocene sediment prism in SE Africa indicate a
315 mid-Holocene to recent age (Pretorius et al., 2016) which correlates with the age at which
316 Holocene sea level stabilized close to the present (Cooper et al., ~~2018~~2018b) and the rhodolith
317 mounds began to form (7406 - 7225 cal yr BP).

318 Surface S2 outcrop represents the seafloor exposure of the Holocene wave ravinement surface.
319 This surface truncates the spit/barrier/lagoon sequences and separates the post-transgressive
320 Holocene material from the underlying transgressive succession. The mixed bioclastic and
321 aeolianite pebbly material (Fig. 6f) is similar to the material forming from the contemporary
322 wave ravinement of beachrocks and aeolianites in SE Africa (Cooper and Green, 2016). The
323 exposure of this material in elongate furrows provides evidence for current furrowing that has
324 denuded the mid to outer shelf of sandy sediment and exposed the underlying wave ravinement
325 ~~to~~ surface to geostrophic current reworking, forming gravel streamers and ribbons (Flemming,
326 1978).

327 The development of rhodolith fields since ca. 7.4 ka yr BP provides further evidence of strong
328 Agulhas Current action since sea levels stabilised close to the present. Prior to this, the current
329 ~~existed~~flowed seaward of the shelf edge and did not support the growth of rhodoliths in this
330 position. Intact rhodoliths that interfinger with the Holocene sediment wedge indicate episodic
331 wedge progradation into current-agitated waters where the rhodoliths nucleated, as opposed to
332 punctuated re-deposition of the rhodoliths by gravity or storm driven processes (evidenced
333 elsewhere by broken rhodoliths, interspersed with pebbly gravels- (Brandano and Ronca,
334 2014).)). This conforms to Flemming's (1981) model of the regional shelf; an inner siliclastic
335 wave-dominated system and an outer Agulhas Current-dominated shelf. In microcosm, this
336 ~~reflects~~matches the shelf/carbonate platform drowning model of Betzler et al. (2013), wherein
337 which swift sea-level rise produces partial shelf drowning and current sweeping of the shelf.
338 This thus places the timing of mid-shelf transgression to a minimum age of 7406 – 7225 cal yr
339 BP and implies a sudden increase in the rate of sea-level rise that post-dates a regional sea-
340 level slowstand recognised by De Lecea et al. (2017) ~ 8000 cal yr BP.

341

342 5.2. Seafloor morphology

343 Several seafloor features bear striking similarity in plan form ~~and scale~~ to contemporary
344 shoreline features on the sandy and wide (40-100 km) Maputaland-Mozambique coastal plain
345 (Fig. 7a), as well as coastal features that are not represented on the modern SE African coast.
346 Below, following Gardner (2005, 2007), we compare the seafloor topographic features with
347 contemporary coastal landforms as an aid to their interpretation.

348 5.2.1. -100 m shoreline

349 The large blocky aeolianite body that occurs at ~ 105 m at the shelf edge (Fig. 4e and f) is
350 ~~equivalent~~similar in ~~scale and~~ shape to the modern barriers of the Maputaland coastline (Table
351 2), and to some modern barrier islands formed on ~~many other~~ wave-dominated coastlines (see
352 Mulhern et al., 2017). Regarding size, the aeolianite body is significantly narrower, with a
353 lower elevation than the contemporary Maputaland coastal barrier. The seafloor depressions
354 and recurved ridges that attach to the depressions and landward sides of the main ridge line are
355 very similar in shape and ~~scale to~~conform to the lower size limits of inlets and associated
356 cusate and recurved spits of contemporary major barrier-inlet systems, (Table 2), both in
357 southern Mozambique and Maputaland (Fig. 7a and b) and from systems of the southern US
358 Atlantic margin (Cooper and Pilkey, 2002; Pilkey, 2003; Davis and FitzGerald, 2009). Breaks
359 in the ridge, marked by topographic lows are of a similar shape and dimension to tidal inlets
360 ~~and,~~ an interpretation that is supported by their location adjacent to recurved features (Fig 4e).
361 These are up to 200 m-wide and ~ 5 m-deep, consistent with figures reported for inlets
362 worldwide (Davis and FitzGerald, 2009). ~~This further supports such an interpretation.~~—The
363 adjacent low relief areas landward of the main inferred barrier positions are interpreted as the
364 palaeo-back barrier environments through which the incised valleys passed during the LGM
365 lowstand (Fig. 6e).

366 The large, semi-circular seafloor depressions (Fig. 7c) that occur slightly distal to the barrier
367 are interpreted as a series of drowned and segmented lagoons. The arcuate prograding ridges
368 along the depression margins, together with the cusate wedges of Unit 1 aeolianite that
369 separate each lagoon, mark prograding lagoon shorelines and down-drift spit termini of the
370 wave-driven littoral cells of the system, respectively (cf. Ashton and Murray, 2010) (Fig. 7c).
371 These are mostly within the lower size range of the modern systems found along the SE African
372 coast (Table 2). The depressions correlate directly to landwards with the outcropping,
373 overspilled muddy facies of Unit 4.

374 These ~~apparently~~ segmented lagoons are fed by several underfilled incised valleys that clearly
375 mark the palaeo-fluvial pathways that entered ~~into~~ these lagoons. These fluvial entrance points
376 are similarly recognised in the contemporary setting of coastal waterbodies in SE Africa (Table
377 2) (Fig. 7d).

378 A significant modern barrier system extends from Richards Bay, ~ 650 km north of the study
379 area into southern Mozambique (Jackson et al., 2014). This system is marked by a series of
380 northeastward oriented, climbing parabolic dunes that can reach up to 120 m high, covered
381 with multiple blowout features. The parabolic ridges and depressions that form in the aeolianite
382 of Unit 1 are very similar in shape and planform scale to those dunes of the contemporary coast,
383 with (Table 2), though their elevations are markedly lower. Small, blowout-like features are
384 also evident (Fig. 7e). We thus consider that a similar large dune system occurred at some point
385 adjacent to and fringing the barrier islands and segmented waterbodies of the outer shelf. ~~This~~
386 appears to be comparable in scale to Though of considerably lower elevation, the width is within
387 the ranges reported for the dune fields of southern Mozambique (Fig. 7a) and marks an
388 approximate shoreline depth of 105 m (c.f. Ramsay, 1995).

389

390 5.2.2. -60 m shoreline

391 At -60 m, a former shoreline lineation is also evident. In planform this is ~~arranged in a series~~
392 of palaeo-embayments. manifest as a series of palaeo-embayments, fringed by small aeolianite
393 ridges of similar widths to the lower limits of the primary dunes found along the embayed
394 mixed-sand and rock coastlines of SE Africa (Jackson et al., 2014). The palaeoheadlands are
395 formed in bedrock of the Karoo Supergroup, separated by crenulate ridges of Quaternary
396 aeolianite (Fig. 8a) that also rest on Karoo bedrock. This is a ~~very~~ similar coastal morphology

397 to that of the present day, where thin outcrops of aeolianite and beachrock rest with marked
398 unconformity on older sedimentary rocks in embayments between prominent bedrock
399 headlands (Fig. 8b and c).

400 Some of the embayments on the contemporary coast are also marked by modern
401 barriers/Holocene age dunes ([Table 2](#)) (Fig. 8c) and this configuration too appears to be
402 reflected on the seafloor (Fig. 8a). Their presence indicates that the coastal evolution at the
403 time of their formation was strongly influenced by the bedrock framework, as is the modern
404 coast (Watkeys, 2006). Similarly, their form and structure point to a shoreline occupation at a
405 depth of 60 m where planform equilibrium forms developed in coastal re-entrants (Carter,
406 1980).

407

408 5.3. Postglacial evolutionary model

409 The contemporary shelf morphology reflects a combination of influences of wave and ocean
410 current processes acting on the pre-existing basement geology. These have operated with
411 varying intensity and at different locations as sea level fluctuated during the last glacial cycle
412 and the deposits and geomorphic features of each successive interval have influenced
413 subsequent evolution. The sequence of events and associated dynamics are discussed below
414 in the context of an evolutionary model for the shelf.

415 Initially, the narrow and shallow shelf was dissected by several fluvial systems during lowstand
416 conditions culminating in the LGM (Fig. 9a). Two main river systems in the area formed
417 valleys of similar scale to those on the modern coast. At this time, wave action was focussed
418 off the modern shelf break, as was the palaeo Agulhas Current. During subsequent sea-level
419 rise wave processes reworked existing sediment and formed distinctive coastal landforms that

420 are preserved at several specific levels on the seafloor. These shoreline features indicate
421 marked differences in shoreline type at various stages of the transgression and their
422 preservation or non-preservation is linked to rates of sea-level change.

423 The generation of a substantial barrier system at ~ 100 m depth (Fig. 9b) can be linked to
424 patterns of stable sea level that allowed planform equilibrium for the palaeo-coastline to be
425 reached. LikeIt contains features similar to the contemporary highstand coastal systems of
426 northern KwaZulu-Natal and southern Mozambique (Green et al., 2013b), ~~we see the same~~
427 ~~coastal forms~~ from which we infer similar conditions of sediment supply, energy and sea level
428 state at the time of formation (~~expanded on~~see below). These strongly contrast with the
429 sediment-poor, headland bound and rocky setting of the contemporary coastline of the Eastern
430 Cape.

431 Stable or slowly rising early Holocene sea levels promoted barrier growth, overspilling of
432 incised valleys and lateral extension of newly forming lagoons, with a general planform
433 equilibrium reached for the lagoon bodies (Fig. 9c). New accommodation was not generated
434 quickly, and the back barrier behind the -100 m barrier could be overfilled to compensate. The
435 prograded lagoon margins on contemporary lagoons in SE Africa (Wright et al., 2000; Botha
436 et al., 2018) are attributed to minor sea-level fall of +/- 2 m from a late Holocene highstand to
437 the present (Cooper et al., ~~2018~~2018b). The prograded lagoon margin features at -100 m may
438 indicate similar patterns of sea-level fall around the LGM (Fig. 9d). This is consistent with
439 new findings regarding the nature of the LGM sea level which dropped from -100 m stillstand
440 to a maximum of -118 m (Yokoyama et al., 2018) between 21 900 and 20 500 yr BP.

441 The behaviour of barrier shorelines in the context of rising sea level is discussed by Carter
442 (2002), who considered three main modes of barrier response, erosion, rollover, and
443 overstepping. A fourth possible mechanism is partial overstepping, whereby remnants of the

444 barrier are left after a portion of the barrier is eroded as the shoreface translates over the barrier
445 form. Overstepping has been considered the main mechanism responsible for the preservation
446 of the palaeo-shorelines from SE Africa, associated with particularly abrupt phases of sea-level
447 rise and in place drowning the coast (Green et al, 2014). We further this hypothesis by linking
448 the overstepping of the -100 m shoreline to melt water pulse 1A (Fig. 9e). This rapid rise in sea
449 level from ~ -100 m (~ 4 m per century, with a 95% probability of between 8.6 and 14.6 m rise
450 globally-Liu et al., 2016) would have been sufficient to overstep the fronting barrier system
451 (Fig. 9d). The lagoonal deposits landward of the -100 m barrier shoreline also bear witness to
452 the rapid creation of accommodation space in the back barrier and an associated reduction in
453 the efficacy of the bay-ravinement process as the barrier and back-barrier were submerged (cf.
454 Storms and Swift, 2003; Storms et al., 2008). The high gradient of the wave ravinement surface
455 (up to 4°), bounding the surface of the lagoonal/back barrier deposits (Fig. 2) indicates a
456 steepened shoreline trajectory during overstepping. Salzmann et al. (2013) consider causes for
457 steepened shoreline trajectories to include steep transgressed topographies, rapid rates of RSL
458 rise and high rates of sediment supply (based on the work of Cattaneo and Steel, 2003). On this
459 sediment-starved shelf, high sedimentation rates during infilling of the back barrier can be
460 discounted (e.g. Green, 2009, 2011; Salzmann et al., 2013).

461 We hypothesise that relatively slower rates of sea-level rise then followed, with widespread
462 shelf ravinement (denoted in red ~~on the figure~~ in Figure 9) removing all but the cores of the
463 barrier system surrounding the segmented lagoons and leaving the low-lying depressions of the
464 lagoons intact (Fig. 9f). This slower rate of sea-level rise is linked to the Younger Dryas period
465 that preceded a second meltwater pulse (MWP 1-B) (see Pretorius et al., 2016 for timing of
466 other shoreline development at the same depth). At this time and where available
467 accommodation occurred, shorelines developed within embayments (Fig. 9f). These were then
468 overstepped by MWP 1-B (11.5–11.1 ka BP-Harrison et al., 2019) (Fig. 9g), leaving a

469 subsequent set of smaller aeolian dune fields, some of which are preserved within embayments
470 as relict shelf features. Sea level has since risen to present day, where the contemporary coast
471 is strongly bedrock-dominated with multiple embayments bounded by rock headlands (Fig.
472 9h).

473

474 5.4. Local controls on stratigraphic and geomorphic evolution.

475 The model that has previously been ~~fitted~~developed to describe the occurrence and preservation
476 of submerged postglacial shorelines ~~as presented here, follows one driven mostly by, is based~~
477 on temporally varying rates of sea-level rise linked to paired slowstands (gradual and slowly
478 rising sea level) and subsequent melt water pulses (see Green et al., 2014; 2018). The present
479 study includes additional observations of submerged shorelines at depths consistently seen at
480 60 and 100 m across the narrow portions of the SE African shelf (c.f. Green et al., 2018;
481 Pretorius et al., 2019). ~~We see a clear pattern forming in the data;~~Across the entire shelf, large
482 volume, submerged planform equilibrium barriers and back barrier environments at -100 m
483 and -60 m, ~~that~~ stretch for over 1000 kms ~~into~~alongshore from southern Mozambique (De
484 Lecea et al., 2017) ~~to the present study area.~~ This ~~even~~ mirrors to some degree, submerged
485 relict shorelines on the western southwestern African margin in Namibia (Kirkpatrick et al.,
486 2019). Repeating forms such as drowned segmented lagoons (e.g. Green et al., 2013a),
487 parabolic dune fields (Green et al., 2018) and underfilled incised valleys (Pretorius et al., 2019)
488 are common, yet occupy areas of significant variation in antecedent shelf setting, e.g. narrow
489 vs wider shelves, numerous steep-sided incised valleys vs flat planation surfaces.

490 Numerous similar examples of submerged shoreline features have been reported from other
491 current-swept sub-tropical shelves. On the Gippsland and Lacepede shelves of SE Australia, a

492 series of coast-parallel ridges are found at depths of ~65-75 m. These were interpreted as relict
493 strandplains and barriers (Brooke et al., 2017). Other examples from similar depth ranges are
494 found on the Recherche and Rottneest shelves of Western Australia, together with relict
495 carbonate-cemented dunes (Brooke et al., 2014). On the Carnarvon shelf, coral reefs and
496 carbonate-cemented dunes are similarly apparent at ~ 60 m (Nichol and Brooke, 2011). Around
497 depths of ~ 100 m, erosional knickpoints (the Lacepede shelf, Hill et al., 2009), coral reefs and
498 occasional associated lagoons (the NW Australian and Sahul shelves, Nichol et al., 2013;
499 Howard et al., 2016) ~~are~~have also ~~found~~been reported.

500 ~~The landforms described above all follow a similar overstepping pattern in their inertial~~
501 ~~response to deglacial sea levels and it appears that the An episodic ~~rate of~~ sea-level rise model~~
502 ~~fits required to develop these well as a dominant driver in preservation of such a~~
503 ~~morphology submerged shoreline features at consistent depths and ages on ~~current swept~~~~
504 ~~shelves throughout the subtropics.~~

505 a global scale. However, antecedent shelf geometry is also an important local consideration on
506 shelf evolution ~~is antecedent shelf geometry. On the East London shelf, the high gradients. The~~
507 steep gradient (up to 2.9°) of the SE African shelf would, theoretically, ~~foster weak~~lower the
508 preservation potential of ~~the shoreline~~ form features due to focused erosion along a steep profile
509 for any given unit of time during transgression (Cattaneo and Steel, 2003). ~~In addition, the~~
510 ~~antecedent back barrier topography is particularly subdued. There are no clearly exposed~~
511 ~~palaeo-valleys and the seafloor directly landwards of the barrier appears remarkably smooth~~
512 ~~(Fig. 4e)~~. Where exposed, the barriers clearly comprise cemented sandy aeolianites and it is
513 thus likely that it is the cementation, in conjunction with the driver of rapid rates of sea-level
514 rise (c.f. Green et al., 2018), that is responsible for the preservation of these relict coastal forms
515 on the shelf.

516 The overall weak preservation of shoreline forms, and a dominantly erosional or current swept
517 seafloor between the outer barrier and the - 60 m shoreline can be related to strong ravinement
518 processes, first by ~~waves~~the aggressive wave climate during landward translation of the wave
519 base, and then by oceanic current denudation once sea level had passed over the palaeo-coastal
520 profile. On this steep shelf (1-3°), the implication is that the shoreline migrated *slowly* between
521 the landward edge of the -100 m shoreline and the seaward edge of the -60 m shoreline. During
522 this period, transgressive erosion was maximised and only small remnants or cores of once
523 much larger dune systems, were left.

524 This contrasts with the higher relief, outer shelf where the ~~barrier island and barrier~~
525 ~~ridges~~former coastal barriers are better preserved. ~~This also explains~~The lack of sediment
526 cover in these areas; ~~as the shoreline transgressed the palaeo-coastal plain,~~ is attributed to
527 sediment ~~is being~~ held in the shoreface under sediment-deficit type conditions as the shoreline
528 transgressed the palaeo-coastal plain (Mellet and Plater, 2018). Any sediment ~~left behind that~~
529 was potentially deposited as a transgressive layer was subsequently removed by the current
530 sweeping that formed the gravel streamers observed: on the modern shelf. Simultaneously, the
531 barrier system would continue to roll over to a point where ~~larger~~smaller parabolic dunes and
532 palaeo-embayments/shorelines could form ~~with a seaward depth of (at -60 m-)~~. This period
533 marks a likely slowing of the rate of relative rise which ~~reconciles with~~ this identified on other
534 shorelines at depths of 60 m from the Durban shelf (Pretorius et al., 2016; Cooper et al.,
535 ~~2018~~2018b) and elsewhere e.g. SE and Western Australia (Brooke et al. 2017), SE Brazil
536 (Cooper et al., 2016, 2018c).

537 When comparing the overall scale and size of the relict barrier features on the seafloor to the
538 modern coastlines of SE Africa, we note that although broadly similar in morphology, the sizes
539 of the relict features are smaller than their modern equivalents. The seafloor features are

540 narrower (850 m vs 2 km), with significantly lower relief (15 m vs 170 m). This implies that a
541 significant amount of sediment (~ an order of magnitude in terms of width and height) was lost
542 as the shoreline translated over the shelf to where it is at present.

543 The current coastal configuration is mostly bedrock-controlled, with small rock-bound
544 embayments that host isolated barrier-dune complexes. These are significantly smaller than the
545 barriers preserved at -100 m and are more like the crenulate shorelines preserved at -60 m. The
546 landward change in barrier size implies a shift from large and contiguous dune cordons forming
547 during the early transgression, to isolated sandy barriers hosted amidst bedrock. This shift
548 marks the increasing influence of bedrock control and coastal squeeze on shoreline adjustment
549 during transgression. The net result is transformation of the Eastern Cape coast from a straight,
550 littoral drift-dominated feature to a strongly compartmentalised shoreline with limited
551 accommodation and littoral sediment supply.

552 The sediment for the early dune building phase appears to have been initially sourced from a
553 well-fed littoral system that adjoined a sandy, linear coastline. The net supply of sediment to
554 the coastline from the Kei River alone is likely to have been substantial, and when coupled to
555 the other large quantities of sediment delivered by the adjoining fluvial systems (Table 2), the
556 shelf and coastline should act as a major sediment depocentre. The Agulhas Current sweeping
557 of the shelf, however, limits the potential for sediment accumulation and rather exposes relict
558 features at -100 m that are indicative of former high sediment supply and retention rates. During
559 the transgression, the landward effect of coastal pinch by the bedrock framework is also
560 coupled to the progressive diminution of the seaward edge of the large quantity of sediment
561 that was formerly hosted in the -100 m dune system. As the Agulhas Current has impinged
562 further landward, this has steadily removed all but the relict and cemented barrier forms and
563 produced the seafloor facies association discussed below. As Flemming (1981) recognised,

564 coast-parallel sediment transport along the shelf and shelf edge extends to locations where a
565 change in shelf orientation occurs and sediment is then lost off-shelf.

566 Rhodoliths began to develop when sea-level stabilised at its present level ca 7000 yrs BP,
567 suggesting that the Agulhas Current was by this stage located on the shelf. During the
568 subsequent 7000 years up to and including the present, thick accumulations of rhodoliths ~~have~~
569 accumulated in current-dominated conditions on the otherwise sediment-starved outer shelf.
570 Sediment denudation has limited burial of the relict shorelines.

571 Multiple, current-controlled sedimentological features have similarly developed, resulting in a
572 specific shelf morphology that comprises gravel-lined furrows and comet marks located in a
573 largely sediment-denuded seascape. Strong current sweeping has further exacerbated the
574 predominance of relict features associated with sea level fluctuations. Exposed wave
575 ravinement surfaces, exhumed and relict incised valley features on the shelf, large exposed
576 lagoonal systems, and intact barrier islands point to limited sediment retention on the shelf,
577 since the repeated impingement of the Agulhas Current ~~on the shelves~~ since ~ 7000 years ago.
578 These seem likely to remain as persistent features in the shelf morphology and represent the
579 nexus between relict geological and contemporary oceanographic processes.

580 Green et al. (2018) consider that subtropical climates particularly favour the preservation of
581 relict shorelines on the shelf, and their occurrence may thus be a unique feature of current swept
582 shelves of the sub tropics. This is strongly supported by the ~~examples outlined from the~~
583 ~~Western and SE Australian shelves.~~ distribution of examples outlined from the Western and
584 SE Australian shelves. However, in those cases, the modern coastlines are wide and sandy and
585 in most part reflect similar geomorphic elements as to the relict shorelines of the adjacent
586 shelves. Likewise, where the submerged shorelines were bedrock controlled, such as in the
587 case of the submerged cliffs offshore the Lacipede shelf (Brooke et al., 2017), these are

588 reflected in the cliffs of the contemporary coastlines. Where bedrock control is reduced or not
589 as extreme, the evolutionary pathway is not constrained, and modern shorelines may mirror the
590 relict features of the shelf. Our study thus provides a unique case study that highlights changing
591 coastal configuration and functioning due to progressive coastal squeeze, exacerbated by rising
592 sea levels, an increased impingement by bedrock framework, and high levels of current
593 sweeping.

594

595 6. Conclusions

596 This study marks the first in South Africa, to identify both the -60 and -100 m submerged
597 shorelines in outcrop, with a degree of unprecedented continuity between the two. The lack of
598 sediment cover and exceptional shoreline preservation makes this area an attractive one for
599 testing the hypothesis of Green et al. (2014); that these features are geomorphic signatures of
600 MWP-1A and 1B.

601 ~~The contemporary shelf morphology reflects the combined effects of relict wave and littoral~~
602 ~~processes and modern ocean current processes as they were mediated by fluctuating rates of~~
603 ~~sea-level rise during the last transgression.~~ Shorelines developed at -100 and -60 are markedly
604 different because of underlying geological influences, and reflect coastline adjustment to
605 changing geological and allocyclic sea-level controls over millennial scales. A lack of shoreline
606 preservation between each major shoreline reflects ravinement processes during slow relative
607 sea-level rise.

608 Rhodolith growth began on the shelf when sea-level stabilised near the present and the Agulhas
609 Current occupied its present position ~ 7000 yr BP. Up to 20 m thick rhodolith accumulations
610 have developed and are strongly associated with other features indicative of sediment

611 denudation and current whittling. Given the current-swept nature of the shelf, the surface
612 expression of palaeoshorelines is exceptional.

613 This study suggests that given the necessary antecedent conditions such as accommodation,
614 sediment supply and favourable diagenetic climate, prominent shorelines can form, and when
615 coupled to rapid rates of sea-level rise and strong current sweeping, can be preserved as
616 persistent morphological features. The coastal evolution can also be tracked using submerged
617 shorelines. These appear to also remain lasting features in the shelf morphology and
618 stratigraphy of current-swept subtropical shelves. Where prominent subsurface bedrock occurs
619 on current-swept shelves, coastal squeeze will be exacerbated due to the increasing disruption
620 of littoral cells, diminishing sediment supply to barrier-shoreline systems and increasing
621 sediment losses to the shelf sediment supply by current sweeping.

622

623

624 Acknowledgements

625 We gratefully acknowledge Eskom and Dr. Peter Ramsay for the donation of multibeam and
626 side scan sonar data sets shown in figures 4e and f, and 5c. Ephan Potgieter of Underwater
627 Surveys kindly rented an INS at cost to the University of KwaZulu-Natal. Andrew Matthew of
628 Underwater Surveys slept little, collected and processed the bulk of the data presented here.
629 This project was funded by the National Research Foundation/African Coelacanth Ecosystem
630 Programme (ACEP; Grant Number 97969), through the Imida Project. Funding was also
631 provided through the Bundesministerium für Bildung und Forschung (BMBF; projects RAiN2
632 and MA-RAIN; Grant No. 03G0862A and 03F0731A). The University of KwaZulu-Natal
633 provided additional funding for extra survey costs for which we are grateful. We appreciate the

634 thoughtful inputs to our paper by Scott Nichol, an anonymous reviewer, and the editor, Prof.
635 Edward Anthony.

636

637 References

638 Ashton, A.D., Murray, A.B., Littlewood, R., Lewis, D.A. and Hong, P., 2009. Fetch-limited
639 self-organization of elongate water bodies. *Geology*, 37, 187-190.

640 Benallack, K., Green, A.N., Humphries, M.S., Cooper, J.A.G., Finch, J.M., Dladla, N.N., 2016.
641 The stratigraphic evolution of a large back-barrier lagoon system with a non-migrating barrier.
642 *Marine Geology* 379, 64-77.

643 Betzler, C., Fürstenau, J., Lüdmann, T., Hübscher, C., Lindhorst, S., Paul, A., Reijmer, J.J.,
644 Droxler, A.W., 2013. Sea-level and ocean-current control on carbonate-platform growth,
645 Maldives, Indian Ocean. *Basin Research*, 25, 172-196.

646 Botha, G.A., Porat, N., Haldorsen, S., Duller, G.A.T., Taylor, R., Roberts, H.M., 2018. Beach
647 ridge sets reflect relative sea-level influence on the Late Holocene evolution of the St Lucia
648 Estuarine lake system, South Africa. *Geomorphology*, 318, 112-127.

649 Brandano, M., Ronca, S., 2014. Depositional processes of the mixed carbonate–siliciclastic
650 rhodolith beds of the Miocene Saint-Florent Basin, northern Corsica. *Facies* 60, 73-90.

651 Brooke, B.P., Olley, J.M., Pietsch, T., Playford, P.E., Haines, P.W., Murray-Wallace, C.V.,
652 Woodroffe, C.D., 2014. Chronology of Quaternary coastal aeolianite deposition and the
653 drowned shorelines of southwestern Western Australia – a reappraisal. *Quat. Sci. Rev.* 93, 106-
654 124.

655 Brooke, B.P., Nichol, S.L., Huang, Z., Beaman, R.J., 2017. Palaeoshorelines on the Australian
656 continental shelf: Morphology, sea-level relationship and applications to environmental
657 management and archaeology. *Continental Shelf Research*, 134, 26-38.

658 Cawthra, H.C., Neumann, F.H., Uken, R., Smith, A.M., Guastella, L., Yates, A.M., 2012.
659 Sedimentation on the narrow (8 km wide), oceanic current-influenced continental shelf off
660 Durban, KwaZulu-Natal, South Africa. *Mar. Geol.* 323, 107-122.

661 Cawthra, H.C., Compton, J.S., Fisher, E.C., Marean, C.W., 2016. Submerged shorelines and
662 landscape features offshore of Mossel Bay, South Africa. In: Harff, J., Bailey, G., Lüth, F.
663 (Eds.), *Geology and Archaeology: Submerged Landscapes of the Continental Shelf*, Special
664 Publication of the Geological Society of London, vol. 411, pp. 219-233.

665 Carter, R.W.G., 1980. Longshore variations in nearshore wave processes at Magilligan Point,
666 Northern Ireland. *Earth Surface Processes*, 5, 81-89.

667 Carter R.W.G., 2002. *Coastal environments: an introduction to the physical, ecological and*
668 *cultural systems of coastlines*. Elsevier, London, 617pp.

669 Cattaneo, A. and Steel, R.J., 2003. Transgressive deposits: a review of their variability. *Earth-*
670 *Science Reviews*, 62, 187-228.

671 Coffey, B.P. and Read, J.F., 2004. Mixed carbonate–siliciclastic sequence stratigraphy of a
672 Paleogene transition zone continental shelf, southeastern USA. *Sedimentary Geology*, 166, 21-
673 57.

674 Cooper, J.A.G., Pilkey, O.H., 2002. The barrier islands of southern Mozambique. *Journal of*
675 *Coastal Research*, Special Issue 36, 164-172.

676 Cooper, J.A.G., Green, A.N., 2016. Geomorphology and preservation potential of coastal and
677 submerged aeolianite: examples from KwaZulu-Natal, South Africa. *Geomorphology*, 271, 1-
678 12.

679 Cooper, J.A.G., Green, A.N., [Meireles, R., Klein, A.H.F. and Toldo, E. 2016. Sandy barrier](#)
680 [overstepping and preservation linked to rapid sea level rise and geological setting. *Marine*](#)
681 [Geology](#), 382, 80-91.

682 [Cooper, J.A.G., Green, A.N. and Loureiro, C. 2018a. Geological constraints on mesoscale](#)
683 [coastal barrier behaviour. *Global and Planetary Change*](#), 168, 15-34

684 [Cooper, J.A.G., Green, A.N., Compton, J.S., 2018](#)~~2018~~[b. Sea-level change in southern Africa](#)
685 since the Last Glacial Maximum. *Quaternary Science Reviews*, 201, 303-318.

686 [Cooper, J.A.G., Meireles, R., Green, A.N., Klein, A.H.F., Toldo, E. 2018c. Late Quaternary](#)
687 [stratigraphic evolution of the inner continental shelf in response to sea-level change, Santa](#)
688 [Catarina, Brazil. *Marine Geology*](#), 397, 1-14.

689 Davis, R.A., Fitzgerald, D.M., 2009. *Beaches and Coasts*. Blackwell Publishing, Malden. 419
690 pp.

691 De Lecea, A.M., Green, A.N., Strachan, K.L., Cooper, J.A.G. and Wiles, E.A., 2017. Stepped
692 Holocene sea-level rise and its influence on sedimentation in a large marine embayment:
693 Maputo Bay, Mozambique. *Estuarine, Coastal and Shelf Science*, 193, 25-36.

694 Dingle, R.V., Siesser, W.G., Newton, A.R., 1983. *Mesozoic and Tertiary Geology of Southern*
695 *Africa*. Balkema, Rotterdam p. 375.

696 Dixon, S., Green, A.N., Cooper, J.A.G., 2015. Storm swash deposition on an embayed rock
697 coastline: facies, formative mechanisms and preservation. *Journal of Sedimentary Research* 85,
698 1155-1165.

699 Dlamini, N.P., 2016. Marine geology of the East London continental shelf. Unpublished MSc
700 Thesis, University of KwaZulu-Natal, Westville, 102 pp.

701 Flemming, B.W., 1978. Underwater sand dunes along the southeast African continental shelf-
702 observations and implications. *Marine Geology* 26, 177–198.

703 Flemming, B.W., 1980. Sand transport and bedform patterns on the continental shelf between
704 Durban and Port Elizabeth (southeast African continental margin). *Sedimentary Geology*, 26,
705 179-205.

706 Flemming, B.W., 1981. Factors controlling shelf sediment dispersal along the southeast
707 African continental margin. *Mar. Geol.* 42, 259-277.

708 Flemming, B.W., Martin, A.K., 2018. The Tsitsikamma coastal shelf, Agulhas Bank, South
709 Africa: example of an isolated Holocene sediment trap. *Geo-Marine Letters*, 38, 107-117.

710 Gardner, J.V., Dartnell, P. Mayer, L.A, Hughes-Clarke, J.E., Calder, B.R., Duffy G., 2005.
711 Shelf-edge deltas and drowned barrier–island complexes on the northwest Florida outer
712 continental shelf. *Geomorphology* 64, 133-166.

713 Gardner, J.V., Calder, B.R., Clarke, J.H., Mayer, L.A., Elston, G., Rzhanov, Y., 2007. Drowned
714 shelf-edge deltas, barrier islands and related features along the outer continental shelf north of
715 the head of De Soto Canyon, NE Gulf of Mexico. *Geomorphology*, 89, 370-390.

716 Green, A.N., 2009. Palaeo-drainage, incised valley fills and transgressive systems tract
717 sedimentation of the northern KwaZulu-Natal continental shelf, South Africa, SW Indian
718 Ocean. *Marine Geology*, 263, 46-63.

719 Green, A.N., 2011. The late Cretaceous to Holocene sequence stratigraphy of a sheared passive
720 upper continental margin, northern KwaZulu-Natal, South Africa. *Marine Geology* 289, 17-28

721 Green, A.N., Garlick, G.L., 2011. A sequence stratigraphic framework for a narrow, current-
722 swept continental shelf: The Durban Bight, central KwaZulu-Natal, South Africa. *Journal of*
723 *African Earth Sciences*, 60, 303-314.

724 Green, A.N., Cooper, J.A.G., Leuci, R. and Thackeray, Z., 2013a. Formation and preservation
725 of an overstepped segmented lagoon complex on a high- energy continental shelf.
726 *Sedimentology*, 60, 1755-1768.

727 Green, A.N., Dladla, N.N., Garlick, G.L., 2013b. Spatial and temporal variations in incised
728 valley systems from the Durban continental shelf, KwaZulu-Natal, South Africa. *Marine*
729 *Geology*, 335, 148-161.

730 Green, A.N., Cooper, J.A.G., Salzmann, L., 2014. Geomorphic and stratigraphic signals of
731 postglacial meltwater pulses on continental shelves. *Geology*, 42, 151-154.

732 Green, A.N., Cooper, J.A.G., Salzmann, L., 2018. The role of shelf morphology and antecedent
733 setting in the preservation of palaeo-shoreline (beachrock and aeolianite) sequences: the SE
734 African shelf. *Geo-Marine Letters*, 38, 5-18.

735 Harrison, S., Smith, D.E., Glasser, N.F., 2019. Late Quaternary meltwater pulses and sea level
736 change. *Journal of Quaternary Science*, 34, 1-15.

737 Hill, P., De Deckker, P., von der Borch, C., Murray-Wallace, C.V., 2009. Ancestral Murray
738 River on the Lacepede Shelf, southern Australia: Late Quaternary migrations of a major river
739 outlet and strandline development. *Aust. J. Earth Sci.* 56, 135-157

740 Hogg, A.G., Hua, Q., Blackwell, P.G., Niu, M., Buck, C.E., Guilderson, T.P., Heaton, T.J.,
741 Palmer, J.G., Reimer, P.J., Reimer, R.W., Turney, C.S.M., Zimmerman, S.R.H., 2013.
742 SHCal13 southern hemisphere calibration, 0–50,000 years cal BP. *Radiocarbon* 55, 1889–
743 1903.

744 Howard, F.J.F., Radke, L., Picard, K., Nichol, S.L., Melrose, R., Lech, M.E., Hackney, R.I.,
745 Grosjean, E., Carroll, A.G., Bernardel, G. and Nicholson, C.J., 2016. A Marine Survey to
746 Investigate Seal Integrity Between Potential CO₂ Storage Reservoirs and Seafloor in the
747 Caswell Sub-basin, Browse Basin, Western Australia: GA0345/GA0346/TAN1411-Post-
748 survey Report. Geoscience Australia.

749 HRU (Hydraulics research Unit), 1968. Wave and wind conditions for the Natal and Western
750 Cape Coastal areas: CSIR Report MEG 665/1 (text) and 665/2 (figures). Pretoria, South Africa.

751 Jackson, D.W.T., Cooper, J.A.G., Green, A.N., 2014. A preliminary classification of coastal
752 sand dunes of KwaZulu-Natal. *Journal of Coastal Research* 70, 718-722.

753 Jarrett, B.D., Hine, A.C., Halley, R.B., Naar, D.F., Locker, S.D., Neumann, A.C., Twichell, D.,
754 Hu, C., Donahue, B.T., Jaap, W.C., Palandro, D., 2005. Strange bedfellows-a deep-water
755 hermatypic coral reef superimposed on a drowned barrier island; southern Pulley Ridge, SW
756 Florida platform margin. *Marine Geology*, 214, 295-307.

757 Kirkpatrick, L.H., Green, A.N., Pether, J., 2019. The seismic stratigraphy of the inner shelf of
758 southern Namibia: The development of an unusual nearshore shelf stratigraphy. *Marine*
759 *Geology*, 408, 18-35.

760 Le Roux, F.G., 1989. Lithostratigraphy of the Nahoon Formation (Algoa Group).
761 *Lithostratigraphic series. South African Committee for Stratigraphy* 9, 14.

762 Liu, J., Milne, G.A., Kopp, R.E., Clark, P.U., Shennan, I., 2016. Sea-level constraints on the
763 amplitude and source distribution of Meltwater Pulse 1A. *Nature Geoscience*, 9, 130.

764 Locker, S.D., Hine, A.C., Tedesco, L.P., Shinn, E.A., 1996. Magnitude and timing of episodic
765 sea-level rise during the last deglaciation. *Geology* 24, 827-830.

766 Mallory, J.K., 1974. Abnormal waves on the south-east coast of South Africa. *International*
767 *Reviews of Hydrology* 51, 99-129.

768 Martin, A.K., Flemming, B.W., 1987. Aeolianites of the South-African coastal zone and
769 continental shelf as sea-level indicators. *South African Journal of Science*, 83, 507-508.

770 Mellet, C.L., Plater, A.J., 2018. Drowned barriers as archives of coastal-response to sea-level
771 rise. In: Moore, L.J., Murray, B. (Eds.), *Barrier Dynamics and Response to Changing Climate*,
772 pp. 57–89.

773 Mulhern, J.S., Johnson, C.L., Martin, J.M., 2017. Is barrier island morphology a function of
774 tidal and wave regime? *Marine Geology*, 387, 74-84.

775 Nichol, S.L., Brooke, B.P., 2011. Shelf habitat distribution as a legacy of Late Quaternary
776 marine transgressions: a case study from a tropical carbonate province. *Continental Shelf*
777 *Research*, 31, 1845-1857.

778 Nichol, S., Howard, F., Kool, J., Stowar, M., Bouchet, P., Radke, L., Siwabessy, J.,
779 Przeslawski, R., Picard, K., Alvarez de Glasby, B., Colquhoun, J., 2013. Oceanic shoals
780 commonwealth marine reserve (Timor sea) biodiversity survey. GA0339/SOL5650, Post-
781 survey report. Record, 38. Geoscience Australia.

782 Novak, B., Pedersen, G.K., 2000. Sedimentology, seismic facies and stratigraphy of a Holocene
783 spit–platform complex interpreted from high-resolution shallow seismics, Lysegrund, southern
784 Kattegat, Denmark. *Marine Geology*, 162, 317-335.

785 Nutz, A., Schuster, M., Ghienne, J-F., Roquin, C., Hay, M.B., Rétif, F., Certain, R., Robin, N.,
786 Raynal, O., Cousineau, P.A., SIROCCO Team, Bouchette, F., 2015. Wind-driven bottom
787 currents and related sedimentary bodies in Lake Saint-Jean (Québec, Canada). *GSA Bulletin*
788 127, 1194–1208.

789 Pearce, A.F., 1978 The shelf circulation off the east coast of South Africa. National Research
790 Institute for Oceanology (South Africa), 1, 220 p.

791 Pilkey, O.H. 2003. A celebration of the world's barrier islands. Columbia University Press.

792 Pretorius, L., Green, A.N., Cooper, J.A.G, 2016. Submerged shoreline preservation and
793 ravinement during rapid postglacial sea-level rise and subsequent “slowstand”. *Bulletin*, 128,
794 1059-1069.

795 Pretorius, L., Green, A.N., Cooper, J.A.G., 2019. Outer- to inner-shelf response to stepped sea-
796 level rise: Insights from incised valleys and submerged shorelines. *Marine Geology* 416,
797 105979.

798 Ramsay, P.J., 1995. 9000 years of sea-level change along the Southern African coastline.
799 *Quaternary International* 31, 71–75.

800 Raynal, O., Bouchette, F., Certain, R., Séranne, M., Dezileau, L., Sabatier, P., Lofi, J., Hy,
801 A.B.X., Briqueu, L., Pezard, P., Tessier, B., 2009. Control of alongshore-oriented sand spits
802 on the dynamics of a wave-dominated coastal system (Holocene deposits, northern Gulf of
803 Lions, France). *Marine Geology*, 264, 242-257.

804 Roberts, D.L., Botha, G.A., Maud, R.R., Pether, J., 2006. Coastal Cenozoic deposits. In:
805 Johnson, M.R., Anhaeusser, C.R. and Thomas, R.J. (Eds), *The Geology of South Africa*.
806 Geological Society of South Africa, Johannesburg/Council for Geoscience, Pretoria, pp. 605-
807 628.

808 Rooseboom A., 1978. Sediment delivery of south African rivers (in Afrikaans). *Water South*
809 *Africa* 4, 14–17.

810 Rossouw., J., 1984, Review of existing wave data, wave climate and design waves for South
811 African and South West African (Namibian) coastal waters. Council for Scientific and
812 Industrial Research, Report T/SEA 8401, Stellenbosch, 66 p.

813 Rucińska-Zjadacz, M., Wróblewski, R., 2018. The complex geomorphology of a barrier spit
814 prograding into deep water, Hel Peninsula, Poland. *Geo-Marine Letters*, 38, 513-525.

815 Salzmann, L., Green, A.N., Cooper, J.A.G., 2013. Submerged barrier shoreline sequences on a
816 high energy, steep and narrow shelf. *Marine Geology*, 346, 366-374.

817 Scrutton, R.A., Du Plessis, A., 1973. Possible marginal fracture ridge south of South Africa.
818 *Nature, Physical Science* 242, 180-182.

819 Shideler, G.L., Swift, D.J., 1972. Seismic reconnaissance of post-Miocene deposits, middle
820 Atlantic continental shelf—Cape Henry, Virginia to Cape Hatteras, North Carolina. *Marine*
821 *Geology*, 12, 165-185.

822 Smith, R., 1976. Giant waves. *Journal of Fluid Mechanics* 11, 417-431.

823 Storms, J.E.A., Swift, D.J.P., 2003. Shallow-marine sequences as the building blocks of
824 stratigraphy: insights from numerical modelling. *Basin Research* 15, 287-303

825 Storms, J.E., Weltje, G.J., Terra, G.J., Cattaneo, A., Trincardi, F., 2008. Coastal dynamics
826 under conditions of rapid sea-level rise: Late Pleistocene to Early Holocene evolution of
827 barrier-lagoon systems on the northern Adriatic shelf (Italy). *Quaternary Science Reviews*, 27,
828 1107-1123.

829 Swift, D.J., 1974. Continental shelf sedimentation. In: Burke, C.A., Drake, C.L. (Eds) *The*
830 *geology of continental margins*. Springer, Berlin, Heidelberg, pp. 117-135.

831 Toscano, F., Sorgente, B., 2002. Rhodalgal-bryomol temperate carbonates from the Apulian
832 Shelf (Southeastern Italy), relict and modern deposits on a current dominated shelf. *Facies*, 46,
833 103-118.

834 Watkeys, M.K., 2006. Gondwana break-up: South African perspective. In: Johnson, M.R.,
835 Anhaeusser, C.R., Thomas, R.J., (eds.), *The Geology of South Africa*. Geological Society of
836 South Africa, Johannesburg/Council for Geoscience, Pretoria, pp. 531-539.

837 Wright, C.I. Miller, W.R. and Cooper, J.A.G., 2000. The Cenozoic evolution of coastal water
838 bodies in northern KwaZulu-Natal, South Africa. *Marine Geology* 167, 207-230.

839 Yokoyama, Y., Esat, T.M., Thompson, W.G., Thomas, A.L., Webster, J.M., Miyairi, Y.,
840 Sawada, C., Aze, T., Matsuzaki, H., Okuno, J.I., Fallon, S., 2018. Rapid glaciation and a two-
841 step sea level plunge into the Last Glacial Maximum. *Nature*, 559, 603.

842

843 Figure captions

844 Figure 1. Locality map of the study area detailing multibeam bathymetric coverage, seismic
845 tracklines (bold white lines) and locations of various seafloor samples or ROV observations
846 (red stars-numbered as portrayed in Figure 6). The -60 m and -100 m isobaths are shown as
847 dashed white lines, and the presence of a large rhodolith field is depicted by the blue polygon.
848 Satellite images from Google EarthTM.

849 Figure 2. Ultra-high-resolution coast-perpendicular seismic reflection profiles and
850 interpretations. Note the pinnacles of Unit 1, underlain by incised valleys into which Unit 3
851 progrades. The abutting and onlapping acoustically transparent Unit 4 overfills the incised
852 valleys and is overlain by the mounded accumulations of Unit 5, which interfinger with Unit
853 6. Inset shows line locations and sample intersections of a large rhodolith field corresponding
854 to Unit 5. Red lines denote Holocene wave ravinement.

855 Figure 3. a) Ultra-high-resolution coast-parallel seismic reflection profile and interpretation
856 detailing an incised valley that has overflowed unit 4 in the middle shelf. This occurs adjacent
857 to pinnacles of Unit 1. Red lines denote Holocene wave ravinement. b) Multibeam bathymetry
858 detailing the underfilled surface expression of the incised valley in a), together with the rugged
859 seafloor expression of the pinnacles of Unit 1. Unit 4 and 5 were sampled from this valley.

860 Figure 4. Multibeam bathymetry showing a) an underfilled incised valley extending from the
861 inner to middle shelf offshore the Kei River. b) A series of crenulate embayment-forming
862 ridges at -60 m, with underfilled incised valleys offshore the Qnube River. c) Semi-circular
863 seafloor depressions offshore the Kei River at ~ 80 m depth, bordered to either side by rugged
864 seafloor of Unit 1. Note the arcuate prograded ridges on the margins of each depression. d)
865 Weakly-developed semi-circular seafloor depression on the middle shelf at -80 m offshore

866 Qnube River. e) A coast-oblique ridge of Unit 1 at -100 m on the outer shelf offshore the Kei
867 River, backed by recurved ridges to landward and intersected by a seafloor depression with
868 subsidiary recurved ridges. f) A coast-oblique ridge of Unit 1 at -100 m on the outer shelf
869 offshore the Qnube River intersected by similar seafloor depression. Note the recurved
870 prograded ridges and single cusate ridge developed to landward of the main ridge feature.

871 Figure 5. Acoustic facies derived from multibeam backscatter and side-scan sonar offshore the
872 Kei River. High backscatter = black, low backscatter = white. The resulting seafloor qualitative
873 interpretations are shown. a) The inner to middle shelf with smooth toned high backscatter
874 interpreted as muddy deposits in the proximal incised valley depression. b) Rugged relief, high
875 backscatter seafloor of Unit 1 in outcrop, interspersed by low relief seafloor of the semi-circular
876 depressions. Occasional linear patches of high backscatter are interpreted as gravel-lined
877 streamers. c) Rugged high relief seafloor of Unit 1 in outcrop, surrounding by lower relief
878 rocky seafloor superimposed by gravel-lined streamers.

879 Figure 6. a) Remote Observation Video (ROV) imagery of stiff mud of Unit 4 cropping out at
880 the seafloor in the underfilled incised valley offshore the Kei River. b) Stiff mud of Unit 4
881 exposed in the troughs of migrating sandy ripples in the most inshore region of the underfilled
882 incised valley. c) Rhodoliths retrieved by seafloor dredging and grab sampling. d) Aeolianite
883 retrieved from pinnacles of Unit 1 using a dredge. f) Mixed unconsolidated shell hash and
884 aeolianite cobbles of surface S2. g) Shell hash and occasional aeolianite granules filling linear
885 seafloor depressions.

886 Figure 7. a) The contemporary coastal geomorphic systems of the sandy Southern Mozambique
887 coastal plain, with interpretative comparisons made to seafloor features of the Eastern Cape
888 shelf (b-e). b) Recurved spits, cusate spits and inlets of a -100 m barrier on the seafloor. c)
889 Lagoon with prograded margins in the backbarrier of the -100 m barrier. d) Fluvial entrances

890 to the lagoons, marked by underfilled incised valleys. e) Parabolic dunes and blowouts formed
891 in the -100 m seaward and landward barriers to the lagoon system. Satellite images from
892 Google Earth™.

893 Figure 8. a) Interpreted multibeam bathymetry of the inner to middle shelf offshore the Qnube
894 River, note how beachrocks and aeolianites comprise the embayment-forming ridges
895 superimposed onto Karoo Supergroup-age strata. b) Contemporary coastal setting immediately
896 adjacent to the above multibeam data. Here beachrock overlies sandstones of the Karoo
897 Supergroup, backed by a Holocene age barrier-dune system (Holidaying Green for scale). c)
898 Beachrocks overlying sandstones of the Karoo Supergroup, forming a headland to an
899 embayment. Note the sandy Holocene-age barrier in the background separating another rocky
900 headland to the north. Satellite images from Google Earth™.

901 Figure 9. A proposed evolutionary model for postglacial shoreline development of the Eastern
902 Cape coast (timing inferred from Pretorius et al., 2016; 2019, details discussed in text).

903

904

Dear Prof. Anthony

I am deeply grateful for the opportunity to revise this paper. I must apologise, firstly to the second reviewer and then to you. I re-read my response and am deeply embarrassed. I say this not because I the paper's fate is in jeopardy, but rather because my reply was childish, rude and above all disrespectful to the reviewer who took the time to read the paper and provide feedback. Likewise, it is deeply unprofessional to place this on your desk. I do not have any excuse, this is not excusable and I am sincerely sorry. My response was rash, and in many instances, I did not truly give the comments their due consideration. Again, inexcusable.

Though some comments are hard to follow through on, I have given these all my full attention and am certain that I have addressed most of the issues that I can, that were highlighted by reviewer 2. I hope I have gone some way to show the novelty of the paper, especially now I have considered the comments on sediment source and sediment fate. I think this pays more than lip service to these comments and has elevated the paper a lot. My responses are all outlined in red below, and the revisions made very clear in the tracked change document.

As an aside to reviewer 2, if we ever meet, I would like to apologise in person and buy you the beverage of your choice (as long as it's not 100-year-old Scotch, remember our currency is weak!)

Kind regards

Andy Green

It was interesting to see a paper focused on the current-swept, passive margin setting of southeastern South Africa. Although the primary conclusions of the paper, which are summarized in the evolutionary model of Figure 9, seem to be generally correct (although need improvement as noted below), the presentation of the work is not up to the standards of a journal like Marine Geology.

I hope that this offering will be different. I have tried to bolster the various areas outlined below with clearer measurements, comparisons, logic and clarity wherever possible.

There are a number of factors that have led to this decision. A primary reason was the manuscript text needs significant improvements. It took several readings to understand the work, its purpose and the details of the results. These elements should be clear with a single reading. These problems seem to arise because the authors know their study area so well that they have forgotten to include important details for the newcomer.

I think this is a good point, overfamiliarity with the paper, I hope this is better portrayed now.

Additionally, there are several leaps made in the logic (e.g., "Units" being defined or described) that are not explained thoroughly in the text.

These have been refined accordingly in the results, and made clear with links to figures, especially the outcrop of Unit 1 and its relating seafloor morphology.

More specifically,

Currently, the paper is written as a summary report, not a scientific paper. No hypotheses are proposed and tested, no research questions are asked.

From what I can gather, there are really few examples in the literature on current-swept shelves and their geomorphic facets. I tried to frame the paper so that we present on an area well-known for its current sweeping, and then try to relate what this may do to the stratigraphic evolution over time, and now, to how this may also produce clear and distinct changes to coastal morphology and dynamics.

We set up the knowledge gap as follows :

Line 52 to 58 ” To date, there are few studies that incorporate current sweeping into models of shelf stratigraphy and morphology (cf. Cawthra et al., 2012) and little is known of the processes that control the development and preservation of such features in the stratigraphic record. A key gap in knowledge is how coastal evolution is influenced by shelf-sweeping, coupled to sea-level rise, i.e. how does a coastline evolve as the shelf is drowned and becomes increasingly swept by oceanic currents?”

We then examine both the development and the preservation of shorelines exposed at the seafloor, a rarity in itself, to state:

Line 65-68“These features provide abundant opportunities to examine shoreline changes in both time and space and importantly provide insight into long-term shoreline behaviour over centennial to millennial scales (Cooper et al., 2018; Mellet and Plater, 2018). Such insights are often lacking from current swept areas where sediment retention is limited by erosion.”

We end our introduction with:

Line 86-93 “(i) sea-level changes during the last glacial cycle and (ii) contemporary ocean dynamics with an aim to (1) describe the shelf stratigraphy and surface morphology; (2) identify modern and relict seafloor features (3) interpret the origin and genesis of seafloor features; and (4) present a model for current-swept shelf evolution driven by relict and modern forcing agents. This is linked with other similar shelves around the globe”

We take this further in the discussion by then demonstrating how over time, sediment retention and barrier building is influenced by increasing bedrock control, coupled with vigorous shelf sweeping. We then compare and contrast to the Australian shelf and how the submerged shorelines evolve towards the modern day coastline.

- (i) The ‘aim’ of the paper as provided in L77-83 is to “investigate the morphological and stratigraphic evolution” of the site in question. However, for what purpose? What fundamental research question will be addressed?

I hope that this is answered in the above. A key gap in knowledge is how coastal evolution is influenced by shelf-sweeping, coupled to sea-level rise, i.e. how does a coastline evolve as the shelf is drowned and becomes increasingly swept by oceanic

currents?” We have also rewritten the abstract to reflect a leaner and more focused research question.

- (ii) What broader scientific understanding could be gained from this investigation? As noted in the Marine Geology Editorial Policies, “Although most papers are based on regional studies, they must demonstrate new findings of international significance.”

Likewise, I really hope this is answered in the above statement.

(ii) The Introduction (L39-83) makes the reader believe that ‘current sweeping’ will be the focus of the work, owing to statements such as, “To date, there are few studies that incorporate current sweeping into model of shelf stratigraphy and morphology...” (L45). However, the paper does not distinguish the effective roles of waves and currents in the sediment transport, the sediment mass balance, or the morphological and stratigraphic evolution of the site (L443-460). As such, no new understanding is provided about current-swept settings.

I hope we have done this adequately now. Its hard to bring address the waves, but the overall littoral transport role, the sediment budget (e.g. from where and to where) and how the coastline evolves is now included.

We include the following sections:

Regional setting:

Line 132-140 Sediment is supplied to the coast via three main river drainage systems, the Kei, Mzimvubu and Great Fish Rivers (Table 1). The Great Fish and Kei River catchments supply 11.48×10^6 m³ and 11.134×10^6 m³ of sediment to the coast respectively (Table 1) (Flemming, 1981). The Mzimvubu River debouches to the north and when combined with the Mbashe River, provides a further 10.458×10^6 m³ of fluvial sediment per year. The zone between the Great Fish and Mzimvubu Rivers was identified by Flemming (1981) as a discrete sediment compartment supplied by the above rivers and mostly dominated by current sweeping of the adjacent shelf. According to Rooseboom (1978), this entire coastal strip is characterised by annual sediment yields that range from 150 t/km² up to 800 150 t/km² per year.

Results:

We include a table showing comparison between measured aspects of the various features observed on the seafloor, vs what we consider to be there contemporary equivalents. We emphasize these dimensions later in the discussion as a means of examining changing sediment budget and changing impacts of bedrock on the littoral regime and sediment supply to barrier.

Discussion:

We have emphasized the aspects the reviewer pointed out as deficiencies.

We retooled our “identical” comparisons and give a much better picture of exactly how similar and different these features are between modern and relict, please see Table 2.

Line 324 to 328 “Several seafloor features bear striking similarity in plan form to contemporary shoreline features on the sandy and wide (40-100 km) Maputaland-Mozambique coastal plain (Fig. 7a), as well as coastal features that are not represented on the modern SE African coast. Below, following Gardner (2005, 2007), we compare the seafloor topographic features with contemporary coastal landforms as an aid to their interpretation.”

Line 330-339 “The large blocky aeolianite body that occurs at ~ 105 m at the shelf edge (Fig. 4e and f) is similar in shape to the modern barriers of the Maputaland coastline (Table 2), and to some modern barrier islands formed on many wave-dominated coastlines (see Mulhern et al., 2017). Regarding size, the aeolianite body is significantly narrower, with a lower elevation. The seafloor depressions and recurved ridges that attach to the depressions and landward sides of the main ridge line are very similar in shape and conform to the lower size limits of inlets and associated cusped and recurved spits of major barrier-inlet systems (Table 2), both in southern Mozambique and Maputaland (Fig. 7a and b) and from systems of the southern US Atlantic margin (Cooper and Pilkey, 2002; Pilkey, 2003; Davis and FitzGerald, 2009)”.

Line 347-353. The arcuate prograding ridges along the depression margins, together with the cusped wedges of Unit 1 aeolianite that separate each lagoon, mark prograding lagoon shorelines and down-drift spit termini of the wave-driven littoral cells of the system, respectively (cf. Ashton and Murray, 2010) (Fig. 7c). These are mostly within the lower size range of the modern systems found along the SE African coasts (Table 2).

Line 360-367. The parabolic ridges and depressions that form in the aeolianite of Unit 1 are very similar in shape and planform scale to those dunes of the contemporary coast (Table 2), though their elevations are markedly lower. Small, blowout-like features are also evident (Fig. 7e). We thus consider that a similar large dune system occurred at some point adjacent to and fringing the barrier islands and segmented waterbodies of the outer shelf. Though of considerably lower elevation, the width is within the ranges reported for the dune fields of southern Mozambique (Fig. 7a) and marks an approximate shoreline depth of 105 m (c.f. Ramsay, 1995).

We have also added new sections as below:

Lines 503-531:

“When comparing the overall scale and size of the relict barrier features on the seafloor to the modern coastlines of SE Africa, we note that although broadly similar in morphology, the sizes of the relict features are diminished when compared to their modern equivalents. The seafloor features are narrower (850 m vs 2 km), with significantly lower relief (15 m vs 170 m). This implies a significant amount of sediment (~ an order of magnitude) was lost as the shoreline translated over the shelf to where it is at present.

The current coastal configuration is mostly bedrock-controlled, with small rock-bound embayments that host isolated barrier-dune complexes. These are significantly smaller than the barriers preserved at -100 m and are more like the crenulate shorelines preserved at -60 m. The landward change in barrier size implies a shift from large and contiguous dune cordons forming during the early transgression, to isolated sandy barriers hosted amidst bedrock. This shift marks the increasing influence of bedrock control and coastal squeeze on shoreline adjustment during transgression. The

net result is transformation of the Eastern Cape coast from a straight, littoral drift-dominated feature to a strongly compartmentalised shoreline with limited accommodation and littoral sediment supply.

The sediment for the early dune building phase appears to have been initially sourced from a well-fed littoral system that adjoined a sandy, linear coastline. The net supply of sediment to the coastline from the Kei River alone is substantial, and when coupled to the other large quantities of sediment delivered by the adjoining fluvial systems (Table 2), the shelf and coastline should act as a major sediment depocentre. The current sweeping of the shelf however limits this and rather only exposes relict features at -100 m that are indicative of higher sediment supply and retention rates. During the transgression, the landward effect of coastal pinch by the bedrock framework is also coupled to the progressive diminution of the seaward edge of the large quantity of sediment that was hosted in the -100 m dune system. As the Agulhas Current has impinged further landward, this has steadily removed all but the relict and cemented barrier forms and produced the seafloor facies association discussed below. As Flemming (1981) recognised, coast-parallel sediment transport along the shelf and shelf edge will continue until a change in shelf orientation occurs where the sediment is then lost off-shelf.

(iii) In the end, it is concluded that, “the contemporary shelf morphology reflects the combined effects of relict wave and littoral processes and modern ocean current processes as they were mediated by fluctuating rates of sea-level rise during the last transgression.” (L31-33). This general conclusion statement could be written for just about any continental shelf setting, active or passive margin.

This is true, and reflects a weak conclusion. We remove this statement and add the following:

Line 578 to 583 “The coastal evolution can also be tracked using submerged shorelines. These appear to also remain lasting features in the shelf morphology and stratigraphy of current-swept subtropical shelves. Where prominent subsurface bedrock occurs on current-swept shelves, coastal squeeze will be exacerbated due to the increasing disruption of littoral cells, diminishing sediment supply to barrier-shoreline systems and increasing sediment losses to the shelf sediment supply by current sweeping”.

(iv) Important parts of the Methods are not reproducible as written. For example, it is stated that, “all (geophysical) data were then interpreted in HIS Kingdom Suite or Hypack SBP...” No information is given about how interpretations were defined and made, how ‘Units’ were defined and delineated, how existing literature was incorporated into the interpretations, etc. Please be descriptive here.

Remedied to include Line 157-161 ” Seismic units were defined by reflector packages, bound by distinct unconformity surfaces where the internal reflectors were either truncated, or where they downlapped, toplapped and onlapped the unconformities (see Mitchum et al., 1977). The units were described according to the internal reflector amplitudes, geometries and continuity and designated a unit name from Unit 1 to 4.”

(v) Several results are not shown or observable in the figures. For example, readers are told of “several coast-parallel elongate furrows” in Figures 3b and 4b (L225), but none are readily seen.

These are now very clearly pointed out with arrows and labels in 3c and 4b, with the aid of new, higher relief sunshaded images and more transparent colour overlays.

Also, “the proximal shelf areas are marked by the surface expression of the S1 paleo-valley that form topographic lows where Unit 4 crops out...” (L212). Huh? Proximal to what?

We rephrase this now to say “Inner shelf”.

“S1 Paleo-valleys” (1st time these are mentioned)? What are these?

I looked at this very carefully and then rephrased it to Line 237-239 “The inner shelf is marked by several underfilled valleys manifest as elongate seafloor depressions. These are correlated in seismic profile to the incisions associated with surface S1. These palaeo-valleys form topographic lows on the inner shelf where Unit 4 crops out”

These valleys are mentioned earlier.

(vi) The data availability (“made available upon request”) does not appear to be consistent with Marine Geology standards. What happens if the communicating author changes email, retires, or is no longer with us?

Unfortunately, we are not allowed to release data before publication by all authors working on these data, but this can be treated on a case by case basis if requests are made. Given the difficulty in collecting even one seismic line here, data is considered sacrosanct.

(vii) Figures are incomplete or not consistent. For example, some of the bathymetric panels in Fig. 4 have relief shading, others do not.

I amended all of these with greater relief exaggeration and more transparent colour overlays.

Different depth ranges are used in most panels of Fig. 4.

These are all now uniform.

The profile in Fig. 2a does not seem to be complete; it should be approximately the same length as b,c,d.

It is the correct length.

No horizontal scales are provided in Fig. 2 and 3.

Thank you for pointing that out, they were on a hidden layer!!! They are now visible.

No geographic information (lat/long) are provided in Fig. 4 and 5.

-These are amended now.

Insets would be very helpful for Fig. 3, 4, 5, just like the inset for Fig. 2.

Amended figure 5, but the other figures are shown in figure 1 and I would rather not clutter things too much.

Many of the key geographical sites are not included in Fig. 1, including these from the Introduction section: Wild Coast, Eastern Cape Province, KwaZulu-Natal, and the locations of previous studies highlighted. Readers will not know the locations of these places.

I have now included the locations for previous studies too, as well as the rivers etc in a new figure 2.

Figure 9 is not complete. The panels are not labeled with a,b,c, etc. Each panel needs an approximate date range. What is the red zone in the 6th panel, and why does it go inland of the water level? Also, include rhodoliths (Unit 5) and new sedimentation (Unit 6), as these are significant features of the study area? Label the final panel with Unit names to show how these were formed/modified?

Have amended as recommended, I am embarrassed I missed that originally.

(viii) The Results define “Units” without presenting the logic for why these are characterized as specific entities.

This is explained in the methods now based on standard seismic stratigraphic procedure.

Presentation of Unit 1 is most problematic, as it is found broadly and intermittently across the shelf (Fig. 2); Unit 4 is similarly intermittent.

These are now very clearly defined on the basis of reflector geometry and spatial distribution

The reader must assume that the authors define the Units with local knowledge, etc., because there is no logic provided for their definition. Please help the reader understand how/why these Units are defined.

We state as above: Seismic units were defined by reflector packages, bound by distinct unconformity surfaces where the internal reflectors were either truncated, or where they downlapped, toplapped and overlapped the unconformities (see Mitchum et al., 1977). The units were described according to the internal reflector amplitudes, geometries and continuity and designated a unit name from Unit 1 to 4. We used the standard practice for defining units.

On a related note, Figure 2 provides a confusing compilation of the Units. Some Units are shown with color, others with text labels.

This is so that the figure is not overwhelmed and only the most important units are coloured so as to draw attention to them. This is mentioned in the figure caption now.

Labels are split between the two panels for each profile. Because Units are an interpretation, shouldn't they solely be placed on the 2nd (ie interpreted) panel? Using color for each Unit would be nice.

These are split like this so as to avoid cramping of labels. I hope this is ok to leave.

(ix) Interpretation of the data is hindered by the general lack of overlapping data collection to ‘tie’ the geophysics data with the bathymetry data (Fig. 1). This makes connecting the dots between geophysical and bathymetric features difficult, if not impossible, for the reader. Although this cannot be remedied, please keep in mind that readers will be significantly challenged with comparison and interpretation of the two data sets.

This is a tough point to address. We simply have such limited budget to get complete coverage of anything, so this is as best I can do. The area itself is so wild, that surveying is a serious challenge given the small vessels (skiboats) we use to collect data. Perhaps in time we will receive a proper oceanographic vessel and that would help a lot. Until then, I wish I could better address this.

(x) The descriptions in the Results are incomplete. For example, the first description of the bathymetric data states, “Where Unit 1 crops out, the seafloor morphology comprises a variety of plan forms (Fig. 4)” (L194). Note that the authors have already concluded that the bathy data has Unit 1 outcrops without describing to the reader how this conclusion was made.

I am still really unsure of this comment, but I amended this to read:

Where Unit 1 crops out (see Figure 2 for example), the seafloor morphology comprises a variety of ridges that exhibit distinct plan form morphologies (Fig. 4).

Where it breaks the surface is where the various ridges etc. are.

Additionally, Fig. 4 does not include any labels with “Unit 1”. Thus, the reader is left confused with questions... Is the entire seafloor shown in Fig. 4 part of Unit 1?

Are the forms labeled in Fig. 4 all Unit 1? These kinds of confusing statements are repeated throughout the Results section.

Amended to show unit 1 outcrop with full labels and arrows.

(xi) Several fundamental research questions should be raised about the evolutionary model (Fig. 9). Why did the massive sand dune fields form during lowstand? What sediment source(s) are attributed to their formation? How is their formation related to the broader coastal morphodynamics? Where did the dune sands go during transgression? Where are they now? A simple order-of-magnitude sediment mass balance would be helpful for this understanding.

I have added much to this, as per the above replies in lines 503-531.

(xii) A number of landforms are described to be “identical”, and these comparisons are overstated. The reader is told that the seafloor characteristics are “identical in shape and scale to inlets and associated cusped and recurved spits of major barrier-inlet systems” (L306), “identical in shape and scale to those dunes of the contemporary coast” (L330), and “identical coastal forms..” (L369). First, measurements of landscape features must be provided to make comparisons, but no measurements were given. These measurements (size, volume, angles, slopes, relief, etc.) would greatly improve the paper. Second, “identical” has a fairly rigorous definition, and it is unlikely to have been met.

You are right, this was not correct. I added a table 2 showing these measurements and their comparisons.

The ‘identical’ coastal forms (L369) are used to infer similar conditions of “sediment supply, energy and sea level state.” Are there instances in coastal morphology where ‘identical’ coastal forms are developed from different conditions?

This is another toughie, I hope I covered it with caveats etc., though I think we provide a convincing argument.

(xii) There are numerous errors, typos, misspellings, although the authors should be able to clean these up.

Noted and cleaned up.

Palaeo-lagoons, inlets and barrier islands mark a -100 m palaeo-shoreline

Barrier complexes formed within embayments mark a -60 m palaeo-shoreline

Rhodolith accumulations, gravel streamers and bedrock exposure signify current-dominated conditions

Current sweeping began ~ 7000 BP

Contemporary morphology reflects relict influences like sea level stillstands, and meltwater pulses

Now strongly current-dominated exposing older shelf morphologies

1 Relict and contemporary influences on the postglacial geomorphology and evolution of a
2 current swept shelf: the Eastern Cape Coast, South Africa

3 Green, A.N.¹, Cooper, J.A.G.^{1,2}, Dlamini, N.P.¹, Dladla, N.N.¹, Parker, D.³, Kerwath, S.E.^{3,4}

4 ¹Geological Sciences, University of KwaZulu-Natal, Westville, Private Bag X54001, South
5 Africa

6 ²School of Geography & Environmental Sciences, University of Ulster, Cromore Road,
7 Coleraine, Northern Ireland, UK

8 ³Department of Agriculture, Forestry and Fisheries, Vlaeberg 8018, Cape Town, South Africa

9 ⁴Biological Sciences, University of Cape Town, Rondebosch 7700, South Africa

10

11 Abstract

12 Few stratigraphic models of continental shelves incorporate the process of geostrophic current-
13 sweeping, consequently its role in the stratigraphic record is often overlooked. We examine the
14 narrow, current-swept Eastern Cape shelf of South Africa using a combination of geophysical
15 techniques, seafloor sampling and video observations and interpret the role of current action
16 on the transgressive stratigraphy of this steep subtropical shelf. During the Last Glacial
17 Maximum, fluvial valleys incised the acoustic basement rocks. During the subsequent
18 transgression, two distinct shorelines were formed and preserved at -105 m and -60 m. Their
19 development and preservation is linked to (i) high sediment supply from adjacent fluvial
20 sources, (ii) early diagenesis and (iii) alternating sea-level stillstands and periods of rapid sea-
21 level rise during melt water pulses 1A and 1B, respectively. The deeper shoreline formed in
22 a sandy, wide coastal plain setting with limited bedrock influence, whereas the shallower

23 shoreline comprised alternating rock headlands and embayments like the contemporary coast.
24 Differences in antecedent topography and geology are responsible for the temporal variability
25 in shoreline type.

26

27 Between the two shoreline complexes, in the mid-shelf, the transgressive stratigraphy records
28 initial valley infill by progradation of coast-parallel sandy spits . These are capped by a stiff
29 lagoonal mud deposited as ongoing sea-level rise overspilled the valley interfluves, onlapping
30 the adjacent aeolianites. The uppermost stratigraphy comprises mounds of rhodoliths which
31 interfinger with a sandy inner to middle shelf highstand wedge.

32

33 After sea-level reached its present position ca 7.4 ka yr BP, the shelf became subject to
34 reworking by the high-energy, geostrophic Agulhas Current. This has had the following major
35 effects on the shelf stratigraphy: 1. the topographic relief of the cemented palaeo-shorelines
36 has been emphasised by removal of the post-transgressive cover; and 2. The shelf no longer
37 acts as a depocenter; instead, the seabed consists of rhodoliths, gravel streamers, bedrock or
38 gravel hash of the wave ravinement surface. Given the necessary antecedent conditions such
39 as accommodation, sediment supply and favourable diagenetic climate, prominent shorelines
40 can form and be preserved on the shelf. Strong current sweeping emphasises these
41 morphological features on subtropical shelves.

42

43 Key words: palaeo-shorelines, barrier islands, melt water pulse, current-dominated shelf,
44 Agulhas Current

45

46 1. Introduction

47 The southeastern shelf of South Africa, off the rocky and high-energy “Wild Coast” of the
48 Eastern Cape Province, is little known in comparison to the adjacent shelves of KwaZulu-Natal
49 (Green et al. 2018; Pretorius et al., 2019) to the north and the Southern Cape to the south
50 (Cawthra et al., 2016; Flemming and Martin, 2018). The combination of a narrow and shallow
51 shelf with the south-westward-flowing Agulhas Current, one of the fastest flowing boundary
52 currents on the globe, results in a shelf that is strongly modified by current activity. To date,
53 there are few studies that incorporate current sweeping into models of shelf stratigraphy and
54 morphology (cf. Cawthra et al., 2012) and little is known of the processes that control the
55 development and preservation of such features in the stratigraphic record. A key gap in
56 knowledge is how coastal evolution is influenced by shelf-sweeping, coupled to sea-level rise,
57 i.e. how does a coastline evolve as the shelf is drowned and becomes increasingly swept by
58 oceanic currents?

59 The morphology and Quaternary/Holocene evolution of the Eastern Cape shelf is poorly
60 studied, and little attention has been paid to shelf geomorphology and stratigraphy despite the
61 current-swept nature of the area having been long identified (Flemming, 1980). Martin and
62 Flemming (1987) notably documented a series of prominent outcropping palaeo-shorelines in
63 the area, which along adjacent shelves, have since been more closely examined and recognised
64 as exceptionally well-preserved and geomorphologically complex shoreline features (Green et
65 al., 2018). These features provide abundant opportunities to examine shoreline changes in both
66 time and space and importantly provide insight into long-term shoreline behaviour over
67 centennial to millennial scales (Cooper et al., 2018a; Mellet and Plater, 2018). Such insights
68 are often lacking from current-swept areas where sediment retention is limited by erosion.

69 Current-swept shelves typically comprise thin veneers of sandy/gravelly sediments (the
70 palimpsest sediments of Swift, 1974), which mantle a relatively flat and low-relief bedrock

71 outcrop (Shideler and Swift, 1972; Toscano and Sorgente, 2002; Coffey and Read, 2004; Green
72 and Garlick, 2011; Flemming and Martin, 2018). However, under certain circumstances, e.g.
73 sufficient antecedent accommodation and sediment supply, rapid sea-level rise and a climate
74 that fosters rapid carbonate diagenesis, large-scale submerged shorelines may be preserved and
75 exposed as spectacular seafloor features by the current action. Notable examples include the
76 Loop Current-exposed Pulley Ridge of SW Florida (e.g. Locker et al., 1996; Jarrett et al.,
77 2005), the Bass Cascade and Bass Strait-influenced Gippsland Shelf of SE Australia (Brooke
78 et al., 2017), the Leeuwin Current-influenced Carnarvon (Nichol and Brooke, 2011) and
79 Rottneest shelves of Western Australia (Brooke et al., 2017) and the Agulhas Current-dominated
80 KwaZulu-Natal shelf of SE Africa (Green et al., 2013a; Green et al., 2014). In these instances,
81 several drivers operate to define the shelf stratigraphy and geomorphology and may include
82 longer-term allocyclic processes such as rate of sea-level fluctuation (Locker et al., 1996;
83 Salzmann et al., 2013), shorter term or near instantaneous allocyclic processes such as
84 oceanographic forcing (Flemming, 1980; 1981), and long-term autocyclic conditioning of shelf
85 gradient and palaeo-topography (e.g. Green et al., 2018; Kirkpatrick et al., 2019).

86 The broad aim of this paper is to investigate the morphological and stratigraphic evolution of
87 a typical current-swept shelf, with focus on the Eastern Cape shelf of South Africa (Fig. 1). We
88 examine the fundamental drivers of shelf evolution including (i) sea-level changes during the
89 last glacial cycle and (ii) contemporary ocean dynamics. Thereby we aim to (1) describe the
90 shelf stratigraphy and surface morphology; (2) identify modern and relict seafloor features (3)
91 interpret the origin and genesis of seafloor features; and (4) present a model for current-swept
92 shelf evolution driven by relict and modern forcing agents. This is compared to other similar
93 shelves around the globe.

95 2. Regional setting

96 The southeast African continental margin is a sheared passive margin along which South
97 America separated from southern Africa during the initial opening of the South Atlantic
98 (Scrutton and Du Plessis, 1973). Regionally, it is exceptionally straight and narrow, but on a
99 local scale, there are extensive variations in morphology, especially in the distribution of
100 canyons and other irregularities on the continental slope (Flemming, 1981; Dingle et al., 1983).
101 The East London shelf break occurs between 110 m and 120 m depth (Fig. 1), with a shelf
102 width that varies between 19 km to 23 km, making it narrower and slightly shallower than the
103 world average of 75 km and 130 m, respectively (Flemming, 1981). The shelf gradient varies,
104 with a shallower gradient ca. 1.4° in the outer shelf, steepening up to 2.9° in the inner to middle
105 shelf (Dlamini, 2018). The adjoining coastline is fragmented by a series of zeta (half-moon)
106 bays of which their origin is related to the brittle deformation phases associated with the break-
107 up of Gondwana (Watkeys, 2006).

108 The continental margin of southeast Africa is a high-energy environment dominated by south-
109 westerly swells. The entire coast is subject to high-energy swells (H_s 2.1 m; T 11 s; HRU
110 1968), where the significant wave heights for 1, 0.1, and 0.01% exceedance are around 3.9 m,
111 5.0 m, and 6.0 m, respectively (Rossouw 1984). Swell heights commonly range between 1 and
112 2 m, with the largest recorded swell (12–13 June 1997) in the last 22 years having a significant
113 wave height (H_s) of 9.3 m (Dixon et al., 2015). Spring tidal range is between 1.8 and 2.0 m,
114 and neap tidal range is 0.6 to 0.8 m (HRU 1968). The mid-outer shelf is dominated by the
115 Agulhas Current, a fast poleward-flowing geostrophic current that can reach surface velocities
116 of >2.5 m/sec (Pearce et al., 1978). Along the shelf margin giant waves may be formed by the
117 propagation of high swells into the current (Mallory, 1974; Smith, 1976).

118 The study area comprises Gondwana-age sedimentary rocks of the Karoo Supergroup that are
119 overlapped by Cretaceous through to Quaternary age sedimentary rocks. Sandstones and shales
120 of the Karoo Supergroup crop out along the coastline and are overlain by limestones of the
121 Cretaceous Igoda Formation (Dingle et al., 1983). Calcareous sandstones of the Neogene
122 Nanaga Formation occur locally, together with shelly sands, soils and middens of the
123 Pleistocene-age Schelmhoek Formation (Roberts et al., 2006).

124 Along the coast and on the shelf, a variety of Pleistocene to Holocene age beachrocks and
125 aeolianites are found (Roberts et al., 2006). These aeolianites comprise the Nahoon Formation,
126 a former parabolic dune complex deposited at ~200 ka (Le Roux, 1989) and since bevelled into
127 a series of raised shore platforms that occur at 4 to 5 m above mean sea level and mean sea
128 level, respectively. The upper platform is mantled by a coquina of assumed Marine Isotope
129 Stage (MIS) 5e age (Roberts et al., 2006). Unconsolidated sediment mantles these in places
130 and occurs as a narrow wedge of shelf sediment that forms the contemporary shoreface
131 (Flemming, 1981).

132 Sediment is supplied to the coast via three main river drainage systems, the Kei, Mzimvubu
133 and Great Fish Rivers (Table 1). The Great Fish and Kei River catchments supply 11.48×10^6
134 m^3 and $11.134 \times 10^6 \text{ m}^3$ of sediment to the coast respectively (Table 1) (Flemming, 1981). The
135 Mzimvubu River debouches to the north and when combined with the Mbashe River, provides
136 a further $10.458 \times 10^6 \text{ m}^3$ of fluvial sediment per year. The zone between the Great Fish and
137 Mzimvubu Rivers was identified by Flemming (1981) as a discrete sediment compartment
138 supplied by the above rivers and mostly dominated by current sweeping of the adjacent shelf.
139 According to Rooseboom (1978), this entire coastal strip is characterised by annual sediment
140 yields that range from 150 t/km² up to 800 150 t/km² per year.

141 Martin and Flemming (1987) identified a series of palaeo-coastlines on the shelf at a depth of
142 60-70 m, and at the shelf edge (-100-105 m). These shorelines extend for over 600 km to the
143 north of the study area (Green et al., 2014) and are thought to have formed when sea levels
144 occupied depths of 100 m ~ 14 600 yr BP (Green et al., 2014) and ~ 60 m between 13 000 and
145 12 500 cal yr BP (Cooper et al., 2018b).

146

147 3. Methods

148 Ultra-high-resolution seismic data were collected aboard the RV Meteor cruise M123 in
149 February 2016. The data were acquired with an Atlas PARASOUND parametric echosounder
150 using a primary low frequency of 4 kHz. Navigation was provided by a differential GPS
151 (DGPS) capable of ~ 1 m accuracy in the X and Y domains.

152 The data were processed with Atlas PARASTORE, where the sea bottom was tracked, the data
153 match-filtered and swell corrected, time varied gains were applied, and the processed data
154 exported in SEG-Y format. All data were then interpreted in IHS Kingdom Suite or Hypack
155 SBP utility. Sound velocity estimates of 1 500 ms⁻¹ in water and 1 600 ms⁻¹ in sediment were
156 applied for all time-depth conversions.

157 Seismic units were defined by reflector packages, bound by distinct unconformity surfaces
158 where the internal reflectors were either truncated, or where they downlapped, toplapped and
159 onlapped the unconformities (see Mitchum et al., 1977). The units were described according
160 to the internal reflector amplitudes, geometries and continuity and designated a unit name from
161 Unit 1 to 4.

162 Multibeam data were collected using two different systems. Data offshore Morgan Bay, East
163 London shelf edge and the Mazeppa Bay area were collected using a Reson 7125 multibeam
164 echosounder coupled to a DGPS and Applanix POS-MV motion reference unit. The data were
165 collected and processed by Marine Geosolutions Pty Ltd., and resolve to a 1 x 1 m grid, with a
166 depth resolution of ~ 30 cm. Backscatter data were collected simultaneously with a Klein 3000
167 side scan sonar system with a scan range of 75 m using the 500 kHz channel. The data were
168 processed using the Klein SonarPro software, where the bottom was manually tracked, the data
169 were filtered, time varied gains applied, the channels colour balanced and the nadir zone
170 removed for seamless mosaicking. The final data set resolve to a mosaic pixel approximating
171 1 x 1 m.

172 The second set of multibeam data were collected aboard the RV Ellen Khuzwayo, voyage 159,
173 using a Reson 7101 ER multibeam system, coupled to a DGPS and a SBG Systems Ekinox-D
174 INS motion reference unit. All soundings were reduced to mean sea level during processing.
175 The final data were output as a 5 x 5 m resolution grid, with a depth resolution of ~ 50 cm. Co-
176 registered pseudo-side scan sonar data were collected as Snippets for backscatter mapping, the
177 final output of these on the same horizontal scale as the bathymetry data.

178 Seafloor materials were sampled using a benthic sled, a Shipek grab and a dredge, depending
179 on the substrate; rocky substrate necessitated a dredge as opposed to the less consolidated
180 materials such as mud and sandy material/gravels. Sampling was mainly done for biological
181 purposes and as such, not all the bathymetric and backscatter features observed were sampled.

182 An intact rhodolith was selected for ^{14}C dating using accelerator mass spectrometry (AMS).
183 Two samples, one from the centre of the rhodolith, the other from the exterior were analysed.
184 Calibrated ages were calculated using the Southern Hemisphere atmospheric curve SHCal13

185 (Hogg et al., 2013). A reservoir correction (DeltaR) of 161 +/- 30 was applied to coralline
186 material. Analyses were performed by Beta Analytic in their Florida radiocarbon facilities.

187

188 4. Results

189 4.1. Seismic stratigraphy

190 The seismic stratigraphy of the study area is shown in figure 3 (a-d). The acoustic basement
191 comprises a series of moderate to high amplitude, inclined parallel reflectors. These dip
192 seawards at ~ 2° and are truncated by an erosional surface, S1, marked by incised valleys up to
193 20 m deep in the middle shelf (Fig. 3c and d). These valleys abut a series of pinnacles and
194 ridges of acoustically opaque material (Unit 1) that span the middle shelf to shelf edge, the
195 bases of which occur at depths of 105 m. To seaward of the most landward ridge, a tangential
196 oblique-prograding wedge of material onlaps the ridges (Unit 2) (Fig. 3a; c and d) and
197 progrades into the valleys (Fig. 3d). In some areas, this wedge appears acoustically transparent
198 (Fig. 3b). A thin (<2 m) body of discontinuous, wavy to horizontal, low amplitude reflectors
199 (Unit 3) locally onlaps Unit 2 and interfingers with the overlying units (Fig. 3a and b).

200 Units 1, 2 and 3 are all in turn onlapped by a finely layered, low amplitude set of reflectors
201 (Unit 4) that spill out of the middle shelf incised valleys (Fig. 4) and terminate behind the main
202 ridges that comprise Unit 1 (Fig. 3b-d). This forms a meter-thick package that is exposed at the
203 seafloor (Fig. 3b-d; 3). In the middle shelf, this forms an acoustically transparent, landward
204 pinching wedge of material that onlaps the ridge on its landward side and overlies the incised
205 valleys in the more proximal middle shelf regions (Fig. 3d).

206 Overlying Unit 4 in the middle to outer shelf is an internally complex mound characterised by
207 chaotic and discontinuous, landward and seaward dipping reflectors (Unit 5) (Fig. 3). These
208 interfinger to landward with moderate amplitude, sigmoidal prograding reflectors of Unit 6.
209 Along coastal strike, Unit 6 forms a coast-parallel prograding body of sediment. These units
210 are separated from the underlying units by a high amplitude erosional reflector, S2, that
211 truncates the lower units (Units 1-4) (Fig. 3 and 4). S2 is exposed along the seafloor from the
212 middle shelf to outer shelf.

213

214 4.2. Seafloor morphology

215 The spatial attributes of the main seafloor morphological features are described in table 2.
216 Where Unit 1 crops out (see Figure 3 for example), the seafloor morphology comprises a
217 variety of ridges that exhibit distinct plan form morphologies (Fig. 5). The shallowest areas are
218 characterised by a series of parabolic-shaped ridges and depressions (Figs 3, 4 and 5a) that crop
219 out at their seaward edge at ~ 60 m depth. The ridge reliefs vary between 1 to 7 m, with the
220 parabolic forms spaced ~ 500 m apart (Table 2). Along strike and at similar depths, Unit 1 takes
221 the form of narrow (≤ 80 m) crenulate ridges 0.5 to 2 m in relief, superimposed on basement
222 rocks that crop out as strongly SE-NW orientated, blocky seafloor (Fig. 5b).

223 In the middle shelf areas, between 60 and 80 m depth, the parabolic ridges and depressions of
224 Unit 1 form cusped features that separate semi-circular seafloor depressions, > 2 km-wide and
225 up to 6 m in vertical relief (Fig. 5c and d; Table 2). The edges of these depressions are
226 characterised by multiple, prograding arcuate ridges, up to 4 m in relief and spaced ~ 200 m
227 apart (Fig. 5c).

228 The outer shelf is mostly characterised by subdued relief seafloor between 80 and 90 m deep.
229 A large, coast parallel ridge of Unit 1 occurs throughout the study area, the seaward fringe of
230 which occurs at -100 m (Fig. 5e and f; Table 2). In some areas, this ridge forms a feature with
231 up to 15 m relief, with multiple recurved ridges attached to its landward flank (Fig. 5e). The
232 recurved ridges are ~ 250 to 350 m-wide, with relief of up to 4 m. Depressions up to 2 m are
233 evident in the ridge (Fig. 5e and f), forming low-lying areas on the seafloor in which smaller,
234 prograded ridges of ~ 0.5 m relief and 40 m spacing occur (Fig. 5e). In other areas, cusped,
235 landward-narrowing ridges occur along the main ridge line, forming triangular seafloor
236 features 300 to 500 m long (Fig. 5f; Table 2).

237 The inner shelf is marked by several underfilled valleys manifest as elongate seafloor
238 depressions. These are correlated in seismic profile to the incisions associated with surface S1.
239 These palaeo-valleys form topographic lows on the inner shelf where Unit 4 crops out. These
240 areas are also characterised by the presence of mounds of Unit 5, where they form in some of
241 the depressions. The palaeo-valleys extend into the semi-circular seafloor depressions and into
242 the low-relief and deeper seafloor landward of the -100 m ridge (Fig. 5).

243

244 4.3. Seafloor backscatter and sediment characteristics

245 The more proximal middle shelf comprises even-toned high backscatter seafloor, confined to
246 the topographic low of the underfilled incised valley (Fig. 6a). This merges with moderate and
247 irregular backscatter where the valley widens towards the semi-circular depressions (Fig. 6a).
248 On either side of the valley, high relief, irregular and alternating moderate to high backscatter
249 seafloor marks the parabolic ridges and depressions of Unit 1, respectively. This seafloor

250 texture to the outer shelf. The lower relief areas of the semi-circular depressions are
251 characterised by moderate, even toned backscatter.

252 Several coast-parallel elongate furrows are evident on the middle to outer shelf (Fig. 4b and
253 4b). These form linear depressions up to 30 cm deep and are associated with linear patches of
254 high backscatter (Fig. 6). These overprint the low relief sea floor features and mark the surface
255 exposure of S2. Throughout the study area, isolated patches of rippled, alternating high to low
256 backscatter seafloor are apparent.

257 Seafloor inspections reveal the even-toned high backscatter areas to comprise weakly
258 laminated, stiff, muddy deposits (Fig. 6; 7a). In the proximal underfilled incised valley, this is
259 mantled by sandy material with mud cropping out in the depressions of current ripples (Fig. 1;
260 7b) The adjoining moderate and irregular backscatter seafloor is paved by a thin cover of
261 rhodoliths (Fig. 6; 7c). In contrast, on the middle to outer shelf, the mounds of Unit 5 comprise
262 stacked accumulations of rhodoliths (Fig. 3; 7c). AMS ^{14}C dates of the interior of the rhodoliths
263 ranged from 7406 - 7225 cal yr BP, with their surface material dating to present day (150 cal
264 yr BP to Post-Bomb).

265 The high relief, alternating high and moderate backscatter ridges and depressions correspond
266 with aeolianites cropping out along the seafloor (Fig. 7d). The lower relief seafloor marks
267 outcrop of subdued relief rocky material. The interleaving seafloor where S2 crops out is
268 marked by pebbles and cobbles of reworked aeolianite, together with finer bioclastic material
269 (Fig. 7e). The linear depressions of high backscatter are likewise lined by similar material (Fig.
270 7f). The isolated areas of rippled, alternating high to low backscatter represent isolated patches
271 of rippled bioclastic material interspersed with quartzose sand.

272

273 5. Discussion

274 5.1. Seismic stratigraphic interpretation

275 Aeolianites of Unit 1 at -105 m and shallower abut and overlie S1, the last glacial maximum
276 (LGM)-age subaerial unconformity that is commonly recognised across the SE African shelf
277 (Green et al., 2013a). We refer to these as the -100 m and -60 m shorelines based on these
278 previous works. Incised valleys formed in S1 relate to the LGM lowstand and constrain the age
279 of the aeolianite sequences to the most recent postglacial period (Pretorius et al., 2016; Cooper
280 et al., 2018b; Pretorius et al., 2019).

281 The tangential oblique-prograding wedge of Unit 2 that onlaps the aeolianites and enters the
282 incised valleys is architecturally similar to spit systems recognised from multiple large incised
283 valley systems, lagoons and lakes of the east coast of South Africa (Wright et al., 2000;
284 Benallack et al., 2016) and from shelf to lake environments elsewhere around the world (Novak
285 and Pederson, 2000; Raynal et al., 2009; Nutz et al., 2015). In keeping with this interpretation,
286 the chaotic and discontinuous reflectors of Unit 3 are similar to features identified elsewhere
287 as small-scale slump or mass wasting packages in waterbodies characterised by active spit
288 progradation (Wright et al., 2000; Rucińska-Zjadacz and Wróblewski, 2018).

289 Seafloor sampling and observations reveal Unit 4 to comprise stiff muddy materials. The
290 stratigraphic position as a capping and overspilling unit of the incised valleys points to
291 deposition in a lagoonal environment that overtopped the interfluves and ponded along the
292 shelf behind the barrier systems of Unit 1 (e.g. Green et al., 2013b; Benallack et al., 2016).

293 The intercalating upper units 5 and 6 represent the contemporary Holocene shelf sediment
294 prism which interfingers with the rhodolith mounds indicating that the two were deposited and
295 evolved contemporaneously. Studies of the Holocene sediment prism in SE Africa indicate a

296 mid-Holocene to recent age (Pretorius et al., 2016) which correlates with the age at which
297 Holocene sea level stabilized close to the present (Cooper et al., 2018b) and the rhodolith
298 mounds began to form (7406 - 7225 cal yr BP).

299 Surface S2 outcrop represents the seafloor exposure of the Holocene wave ravinement surface.
300 This surface truncates the spit/barrier/lagoon sequences and separates the post-transgressive
301 Holocene material from the underlying transgressive succession. The mixed bioclastic and
302 aeolianite pebbly material (Fig. 7f) is similar to the material forming from the contemporary
303 wave ravinement of beachrocks and aeolianites in SE Africa (Cooper and Green, 2016). The
304 exposure of this material in elongate furrows provides evidence for current furrowing that has
305 denuded the mid to outer shelf of sandy sediment and exposed the underlying wave ravinement
306 surface to geostrophic current reworking, forming gravel streamers and ribbons (Flemming,
307 1978).

308 The development of rhodolith fields since ca. 7.4 ka yr BP provides further evidence of strong
309 Agulhas Current action since sea levels stabilised close to the present. Prior to this, the current
310 flowed seaward of the shelf edge and did not support the growth of rhodoliths in this position.
311 Intact rhodoliths that interfinger with the Holocene sediment wedge indicate episodic wedge
312 progradation into current-agitated waters where the rhodoliths nucleated, as opposed to
313 punctuated re-deposition of the rhodoliths by gravity or storm driven processes (evidenced
314 elsewhere by broken rhodoliths, interspersed with pebbly gravels (Brandano and Ronca,
315 2014)). This conforms to Flemming's (1981) model of the regional shelf; an inner siliclastic
316 wave-dominated system and an outer Agulhas Current-dominated shelf. In microcosm, this
317 matches the shelf/carbonate platform-drowning model of Betzler et al. (2013), in which swift
318 sea-level rise produces partial shelf drowning and current sweeping of the shelf. This thus
319 places the timing of mid-shelf transgression to a minimum age of 7406 – 7225 cal yr BP and

320 implies a sudden increase in the rate of sea-level rise that post-dates a regional sea-level
321 slowstand recognised by De Lecea et al. (2017) ~ 8000 cal yr BP.

322

323 5.2. Seafloor morphology

324 Several seafloor features bear striking similarity in plan form to contemporary shoreline
325 features on the sandy and wide (40-100 km) Maputaland-Mozambique coastal plain (Fig. 8a),
326 as well as coastal features that are not represented on the modern SE African coast. Below,
327 following Gardner (2005, 2007), we compare the seafloor topographic features with
328 contemporary coastal landforms as an aid to their interpretation.

329 5.2.1. -100 m shoreline

330 The large blocky aeolianite body that occurs at ~ 105 m at the shelf edge (Fig. 5e and f) is
331 similar in shape to the modern barriers of the Maputaland coastline (Table 2), and to some
332 modern barrier islands formed on other wave-dominated coastlines (see Mulhern et al., 2017).
333 Regarding size, the aeolianite body is significantly narrower, with a lower elevation than the
334 contemporary Maputaland coastal barrier. The seafloor depressions and recurved ridges that
335 attach to the depressions and landward sides of the main ridge line are very similar in shape
336 and conform to the lower size limits of inlets and associated cusped and recurved spits of
337 contemporary major barrier-inlet systems (Table 2), both in southern Mozambique and
338 Maputaland (Fig. 8a and b) and from systems of the southern US Atlantic margin (Cooper and
339 Pilkey, 2002; Pilkey, 2003; Davis and FitzGerald, 2009). Breaks in the ridge, marked by
340 topographic lows are of a similar shape and dimension to tidal inlets, an interpretation that is
341 supported by their location adjacent to recurved features (Fig 4e). These are up to 200 m-wide
342 and ~ 5 m-deep, consistent with figures reported for inlets worldwide (Davis and FitzGerald,

343 2009). The adjacent low relief areas landward of the main inferred barrier positions are
344 interpreted as the palaeo-back barrier environments through which the incised valleys passed
345 during the LGM lowstand (Fig. 7e).

346 The large, semi-circular seafloor depressions (Fig. 8c) that occur slightly distal to the barrier
347 are interpreted as a series of drowned and segmented lagoons. The arcuate prograding ridges
348 along the depression margins, together with the cusped wedges of Unit 1 aeolianite that
349 separate each lagoon, mark prograding lagoon shorelines and down-drift spit termini of the
350 wave-driven littoral cells of the system, respectively (cf. Ashton and Murray, 2010) (Fig. 8c).
351 These are mostly within the lower size range of the modern systems found along the SE African
352 coast (Table 2). The depressions correlate directly to landwards with the outcropping,
353 overspilled muddy facies of Unit 4.

354 These segmented lagoons are fed by several underfilled incised valleys that clearly mark the
355 palaeo-fluvial pathways that entered these lagoons. These fluvial entrance points are similarly
356 recognised in the contemporary setting of coastal waterbodies in SE Africa (Table 2) (Fig. 8d).

357 A significant modern barrier system extends from Richards Bay, ~ 650 km north of the study
358 area into southern Mozambique (Jackson et al., 2014). This system is marked by a series of
359 northeastward oriented, climbing parabolic dunes that can reach up to 120 m high, covered
360 with multiple blowout features. The parabolic ridges and depressions that form in the aeolianite
361 of Unit 1 are very similar in shape and planform scale to those dunes of the contemporary coast
362 (Table 2), though their elevations are markedly lower. Small, blowout-like features are also
363 evident (Fig. 8e). We thus consider that a similar large dune system occurred at some point
364 adjacent to and fringing the barrier islands and segmented waterbodies of the outer shelf.
365 Though of considerably lower elevation, the width is within the ranges reported for the dune

366 fields of southern Mozambique (Fig. 8a) and marks an approximate shoreline depth of 105 m
367 (c.f. Ramsay, 1995).

368

369 5.2.2. -60 m shoreline

370 At -60 m, a former shoreline lineation is also evident. In planform this is manifest as a series
371 of palaeo-embayments, fringed by small aeolianite ridges of similar widths to the lower limits
372 of the primary dunes found along the embayed mixed-sand and rock coastlines of SE Africa
373 (Jackson et al., 2014). The palaeoheadlands are formed in bedrock of the Karoo Supergroup,
374 separated by crenulate ridges of Quaternary aeolianite (Fig. 9a) that also rest on Karoo bedrock.
375 This is a similar coastal morphology to that of the present day, where thin outcrops of aeolianite
376 and beachrock rest with marked unconformity on older sedimentary rocks in embayments
377 between prominent bedrock headlands (Fig. 9b and c).

378 Some of the embayments on the contemporary coast are also marked by modern
379 barriers/Holocene age dunes (Table 2) (Fig. 9c) and this configuration too appears to be
380 reflected on the seafloor (Fig. 9a). Their presence indicates that the coastal evolution at the
381 time of their formation was strongly influenced by the bedrock framework, as is the modern
382 coast (Watkeys, 2006). Similarly, their form and structure point to a shoreline occupation at a
383 depth of 60 m where planform equilibrium forms developed in coastal re-entrants (Carter,
384 1980).

385

386 5.3. Postglacial evolutionary model

387 The contemporary shelf morphology reflects a combination of influences of wave and ocean
388 current processes acting on the pre-existing basement geology. These have operated with
389 varying intensity and at different locations as sea level fluctuated during the last glacial cycle
390 and the deposits and geomorphic features of each successive interval have influenced
391 subsequent evolution. The sequence of events and associated dynamics are discussed below
392 in the context of an evolutionary model for the shelf.

393 Initially, the narrow and shallow shelf was dissected by several fluvial systems during lowstand
394 conditions culminating in the LGM (Fig. 10a). Two main river systems in the area formed
395 valleys of similar scale to those on the modern coast. At this time, wave action was focussed
396 off the modern shelf break, as was the palaeo Agulhas Current. During subsequent sea-level
397 rise wave processes reworked existing sediment and formed distinctive coastal landforms that
398 are preserved at several specific levels on the seafloor. These shoreline features indicate
399 marked differences in shoreline type at various stages of the transgression and their
400 preservation or non-preservation is linked to rates of sea-level change.

401 The generation of a substantial barrier system at ~ 100 m depth (Fig. 10b) can be linked to
402 patterns of stable sea level that allowed planform equilibrium for the palaeo-coastline to be
403 reached. It contains features similar to the contemporary highstand coastal systems of northern
404 KwaZulu-Natal and southern Mozambique (Green et al., 2013b), from which we infer similar
405 conditions of sediment supply, energy and sea level state at the time of formation (see below).
406 These strongly contrast with the sediment-poor, headland bound and rocky setting of the
407 contemporary coastline of the Eastern Cape.

408 Stable or slowly rising early Holocene sea levels promoted barrier growth, overspilling of
409 incised valleys and lateral extension of newly forming lagoons, with a general planform
410 equilibrium reached for the lagoon bodies (Fig. 10c). New accommodation was not generated

411 quickly, and the back barrier behind the -100 m barrier could be overfilled to compensate. The
412 prograded lagoon margins on contemporary lagoons in SE Africa (Wright et al., 2000; Botha
413 et al., 2018) are attributed to minor sea-level fall of +/- 2 m from a late Holocene highstand to
414 the present (Cooper et al., 2018b). The prograded lagoon margin features at -100 m may
415 indicate similar patterns of sea-level fall around the LGM (Fig. 10d). This is consistent with
416 new findings regarding the nature of the LGM sea level which dropped from -100 m stillstand
417 to a maximum of -118 m (Yokoyama et al., 2018) between 21 900 and 20 500 yr BP.

418 The behaviour of barrier shorelines in the context of rising sea level is discussed by Carter
419 (2002), who considered three main modes of barrier response, erosion, rollover, and
420 overstepping. A fourth possible mechanism is partial overstepping, whereby remnants of the
421 barrier are left after a portion of the barrier is eroded as the shoreface translates over the barrier
422 form. Overstepping has been considered the main mechanism responsible for the preservation
423 of the palaeo-shorelines from SE Africa, associated with particularly abrupt phases of sea-level
424 rise and in place drowning the coast (Green et al, 2014). We further this hypothesis by linking
425 the overstepping of the -100 m shoreline to melt water pulse 1A (Fig. 10e). This rapid rise in
426 sea level from ~ -100 m (~ 4 m per century, with a 95% probability of between 8.6 and 14.6 m
427 rise globally-Liu et al., 2016) would have been sufficient to overstep the fronting barrier system
428 (Fig. 10d). The lagoonal deposits landward of the -100 m barrier shoreline also bear witness to
429 the rapid creation of accommodation space in the back barrier and an associated reduction in
430 the efficacy of the bay-ravinement process as the barrier and back-barrier were submerged (cf.
431 Storms and Swift, 2003; Storms et al., 2008). The high gradient of the wave ravinement surface
432 (up to 4°), bounding the surface of the lagoonal/back barrier deposits (Fig. 3) indicates a
433 steepened shoreline trajectory during overstepping. Salzmann et al. (2013) consider causes for
434 steepened shoreline trajectories to include steep transgressed topographies, rapid rates of RSL
435 rise and high rates of sediment supply (based on the work of Cattaneo and Steel, 2003). On this

436 sediment-starved shelf, high sedimentation rates during infilling of the back barrier can be
437 discounted (e.g. Green, 2009, 2011; Salzmann et al., 2013).

438 We hypothesise that relatively slower rates of sea-level rise then followed, with widespread
439 shelf ravinement (denoted in red in Figure 10) removing all but the cores of the barrier system
440 surrounding the segmented lagoons and leaving the low-lying depressions of the lagoons intact
441 (Fig. 10f). This slower rate of sea-level rise is linked to the Younger Dryas period that preceded
442 a second meltwater pulse (MWP 1-B) (see Pretorius et al., 2016 for timing of other shoreline
443 development at the same depth). At this time and where available accommodation occurred,
444 shorelines developed within embayments (Fig. 10f). These were then overstepped by MWP 1-
445 B (11.5–11.1 ka BP-Harrison et al., 2019) (Fig. 10g), leaving a subsequent set of smaller
446 aeolian dune fields, some of which are preserved within embayments as relict shelf features.
447 Sea level has since risen to present day, where the contemporary coast is strongly bedrock-
448 dominated with multiple embayments bounded by rock headlands (Fig. 10h).

449

450 5.4. Local controls on stratigraphic and geomorphic evolution.

451 The model that has previously been developed to describe the occurrence and preservation of
452 submerged postglacial shorelines, is based on temporally varying rates of sea-level rise linked
453 to paired slowstands (gradual and slowly rising sea level) and subsequent melt water pulses
454 (see Green et al., 2014; 2018). The present study includes additional observations of submerged
455 shorelines at depths consistently seen at 60 and 100 m across the narrow portions of the SE
456 African shelf (c.f. Green et al., 2018; Pretorius et al., 2019). Across the entire shelf, large
457 volume, submerged planform equilibrium barriers and back barrier environments at -100 m
458 and -60 m, stretch for over 1000 kms alongshore from southern Mozambique (De Lecea et al.,

459 2017) to the present study area. This mirrors to some degree, submerged relict shorelines on
460 the southwestern African margin in Namibia (Kirkpatrick et al., 2019). Repeating forms such
461 as drowned segmented lagoons (e.g. Green et al., 2013a), parabolic dune fields (Green et al.,
462 2018) and underfilled incised valleys (Pretorius et al., 2019) are common, yet occupy areas of
463 significant variation in antecedent shelf setting, e.g. narrow vs wider shelves, numerous steep-
464 sided incised valleys vs flat planation surfaces.

465 Numerous similar examples of submerged shoreline features have been reported from other
466 current-swept sub-tropical shelves. On the Gippsland and Lacepede shelves of SE Australia, a
467 series of coast-parallel ridges are found at depths of ~65-75 m. These were interpreted as relict
468 strandplains and barriers (Brooke et al., 2017). Other examples from similar depth ranges are
469 found on the Recherche and Rottnest shelves of Western Australia, together with relict
470 carbonate-cemented dunes (Brooke et al., 2014). On the Carnarvon shelf, coral reefs and
471 carbonate-cemented dunes are similarly apparent at ~ 60 m (Nichol and Brooke, 2011). Around
472 depths of ~ 100 m, erosional knickpoints (the Lacepede shelf, Hill et al., 2009), coral reefs and
473 occasional associated lagoons (the NW Australian and Sahul shelves, Nichol et al., 2013;
474 Howard et al., 2016) have also been reported.

475 An episodic sea-level rise model is required to develop these submerged shoreline features at
476 consistent depths and ages on a global scale. However, antecedent shelf geometry is also an
477 important local consideration on shelf evolution. The steep gradient (up to 2.9°) of the SE
478 African shelf would, theoretically, lower the preservation potential of shoreline features due to
479 focused erosion along a steep profile for any given unit of time during transgression (Cattaneo
480 and Steel, 2003). Where exposed, the barriers clearly comprise cemented sandy aeolianites
481 and it is thus likely that it is the cementation, in conjunction with the driver of rapid rates of

482 sea-level rise (c.f. Green et al., 2018), that is responsible for the preservation of these relict
483 coastal forms on the shelf.

484 The overall weak preservation of shoreline forms, and a dominantly erosional or current swept
485 seafloor between the outer barrier and the - 60 m shoreline can be related to strong ravinement
486 processes, first by the aggressive wave climate during landward translation of the wave base,
487 and then by oceanic current denudation once sea level had passed over the palaeo-coastal
488 profile. On this steep shelf (1-3°), the implication is that the shoreline migrated *slowly* between
489 the landward edge of the -100 m shoreline and the seaward edge of the -60 m shoreline. During
490 this period, transgressive erosion was maximised and only small remnants or cores of once
491 much larger dune systems, were left.

492 This contrasts with the higher relief, outer shelf where the former coastal barriers are better
493 preserved. The lack of sediment cover in these areas is attributed to sediment being held in the
494 shoreface under sediment-deficit type conditions as the shoreline transgressed the palaeo-
495 coastal plain (Mellet and Plater, 2018). Any sediment that was potentially deposited as a
496 transgressive layer was subsequently removed by the current sweeping that formed the gravel
497 streamers observed on the modern shelf. Simultaneously, the barrier system would continue to
498 roll over to a point where smaller parabolic dunes and palaeo-embayments/shorelines could
499 form (at -60 m). This period marks a likely slowing of the rate of relative rise which is identified
500 on other shorelines at depths of 60 m from the Durban shelf (Pretorius et al., 2016; Cooper et
501 al., 2018b) and elsewhere e.g. SE and Western Australia (Brooke et al. 2017), SE Brazil
502 (Cooper et al., 2016, 2018c).

503 When comparing the overall scale and size of the relict barrier features on the seafloor to the
504 modern coastlines of SE Africa, we note that although broadly similar in morphology, the sizes
505 of the relict features are smaller than their modern equivalents. The seafloor features are

506 narrower (850 m vs 2 km), with significantly lower relief (15 m vs 170 m). This implies that a
507 significant amount of sediment (~ an order of magnitude in terms of width and height) was lost
508 as the shoreline translated over the shelf to where it is at present.

509 The current coastal configuration is mostly bedrock-controlled, with small rock-bound
510 embayments that host isolated barrier-dune complexes. These are significantly smaller than the
511 barriers preserved at -100 m and are more like the crenulate shorelines preserved at -60 m. The
512 landward change in barrier size implies a shift from large and contiguous dune cordons forming
513 during the early transgression, to isolated sandy barriers hosted amidst bedrock. This shift
514 marks the increasing influence of bedrock control and coastal squeeze on shoreline adjustment
515 during transgression. The net result is transformation of the Eastern Cape coast from a straight,
516 littoral drift-dominated feature to a strongly compartmentalised shoreline with limited
517 accommodation and littoral sediment supply.

518 The sediment for the early dune building phase appears to have been initially sourced from a
519 well-fed littoral system that adjoined a sandy, linear coastline. The net supply of sediment to
520 the coastline from the Kei River alone is likely to have been substantial, and when coupled to
521 the other large quantities of sediment delivered by the adjoining fluvial systems (Table 2), the
522 shelf and coastline should act as a major sediment depocentre. The Agulhas Current sweeping
523 of the shelf, however, limits the potential for sediment accumulation and rather exposes relict
524 features at -100 m that are indicative of former high sediment supply and retention rates. During
525 the transgression, the landward effect of coastal pinch by the bedrock framework is also
526 coupled to the progressive diminution of the seaward edge of the large quantity of sediment
527 that was formerly hosted in the -100 m dune system. As the Agulhas Current has impinged
528 further landward, this has steadily removed all but the relict and cemented barrier forms and
529 produced the seafloor facies association discussed below. As Flemming (1981) recognised,

530 coast-parallel sediment transport along the shelf and shelf edge extends to locations where a
531 change in shelf orientation occurs and sediment is then lost off-shelf.

532 Rhodoliths began to develop when sea-level stabilised at its present level ca 7000 yrs BP,
533 suggesting that the Agulhas Current was by this stage located on the shelf. During the
534 subsequent 7000 years up to and including the present, thick accumulations of rhodoliths
535 accumulated in current-dominated conditions on the otherwise sediment-starved outer shelf.
536 Sediment denudation has limited burial of the relict shorelines.

537 Multiple, current-controlled sedimentological features have similarly developed, resulting in a
538 specific shelf morphology that comprises gravel-lined furrows and comet marks located in a
539 largely sediment-denuded seascape. Strong current sweeping has further exacerbated the
540 predominance of relict features associated with sea level fluctuations. Exposed wave
541 ravinement surfaces, exhumed and relict incised valley features on the shelf, large exposed
542 lagoonal systems, and intact barrier islands point to limited sediment retention on the shelf,
543 since the repeated impingement of the Agulhas Current since ~ 7000 years ago. These seem
544 likely to remain as persistent features in the shelf morphology and represent the nexus between
545 relict geological and contemporary oceanographic processes.

546 Green et al. (2018) consider that subtropical climates particularly favour the preservation of
547 relict shorelines on the shelf, and their occurrence may thus be a unique feature of current swept
548 shelves of the sub tropics. This is strongly supported by the distribution of examples outlined
549 from the Western and SE Australian shelves. However, in those cases, the modern coastlines
550 are wide and sandy and in most part reflect similar geomorphic elements as to the relict
551 shorelines of the adjacent shelves. Likewise, where the submerged shorelines were bedrock
552 controlled, such as in the case of the submerged cliffs offshore the Lacipede shelf (Brooke et
553 al., 2017), these are reflected in the cliffs of the contemporary coastlines. Where bedrock

554 control is reduced or not as extreme, the evolutionary pathway is not constrained, and modern
555 shorelines may mirror the relict features of the shelf. Our study thus provides a unique case
556 study that highlights changing coastal configuration and functioning due to progressive coastal
557 squeeze, exacerbated by rising sea levels, an increased impingement by bedrock framework,
558 and high levels of current sweeping.

559

560 6. Conclusions

561 This study marks the first in South Africa, to identify both the -60 and -100 m submerged
562 shorelines in outcrop, with a degree of unprecedented continuity between the two. The lack of
563 sediment cover and exceptional shoreline preservation makes this area an attractive one for
564 testing the hypothesis of Green et al. (2014); that these features are geomorphic signatures of
565 MWP-1A and 1B.

566 Shorelines developed at -100 and -60 are markedly different because of underlying geological
567 influences, and reflect coastline adjustment to changing geological and allocyclic sea-level
568 controls over millennial scales. A lack of shoreline preservation between each major shoreline
569 reflects ravinement processes during slow relative sea-level rise.

570 Rhodolith growth began on the shelf when sea-level stabilised near the present and the Agulhas
571 Current occupied its present position ~ 7000 yr BP. Up to 20 m thick rhodolith accumulations
572 have developed and are strongly associated with other features indicative of sediment
573 denudation and current whittling. Given the current-swept nature of the shelf, the surface
574 expression of palaeoshorelines is exceptional.

575 This study suggests that given the necessary antecedent conditions such as accommodation,
576 sediment supply and favourable diagenetic climate, prominent shorelines can form, and when
577 coupled to rapid rates of sea-level rise and strong current sweeping, can be preserved as
578 persistent morphological features. The coastal evolution can also be tracked using submerged
579 shorelines. These appear to also remain lasting features in the shelf morphology and
580 stratigraphy of current-swept subtropical shelves. Where prominent subsurface bedrock occurs
581 on current-swept shelves, coastal squeeze will be exacerbated due to the increasing disruption
582 of littoral cells, diminishing sediment supply to barrier-shoreline systems and increasing
583 sediment losses to the shelf sediment supply by current sweeping.

584

585

586 Acknowledgements

587 We gratefully acknowledge Eskom and Dr. Peter Ramsay for the donation of multibeam and
588 side scan sonar data sets shown in figures 4e and f, and 5c. Ephan Potgieter of Underwater
589 Surveys kindly rented an INS at cost to the University of KwaZulu-Natal. Andrew Matthew of
590 Underwater Surveys slept little, collected and processed the bulk of the data presented here.
591 This project was funded by the National Research Foundation/African Coelacanth Ecosystem
592 Programme (ACEP; Grant Number 97969), through the Imida Project. Funding was also
593 provided through the Bundesministerium für Bildung und Forschung (BMBF; projects RAIN2
594 and MA-RAIN; Grant No. 03G0862A and 03F0731A). The University of KwaZulu-Natal
595 provided additional funding for extra survey costs for which we are grateful. We appreciate the
596 thoughtful inputs to our paper by Scott Nichol, an anonymous reviewer, and the editor, Prof.
597 Edward Anthony.

599 References

- 600 Ashton, A.D., Murray, A.B., Littlewood, R., Lewis, D.A. and Hong, P., 2009. Fetch-limited
601 self-organization of elongate water bodies. *Geology*, 37, 187-190.
- 602 Benallack, K., Green, A.N., Humphries, M.S., Cooper, J.A.G., Finch, J.M., Dladla, N.N., 2016.
603 The stratigraphic evolution of a large back-barrier lagoon system with a non-migrating barrier.
604 *Marine Geology* 379, 64-77.
- 605 Betzler, C., Fürstenau, J., Lüdmann, T., Hübscher, C., Lindhorst, S., Paul, A., Reijmer, J.J.,
606 Droxler, A.W., 2013. Sea-level and ocean-current control on carbonate-platform growth,
607 Maldives, Indian Ocean. *Basin Research*, 25, 172-196.
- 608 Botha, G.A., Porat, N., Haldorsen, S., Duller, G.A.T., Taylor, R., Roberts, H.M., 2018. Beach
609 ridge sets reflect relative sea-level influence on the Late Holocene evolution of the St Lucia
610 Estuarine lake system, South Africa. *Geomorphology*, 318, 112-127.
- 611 Brandano, M., Ronca, S., 2014. Depositional processes of the mixed carbonate–siliciclastic
612 rhodolith beds of the Miocene Saint-Florent Basin, northern Corsica. *Facies* 60, 73-90.
- 613 Brooke, B.P., Olley, J.M., Pietsch, T., Playford, P.E., Haines, P.W., Murray-Wallace, C.V.,
614 Woodroffe, C.D., 2014. Chronology of Quaternary coastal aeolianite deposition and the
615 drowned shorelines of southwestern Western Australia – a reappraisal. *Quat. Sci. Rev.* 93, 106-
616 124.

617 Brooke, B.P., Nichol, S.L., Huang, Z., Beaman, R.J., 2017. Palaeoshorelines on the Australian
618 continental shelf: Morphology, sea-level relationship and applications to environmental
619 management and archaeology. *Continental Shelf Research*, 134, 26-38.

620 Cawthra, H.C., Neumann, F.H., Uken, R., Smith, A.M., Guastella, L., Yates, A.M., 2012.
621 Sedimentation on the narrow (8 km wide), oceanic current-influenced continental shelf off
622 Durban, KwaZulu-Natal, South Africa. *Mar. Geol.* 323, 107-122.

623 Cawthra, H.C., Compton, J.S., Fisher, E.C., Marean, C.W., 2016. Submerged shorelines and
624 landscape features offshore of Mossel Bay, South Africa. In: Harff, J., Bailey, G., Lüth, F.
625 (Eds.), *Geology and Archaeology: Submerged Landscapes of the Continental Shelf*, Special
626 Publication of the Geological Society of London, vol. 411, pp. 219-233.

627 Carter, R.W.G., 1980. Longshore variations in nearshore wave processes at Magilligan Point,
628 Northern Ireland. *Earth Surface Processes*, 5, 81-89.

629 Carter R.W.G., 2002. *Coastal environments: an introduction to the physical, ecological and*
630 *cultural systems of coastlines*. Elsevier, London, 617pp.

631 Cattaneo, A. and Steel, R.J., 2003. Transgressive deposits: a review of their variability. *Earth-*
632 *Science Reviews*, 62, 187-228.

633 Coffey, B.P. and Read, J.F., 2004. Mixed carbonate–siliciclastic sequence stratigraphy of a
634 Paleogene transition zone continental shelf, southeastern USA. *Sedimentary Geology*, 166, 21-
635 57.

636 Cooper, J.A.G., 2001. Geomorphological variability among microtidal estuaries from the wave
637 dominated South African coast. *Geomorphology* 40, 99-122.

638 Cooper, J.A.G., Pilkey, O.H., 2002. The barrier islands of southern Mozambique. *Journal of*
639 *Coastal Research*, Special Issue 36, 164-172.

640 Cooper, J.A.G., Green, A.N., 2016. Geomorphology and preservation potential of coastal and
641 submerged aeolianite: examples from KwaZulu-Natal, South Africa. *Geomorphology*, 271, 1-
642 12.

643 Cooper, J.A.G., Green, A.N., Wright, C.I., 2011. Evolution of an incised valley coastal plain
644 estuary under low sediment supply: a give-up estuary. *Sedimentology*, 59, 899-916.

645 Cooper, J.A.G., Green, A.N., Meireles, R., Klein, A.H.F. and Toldo, E. 2016. Sandy barrier
646 overstepping and preservation linked to rapid sea level rise and geological setting. *Marine*
647 *Geology*, 382, 80-91.

648 Cooper, J.A.G., Green, A.N. and Loureiro, C. 2018a. Geological constraints on mesoscale
649 coastal barrier behaviour. *Global and Planetary Change*, 168, 15-34

650 Cooper, J.A.G., Green, A.N., Compton, J.S., 2018b. Sea-level change in southern Africa since
651 the Last Glacial Maximum. *Quaternary Science Reviews*, 201, 303-318.

652 Cooper, J.A.G., Meireles, R., Green, A.N., Klein, A.H.F., Toldo, E. 2018c. Late Quaternary
653 stratigraphic evolution of the inner continental shelf in response to sea-level change, Santa
654 Catarina, Brazil. *Marine Geology*, 397, 1-14.

655 Davis, R.A., Fitzgerald, D.M., 2009. *Beaches and Coasts*. Blackwell Publishing, Malden. 419
656 pp.

657 De Lecea, A.M., Green, A.N., Strachan, K.L., Cooper, J.A.G. and Wiles, E.A., 2017. Stepped
658 Holocene sea-level rise and its influence on sedimentation in a large marine embayment:
659 Maputo Bay, Mozambique. *Estuarine, Coastal and Shelf Science*, 193, 25-36.

660 Dingle, R.V., Siesser, W.G., Newton, A.R., 1983. *Mesozoic and Tertiary Geology of Southern*
661 *Africa*. Balkema, Rotterdam p. 375.

662 Dixon, S., Green, A.N., Cooper, J.A.G., 2015. Storm swash deposition on an embayed rock
663 coastline: facies, formative mechanisms and preservation. *Journal of Sedimentary Research* 85,
664 1155-1165.

665 Dlamini, N.P., 2016. Marine geology of the East London continental shelf. Unpublished MSc
666 Thesis, University of KwaZulu-Natal, Westville, 102 pp.

667 Dorschel, B., Jensen, L., Arndt, J.E., Brummer, G.J., de Haas, H., Fielies, A., Franke, D., Jokat,
668 W., Krockner, R., Kroon, D., Pätzold, J., Schneider R.R., Spieß, V., Stollhofen, H., Uenzelmann-
669 Neben, G., Watkeys, M.K., Wiles, E.A., 2018. The Southwest Indian Ocean Bathymetric
670 Compilation (swIOBC). *Geochemistry, Geophysics, Geosystems*, 19, 968-976.

671 Flemming, B.W., 1978. Underwater sand dunes along the southeast African continental shelf-
672 observations and implications. *Marine Geology* 26, 177–198.

673 Flemming, B.W., 1980. Sand transport and bedform patterns on the continental shelf between
674 Durban and Port Elizabeth (southeast African continental margin). *Sedimentary Geology*, 26,
675 179-205.

676 Flemming, B.W., 1981. Factors controlling shelf sediment dispersal along the southeast
677 African continental margin. *Mar. Geol.* 42, 259-277.

678 Flemming, B.W., Martin, A.K., 2018. The Tsitsikamma coastal shelf, Agulhas Bank, South
679 Africa: example of an isolated Holocene sediment trap. *Geo-Marine Letters*, 38, 107-117.

680 Gardner, J.V., Dartnell, P. Mayer, L.A, Hughes-Clarke, J.E., Calder, B.R., Duffy G., 2005.
681 Shelf-edge deltas and drowned barrier–island complexes on the northwest Florida outer
682 continental shelf. *Geomorphology* 64, 133-166.

683 Gardner, J.V., Calder, B.R., Clarke, J.H., Mayer, L.A., Elston, G., Rzhanov, Y., 2007. Drowned
684 shelf-edge deltas, barrier islands and related features along the outer continental shelf north of
685 the head of De Soto Canyon, NE Gulf of Mexico. *Geomorphology*, 89, 370-390.

686 Green, A.N., 2009. Palaeo-drainage, incised valley fills and transgressive systems tract
687 sedimentation of the northern KwaZulu-Natal continental shelf, South Africa, SW Indian
688 Ocean. *Marine Geology*, 263, 46-63.

689 Green, A.N., 2011. The late Cretaceous to Holocene sequence stratigraphy of a sheared passive
690 upper continental margin, northern KwaZulu-Natal, South Africa. *Marine Geology* 289, 17-28

691 Green, A.N, Garlick, G.L., 2011. A sequence stratigraphic framework for a narrow, current-
692 swept continental shelf: The Durban Bight, central KwaZulu-Natal, South Africa. *Journal of*
693 *African Earth Sciences*, 60, 303-314.

694 Green, A.N., Cooper, J.A.G., Leuci, R. and Thackeray, Z., 2013a. Formation and preservation
695 of an overstepped segmented lagoon complex on a high- energy continental shelf.
696 *Sedimentology*, 60, 1755-1768.

697 Green, A.N., Dladla, N.N., Garlick, G.L., 2013b. Spatial and temporal variations in incised
698 valley systems from the Durban continental shelf, KwaZulu-Natal, South Africa. *Marine*
699 *Geology*, 335, 148-161.

700 Green, A.N., Cooper, J.A.G., Salzmann, L., 2014. Geomorphic and stratigraphic signals of
701 postglacial meltwater pulses on continental shelves. *Geology*, 42, 151-154.

702 Green, A.N., Cooper, J.A.G., Salzmann, L., 2018. The role of shelf morphology and antecedent
703 setting in the preservation of palaeo-shoreline (beachrock and aeolianite) sequences: the SE
704 African shelf. *Geo-Marine Letters*, 38, 5-18.

705 Harrison, S., Smith, D.E., Glasser, N.F., 2019. Late Quaternary meltwater pulses and sea level
706 change. *Journal of Quaternary Science*, 34, 1-15.

707 Hill, P., De Deckker, P., von der Borch, C., Murray-Wallace, C.V., 2009. Ancestral Murray
708 River on the Lacepede Shelf, southern Australia: Late Quaternary migrations of a major river
709 outlet and strandline development. *Aust. J. Earth Sci.* 56, 135-157

710 Hogg, A.G., Hua, Q., Blackwell, P.G., Niu, M., Buck, C.E., Guilderson, T.P., Heaton, T.J.,
711 Palmer, J.G., Reimer, P.J., Reimer, R.W., Turney, C.S.M., Zimmerman, S.R.H., 2013.
712 SHCal13 southern hemisphere calibration, 0–50,000 years cal BP. *Radiocarbon* 55, 1889–
713 1903.

714 Howard, F.J.F., Radke, L., Picard, K., Nichol, S.L., Melrose, R., Lech, M.E., Hackney, R.I.,
715 Grosjean, E., Carroll, A.G., Bernardel, G. and Nicholson, C.J., 2016. A Marine Survey to
716 Investigate Seal Integrity Between Potential CO2 Storage Reservoirs and Seafloor in the
717 Caswell Sub-basin, Browse Basin, Western Australia: GA0345/GA0346/TAN1411-Post-
718 survey Report. Geoscience Australia.

719 HRU (Hydraulics research Unit), 1968. Wave and wind conditions for the Natal and Western
720 Cape Coastal areas: CSIR Report MEG 665/1 (text) and 665/2 (figures). Pretoria, South Africa.

721 Jackson, D.W.T., Cooper, J.A.G., Green, A.N., 2014. A preliminary classification of coastal
722 sand dunes of KwaZulu-Natal. *Journal of Coastal Research* 70, 718-722.

723 Jarrett, B.D., Hine, A.C., Halley, R.B., Naar, D.F., Locker, S.D., Neumann, A.C., Twichell, D.,
724 Hu, C., Donahue, B.T., Jaap, W.C., Palandro, D., 2005. Strange bedfellows-a deep-water
725 hermatypic coral reef superimposed on a drowned barrier island; southern Pulley Ridge, SW
726 Florida platform margin. *Marine Geology*, 214, 295-307.

727 Kirkpatrick, L.H., Green, A.N., Pether, J., 2019. The seismic stratigraphy of the inner shelf of
728 southern Namibia: The development of an unusual nearshore shelf stratigraphy. *Marine*
729 *Geology*, 408, 18-35.

730 Le Roux, F.G., 1989. Lithostratigraphy of the Nahoon Formation (Algoa Group).
731 Lithostratigraphic series. *South African Committee for Stratigraphy* 9, 14.

732 Liu, J., Milne, G.A., Kopp, R.E., Clark, P.U., Shennan, I., 2016. Sea-level constraints on the
733 amplitude and source distribution of Meltwater Pulse 1A. *Nature Geoscience*, 9, 130.

734 Locker, S.D., Hine, A.C., Tedesco, L.P., Shinn, E.A., 1996. Magnitude and timing of episodic
735 sea-level rise during the last deglaciation. *Geology* 24, 827-830.

736 Mallory, J.K., 1974. Abnormal waves on the south-east coast of South Africa. *International*
737 *Reviews of Hydrology* 51, 99-129.

738 Martin, A.K., Flemming, B.W., 1987. Aeolianites of the South-African coastal zone and
739 continental shelf as sea-level indicators. *South African Journal of Science*, 83, 507-508.

740 Mellet, C.L., Plater, A.J., 2018. Drowned barriers as archives of coastal-response to sea-level
741 rise. In: Moore, L.J., Murray, B. (Eds.), *Barrier Dynamics and Response to Changing Climate*,
742 pp. 57–89.

743 Mulhern, J.S., Johnson, C.L., Martin, J.M., 2017. Is barrier island morphology a function of
744 tidal and wave regime? *Marine Geology*, 387, 74-84.

745 Nichol, S.L., Brooke, B.P., 2011. Shelf habitat distribution as a legacy of Late Quaternary
746 marine transgressions: a case study from a tropical carbonate province. *Continental Shelf*
747 *Research*, 31, 1845-1857.

748 Nichol, S., Howard, F., Kool, J., Stowar, M., Bouchet, P., Radke, L., Siwabessy, J.,
749 Przeslawski, R., Picard, K., Alvarez de Glasby, B., Colquhoun, J., 2013. Oceanic shoals
750 commonwealth marine reserve (Timor sea) biodiversity survey. GA0339/SOL5650, Post-
751 survey report. Record, 38. Geoscience Australia.

752 Novak, B., Pedersen, G.K., 2000. Sedimentology, seismic facies and stratigraphy of a Holocene
753 spit–platform complex interpreted from high-resolution shallow seismics, Lysegrund, southern
754 Kattegat, Denmark. *Marine Geology*, 162, 317-335.

755 Nutz, A., Schuster, M., Ghienne, J-F., Roquin, C., Hay, M.B., Rétif, F., Certain, R., Robin, N.,
756 Raynal, O., Cousineau, P.A., SIROCCO Team, Bouchette, F., 2015. Wind-driven bottom
757 currents and related sedimentary bodies in Lake Saint-Jean (Québec, Canada). *GSA Bulletin*
758 127, 1194–1208.

759 Pearce, A.F., 1978 The shelf circulation off the east coast of South Africa. National Research
760 Institute for Oceanology (South Africa), 1, 220 p.

761 Pilkey, O.H. 2003. A celebration of the world's barrier islands. Columbia University Press.

762 Pretorius, L., Green, A.N., Cooper, J.A.G, 2016. Submerged shoreline preservation and
763 ravinement during rapid postglacial sea-level rise and subsequent “slowstand”. *Bulletin*, 128,
764 1059-1069.

765 Pretorius, L., Green, A.N., Cooper, J.A.G., 2019. Outer- to inner-shelf response to stepped sea-
766 level rise: Insights from incised valleys and submerged shorelines. *Marine Geology* 416,
767 105979.

768 Ramsay, P.J., 1995. 9000 years of sea-level change along the Southern African coastline.
769 *Quaternary International* 31, 71–75.

770 Raynal, O., Bouchette, F., Certain, R., Séranne, M., Dezileau, L., Sabatier, P., Lofi, J., Hy,
771 A.B.X., Briquieu, L., Pezard, P., Tessier, B., 2009. Control of alongshore-oriented sand spits
772 on the dynamics of a wave-dominated coastal system (Holocene deposits, northern Gulf of
773 Lions, France). *Marine Geology*, 264, 242-257.

774 Roberts, D.L., Botha, G.A., Maud, R.R., Pether, J., 2006. Coastal Cenozoic deposits. In:
775 Johnson, M.R., Anhaeusser, C.R. and Thomas, R.J. (Eds), *The Geology of South Africa*.
776 Geological Society of South Africa, Johannesburg/Council for Geoscience, Pretoria, pp. 605-
777 628.

778 Rooseboom A., 1978. Sediment delivery of south African rivers (in Afrikaans). *Water South*
779 *Africa* 4, 14–17.

780 Rossouw., J., 1984, Review of existing wave data, wave climate and design waves for South
781 African and South West African (Namibian) coastal waters. Council for Scientific and
782 Industrial Research, Report T/SEA 8401, Stellenbosch, 66 p.

783 Rucińska-Zjadacz, M., Wróblewski, R., 2018. The complex geomorphology of a barrier spit
784 prograding into deep water, Hel Peninsula, Poland. *Geo-Marine Letters*, 38, 513-525.

785 Salzmann, L., Green, A.N., Cooper, J.A.G., 2013. Submerged barrier shoreline sequences on a
786 high energy, steep and narrow shelf. *Marine Geology*, 346, 366-374.

787 Scrutton, R.A., Du Plessis, A., 1973. Possible marginal fracture ridge south of South Africa.
788 *Nature, Physical Science* 242, 180-182.

789 Shideler, G.L., Swift, D.J., 1972. Seismic reconnaissance of post-Miocene deposits, middle
790 Atlantic continental shelf—Cape Henry, Virginia to Cape Hatteras, North Carolina. *Marine*
791 *Geology*, 12, 165-185.

792 Smith, R., 1976. Giant waves. *Journal of Fluid Mechanics* 11, 417-431.

793 Storms, J.E.A., Swift, D.J.P., 2003. Shallow-marine sequences as the building blocks of
794 stratigraphy: insights from numerical modelling. *Basin Research* 15, 287-303

795 Storms, J.E., Weltje, G.J., Terra, G.J., Cattaneo, A., Trincardi, F., 2008. Coastal dynamics
796 under conditions of rapid sea-level rise: Late Pleistocene to Early Holocene evolution of
797 barrier-lagoon systems on the northern Adriatic shelf (Italy). *Quaternary Science Reviews*, 27,
798 1107-1123.

799 Swift, D.J., 1974. Continental shelf sedimentation. In: Burke, C.A., Drake, C.L. (Eds) *The*
800 *geology of continental margins*. Springer, Berlin, Heidelberg, pp. 117-135.

801 Toscano, F., Sorgente, B., 2002. Rhodalgae-bryomorph temperate carbonates from the Apulian
802 Shelf (Southeastern Italy), relict and modern deposits on a current dominated shelf. *Facies*, 46,
803 103-118.

804 Watkeys, M.K., 2006. Gondwana break-up: South African perspective. In: Johnson, M.R.,
805 Anhaeusser, C.R., Thomas, R.J., (eds.), The Geology of South Africa. Geological Society of
806 South Africa, Johannesburg/Council for Geoscience, Pretoria, pp. 531-539.

807 Wright, C.I. Miller, W.R. and Cooper, J.A.G., 2000. The Cenozoic evolution of coastal water
808 bodies in northern KwaZulu-Natal, South Africa. *Marine Geology* 167, 207-230.

809 Yokoyama, Y., Esat, T.M., Thompson, W.G., Thomas, A.L., Webster, J.M., Miyairi, Y.,
810 Sawada, C., Aze, T., Matsuzaki, H., Okuno, J.I., Fallon, S., 2018. Rapid glaciation and a two-
811 step sea level plunge into the Last Glacial Maximum. *Nature*, 559, 603.

812

813 Figure captions

814 Figure 1. Locality map of the study area detailing multibeam bathymetric coverage, seismic
815 tracklines (bold white lines) and locations of various seafloor samples or ROV observations
816 (red stars-numbered as portrayed in Figure 7). The -60 m and -100 m isobaths are shown as
817 dashed white lines, and the presence of a large rhodolith field is depicted by the blue polygon.
818 The Agulhas Current is portrayed as an idealised cartoon representing shelf sweeping of the
819 area. Satellite images from Google Earth™.

820 Figure 2. Fluvial sediment supply to the shelf. The main rivers and sub-catchments that
821 contribute to the study area, as outlined in table 1, are depicted (Q-T). The sediment yield in
822 tonnes per km² per year are provided based on Rooseboom's (1978) data, modified after
823 Flemming and Martin (2018). Red line denotes the 100 m isobath which approximates the shelf
824 break for the study area. Note the shelf sediment compartment identified by Flemming (1981).
825 The terrain model is based on the data of Dorschel et al. (2018).

826 Figure 3. Ultra-high-resolution coast-perpendicular seismic reflection profiles and
827 interpretations. Note the pinnacles of Unit 1, underlain by incised valleys into which Unit 3
828 progrades. The abutting and onlapping acoustically transparent Unit 4 overfills the incised
829 valleys and is overlain by the mounded accumulations of Unit 5, which interfinger with Unit
830 6. Inset shows line locations and sample intersections of a large rhodolith field corresponding
831 to Unit 5. Red lines denote Holocene wave ravinement. Only the most important units are
832 depicted in colour overlay.

833 Figure 4. a) Ultra-high-resolution coast-parallel seismic reflection profile and interpretation
834 detailing an incised valley that has overflowed unit 4 in the middle shelf. This occurs adjacent
835 to pinnacles of Unit 1. Red lines denote Holocene wave ravinement. b) Multibeam bathymetry
836 detailing the underfilled surface expression of the incised valley in a), together with the rugged
837 seafloor expression of the pinnacles of Unit 1. Unit 4 and 5 were sampled from this valley.
838 Only the most important units are depicted in colour overlay.

839 Figure 5. Multibeam bathymetry showing a) an underfilled incised valley extending from the
840 inner to middle shelf offshore the Kei River. b) A series of crenulate embayment-forming
841 ridges at -60 m, with underfilled incised valleys offshore the Qnube River. c) Semi-circular
842 seafloor depressions offshore the Kei River at ~ 80 m depth, bordered to either side by rugged
843 seafloor of Unit 1. Note the arcuate prograded ridges on the margins of each depression. d)
844 Weakly-developed semi-circular seafloor depression on the middle shelf at -80 m offshore
845 Qnube River. e) A coast-oblique ridge of Unit 1 at -100 m on the outer shelf offshore the Kei
846 River, backed by recurved ridges to landward and intersected by a seafloor depression with
847 subsidiary recurved ridges. f) A coast-oblique ridge of Unit 1 at -100 m on the outer shelf
848 offshore the Qnube River intersected by similar seafloor depression. Note the recurved
849 prograded ridges and single cusped ridge developed to landward of the main ridge feature.

850 Figure 6. Acoustic facies derived from multibeam backscatter and side-scan sonar offshore the
851 Kei River. High backscatter = black, low backscatter = white. The resulting seafloor qualitative
852 interpretations are shown. a) The inner to middle shelf with smooth toned high backscatter
853 interpreted as muddy deposits in the proximal incised valley depression. b) Rugged relief, high
854 backscatter seafloor of Unit 1 in outcrop, interspersed by low relief seafloor of the semi-circular
855 depressions. Occasional linear patches of high backscatter are interpreted as gravel-lined
856 streamers. c) Rugged high relief seafloor of Unit 1 in outcrop, surrounding by lower relief
857 rocky seafloor superimposed by gravel-lined streamers.

858 Figure 7. a) Remote Observation Video (ROV) imagery of stiff mud of Unit 4 cropping out at
859 the seafloor in the underfilled incised valley offshore the Kei River. b) Stiff mud of Unit 4
860 exposed in the troughs of migrating sandy ripples in the most inshore region of the underfilled
861 incised valley. c) Rhodoliths retrieved by seafloor dredging and grab sampling. d) Aeolianite
862 retrieved from pinnacles of Unit 1 using a dredge. f) Mixed unconsolidated shell hash and
863 aeolianite cobbles of surface S2. g) Shell hash and occasional aeolianite granules filling linear
864 seafloor depressions.

865 Figure 8. a) The contemporary coastal geomorphic systems of the sandy Southern Mozambique
866 coastal plain, with interpretative comparisons made to seafloor features of the Eastern Cape
867 shelf (b-e). b) Recurved spits, cusped spits and inlets of a -100 m barrier on the seafloor. c)
868 Lagoon with prograded margins in the backbarrier of the -100 m barrier. d) Fluvial entrances
869 to the lagoons, marked by underfilled incised valleys. e) Parabolic dunes and blowouts formed
870 in the -100 m seaward and landward barriers to the lagoon system. Satellite images from
871 Google Earth™.

872 Figure 9. a) Interpreted multibeam bathymetry of the inner to middle shelf offshore the Qnube
873 River, note how beachrocks and aeolianites comprise the embayment-forming ridges

874 superimposed onto Karoo Supergroup-age strata. b) Contemporary coastal setting immediately
875 adjacent to the above multibeam data. Here beachrock overlies sandstones of the Karoo
876 Supergroup, backed by a Holocene age barrier-dune system (Holidaying Green for scale). c)
877 Beachrocks overlying sandstones of the Karoo Supergroup, forming a headland to an
878 embayment. Note the sandy Holocene-age barrier in the background separating another rocky
879 headland to the north. Satellite images from Google Earth™.

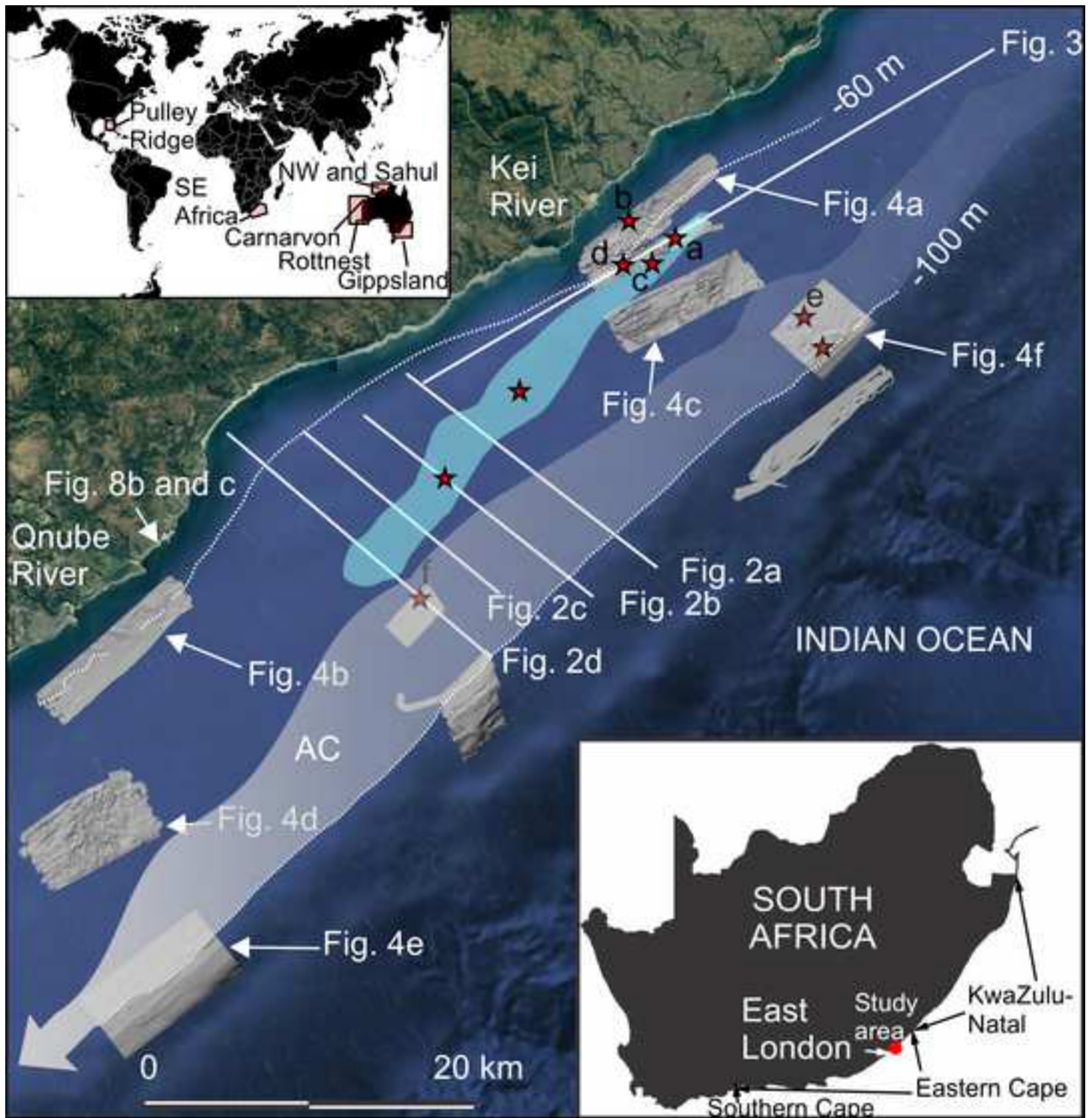
880 Figure 10. A proposed evolutionary model for postglacial shoreline development of the Eastern
881 Cape coast (timing inferred from Pretorius et al., 2016; 2019, details discussed in text).

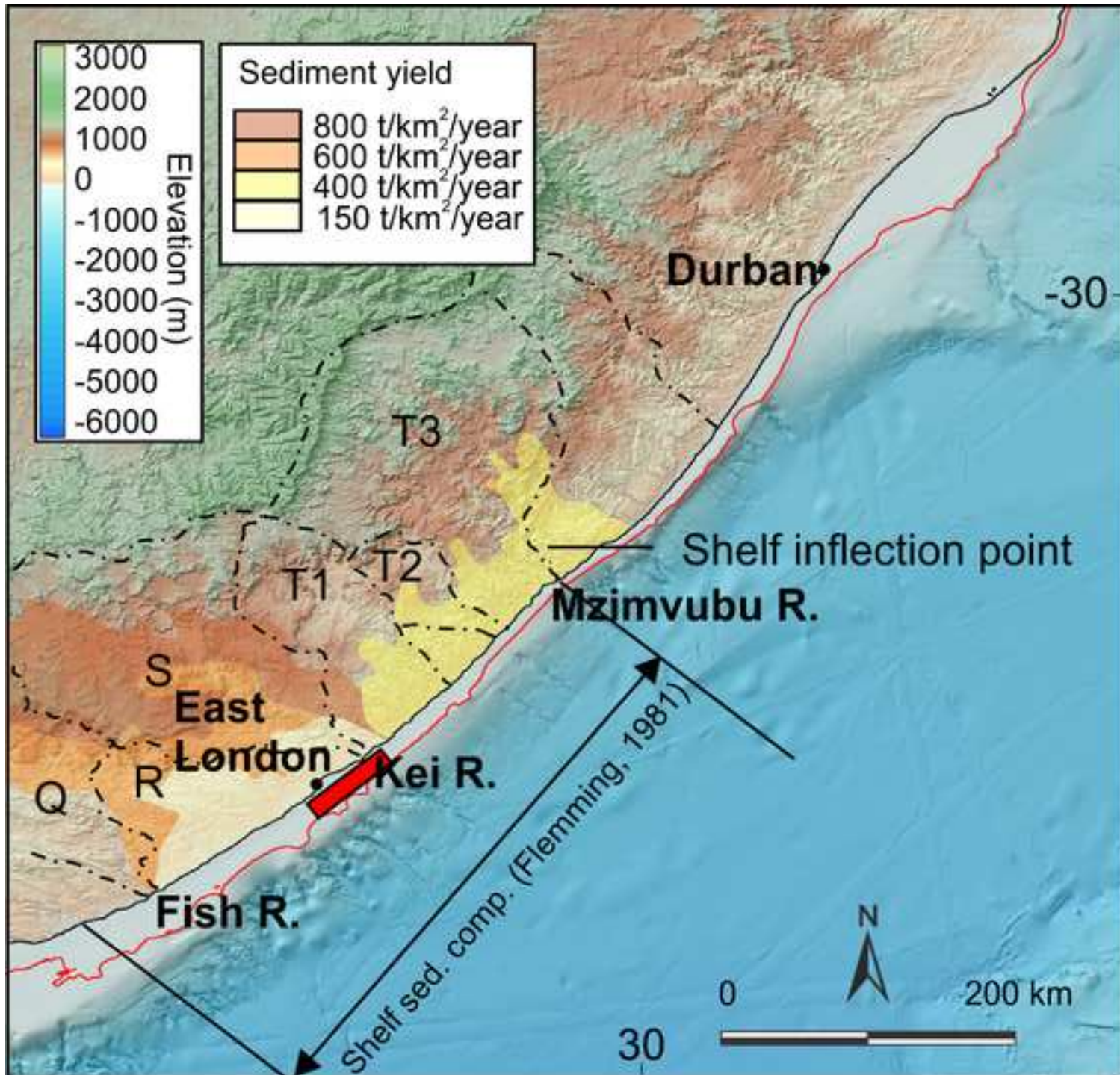
882 Table 1. Physical characteristics of the regional drainage basins for the Fish, Kei and
883 Mzimvubu Rivers. Sediment yield for each sub-catchment is based on figures reported by
884 Flemming (1981).

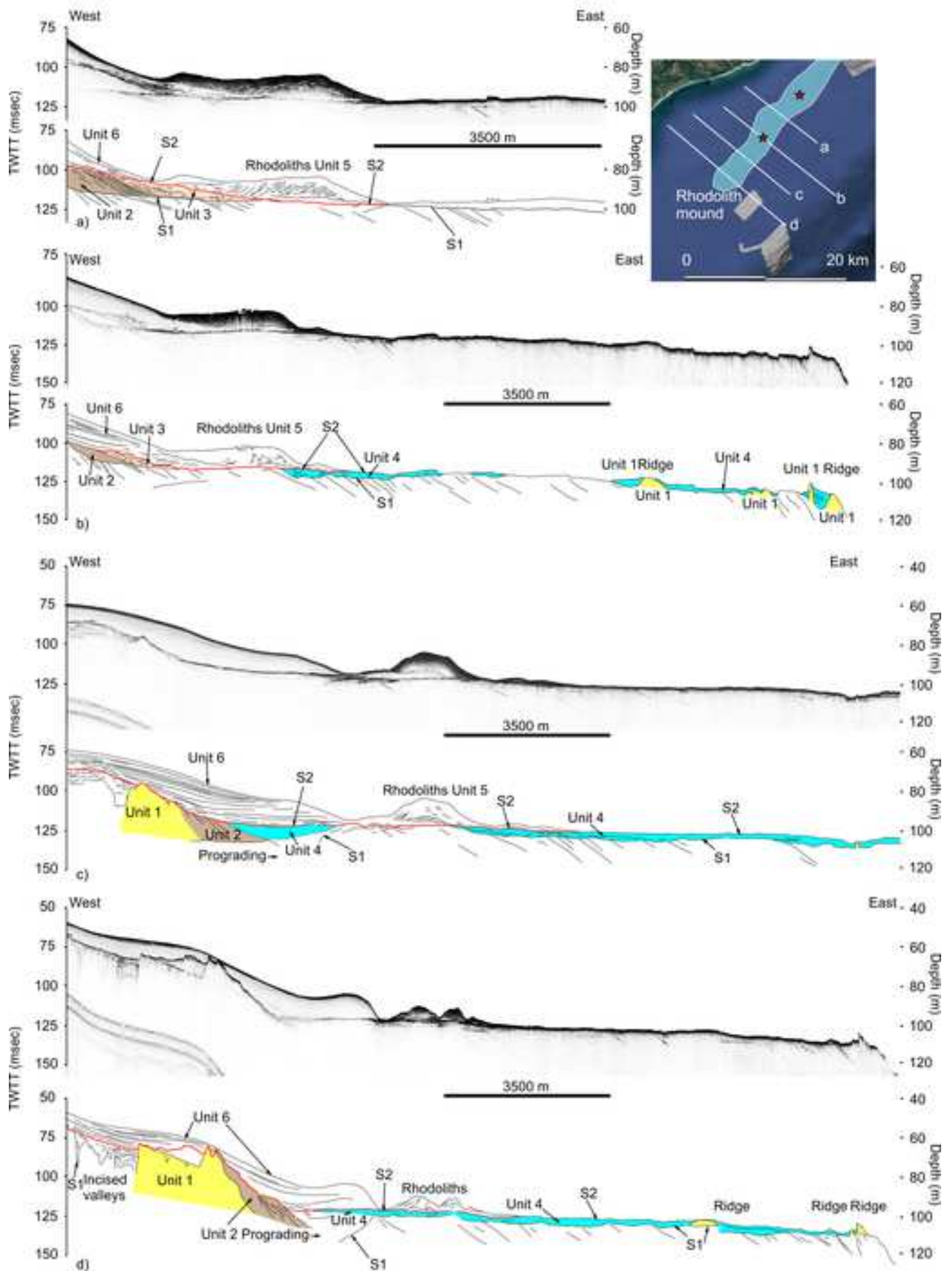
885 Table 2. Dimensions of relict seafloor features. Wherever possible the seismic unit, relief,
886 width, length and spacing are provided and compared to dimensions of modern systems from
887 the contemporary coastline of SE Africa.

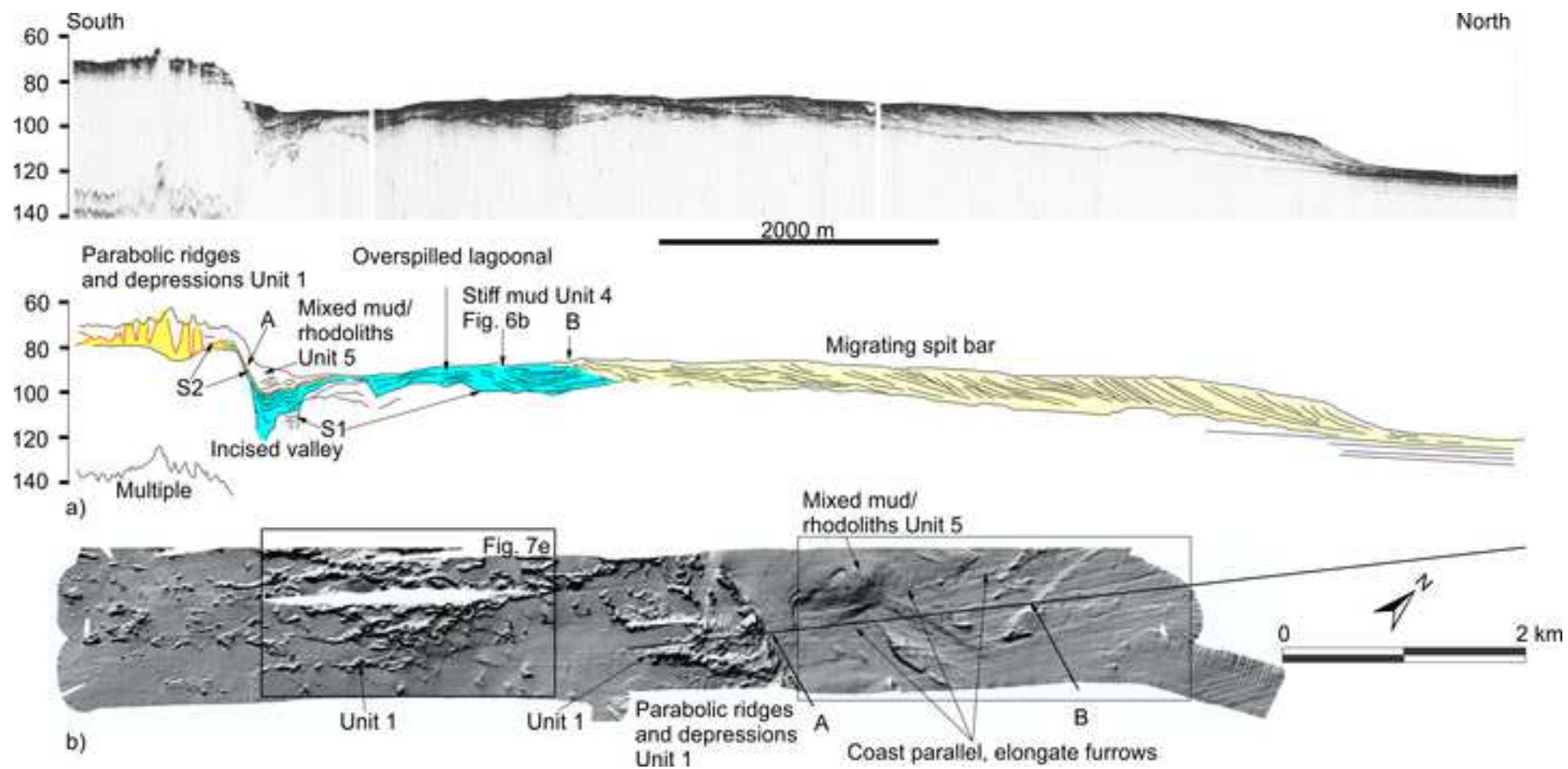
888

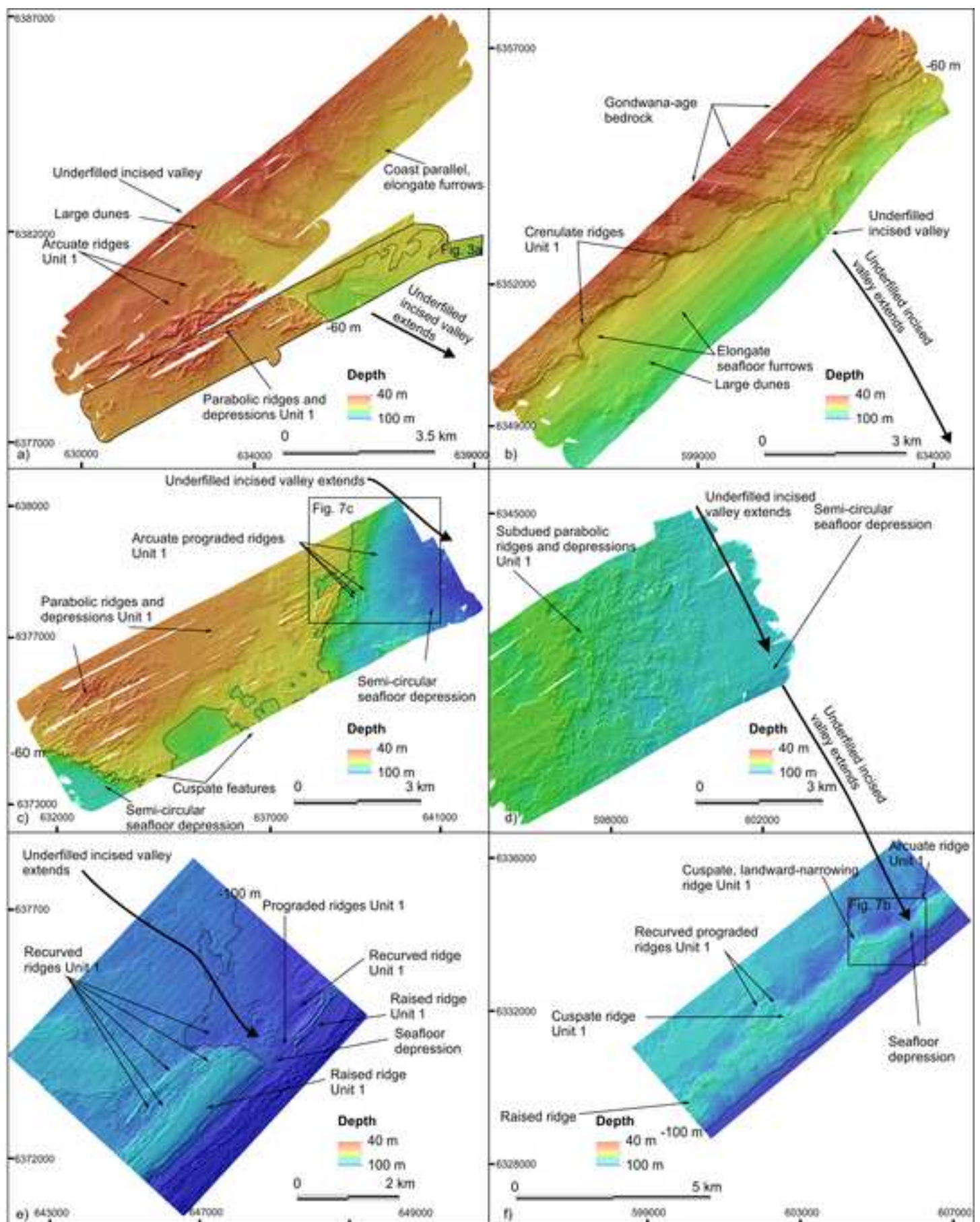
889

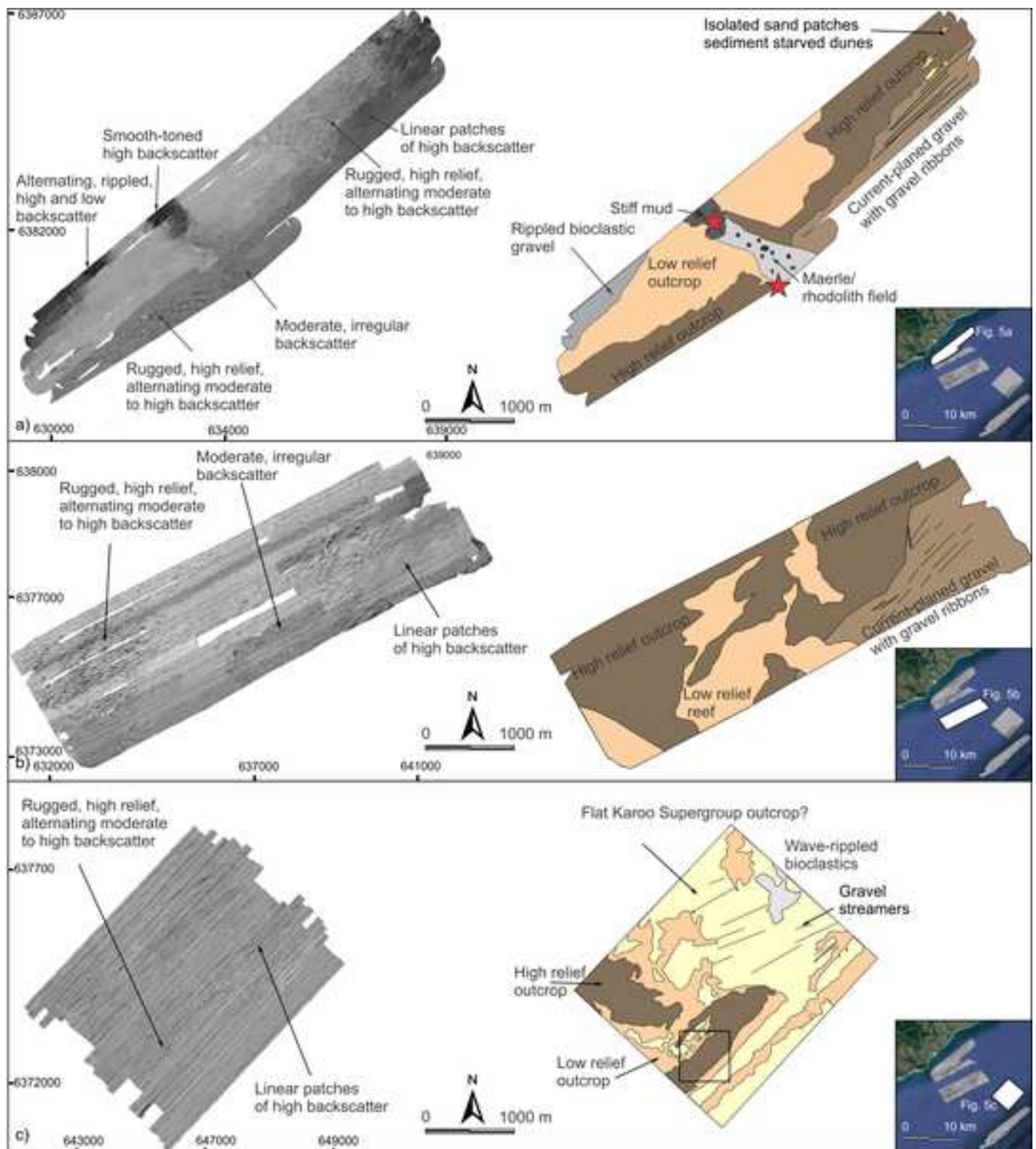


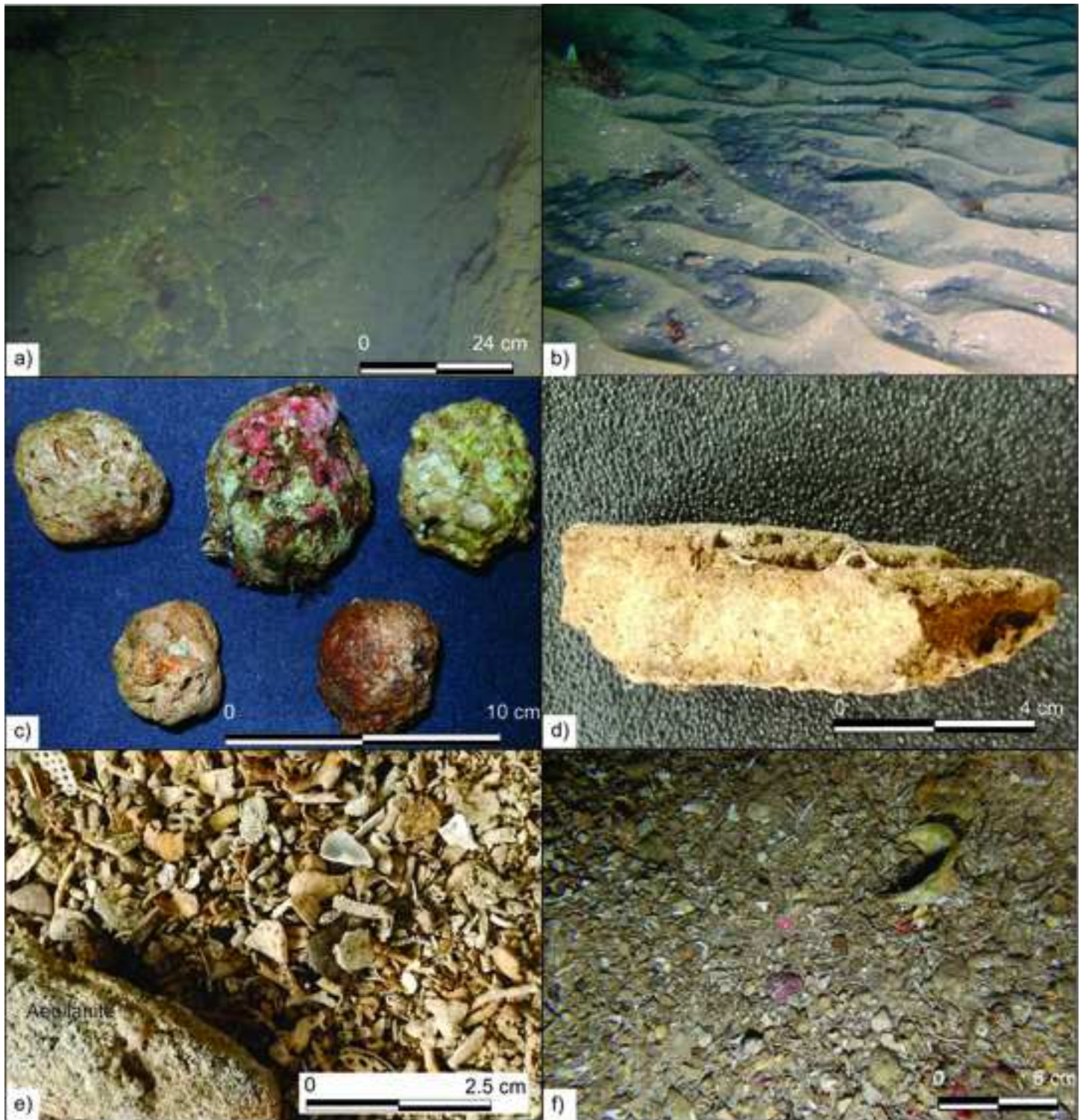


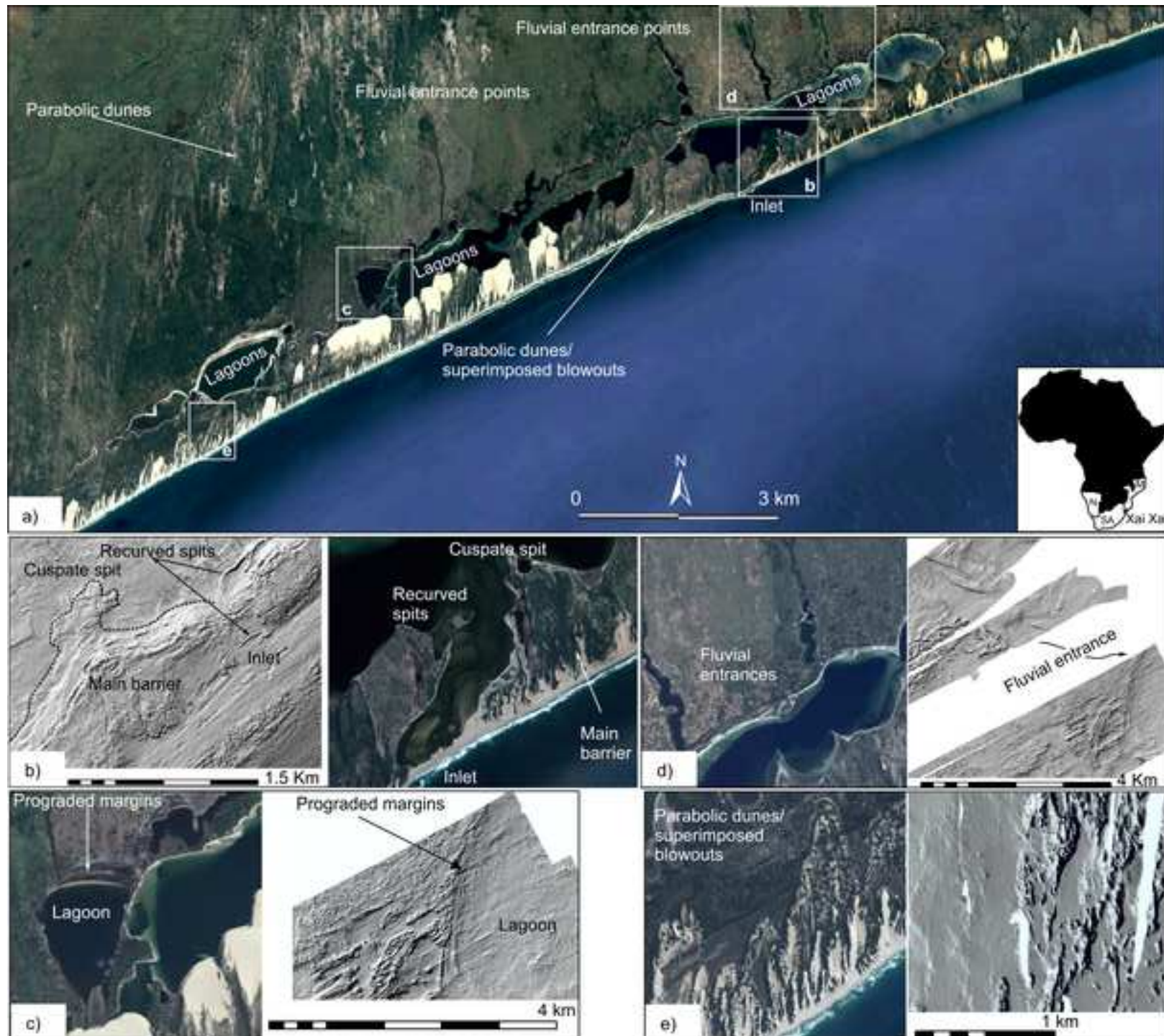


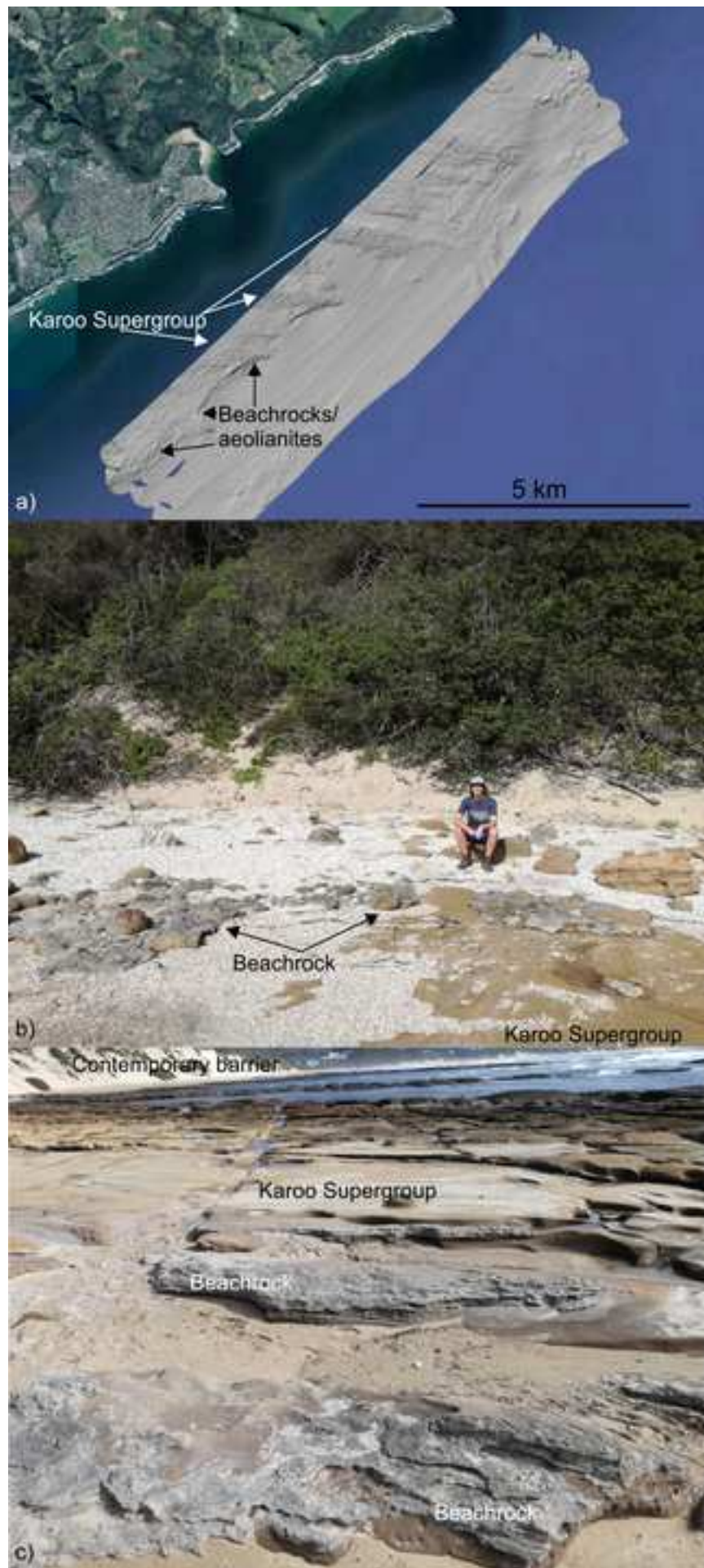


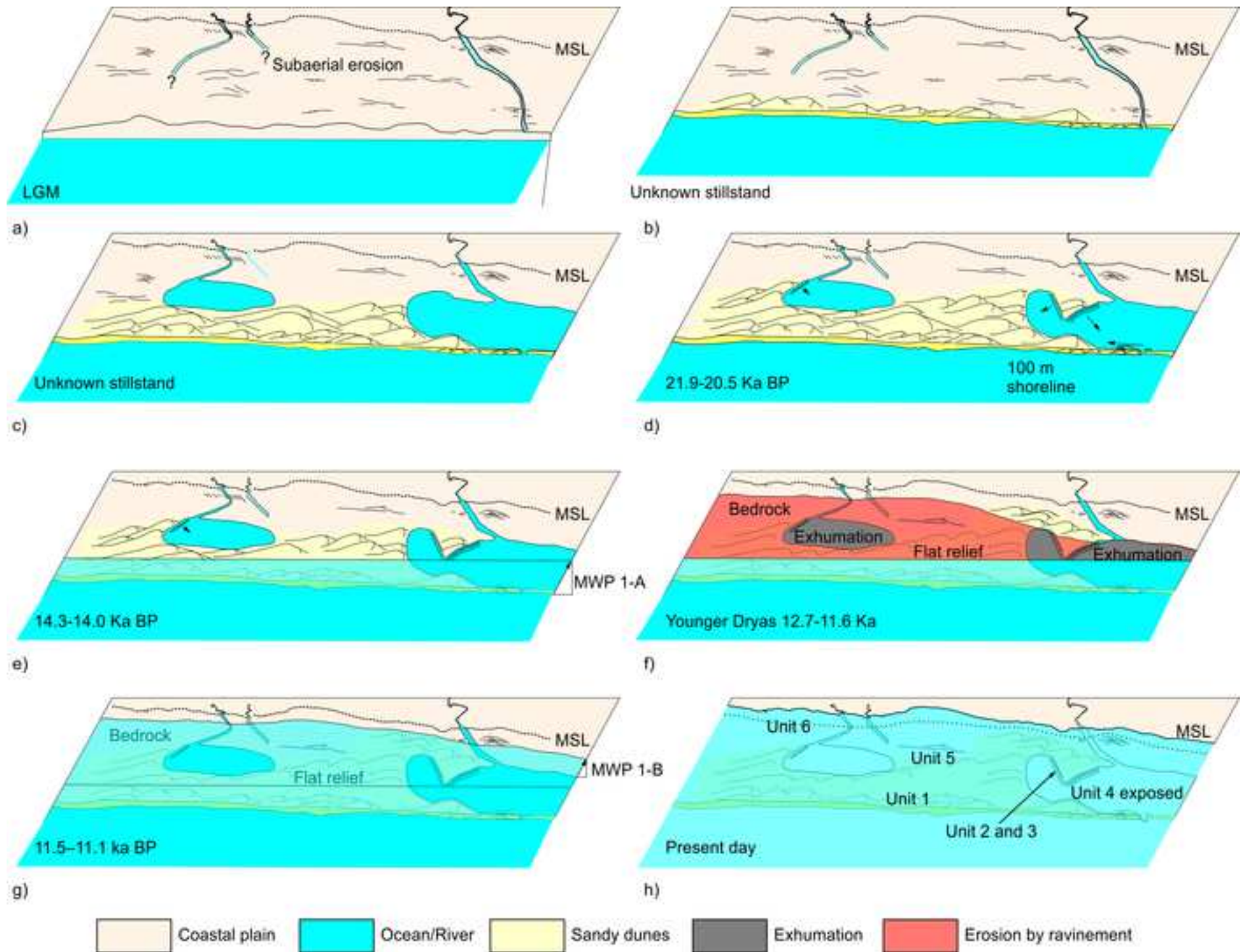














Click here to access/download

Table

Table 1.docx





Click here to access/download

Table

Table 2.docx



Author declaration

[Instructions: Please check all applicable boxes and provide additional information as requested.]

1. Conflict of Interest

Potential conflict of interest exists:

We wish to draw the attention of the Editor to the following facts, which may be considered as potential conflicts of interest, and to significant financial contributions to this work:

The nature of potential conflict of interest is described below:

No conflict of interest exists.

We wish to confirm that there are no known conflicts of interest associated with this publication and there has been no significant financial support for this work that could have influenced its outcome.

2. Funding

Funding was received for this work.

All of the sources of funding for the work described in this publication are acknowledged below:

[List funding sources and their role in study design, data analysis, and result interpretation]

No funding was received for this work.

3. Intellectual Property

We confirm that we have given due consideration to the protection of intellectual property associated with this work and that there are no impediments to publication, including the timing of publication, with respect to intellectual property. In so doing we confirm that we have followed the regulations of our institutions concerning intellectual property.

4. Research Ethics

We further confirm that any aspect of the work covered in this manuscript that has involved human patients has been conducted with the ethical approval of all relevant bodies and that such approvals are acknowledged within the manuscript.

IRB approval was obtained (required for studies and series of 3 or more cases)

Written consent to publish potentially identifying information, such as details or the case and photographs, was obtained from the patient(s) or their legal guardian(s).

5. Authorship

The International Committee of Medical Journal Editors (ICMJE) recommends that authorship be based on the following four criteria:

1. Substantial contributions to the conception or design of the work; or the acquisition, analysis, or interpretation of data for the work; AND
2. Drafting the work or revising it critically for important intellectual content; AND
3. Final approval of the version to be published; AND
4. Agreement to be accountable for all aspects of the work in ensuring that questions related to the accuracy or integrity of any part of the work are appropriately investigated and resolved.

All those designated as authors should meet all four criteria for authorship, and all who meet the four criteria should be identified as authors. For more information on authorship, please see <http://www.icmje.org/recommendations/browse/roles-and-responsibilities/defining-the-role-of-authors-and-contributors.html#two>.

All listed authors meet the ICMJE criteria. We attest that all authors contributed significantly to the creation of this manuscript, each having fulfilled criteria as established by the ICMJE.

One or more listed authors do(es) not meet the ICMJE criteria.

We believe these individuals should be listed as authors because:

[Please elaborate below]

AG, JAGC wrote the paper, ND and ND were the students on the paper, SK and DP secured funding and assisted with data collection

We confirm that the manuscript has been read and approved by all named authors.

We confirm that the order of authors listed in the manuscript has been approved by all named authors.

6. Contact with the Editorial Office

The Corresponding Author declared on the title page of the manuscript is:

[Insert name below]

Andrew Green

This author submitted this manuscript using his/her account in EVISE.

We understand that this Corresponding Author is the sole contact for the Editorial process (including EVISE and direct communications with the office). He/she is responsible for communicating with the other authors about progress, submissions of revisions and final approval of proofs.

We confirm that the email address shown below is accessible by the Corresponding Author, is the address to which Corresponding Author's EVISE account is linked, and has been configured to accept email from the editorial office of American Journal of Ophthalmology Case Reports:

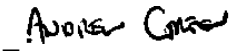
[Insert email address you wish to use for communication with the journal here]

Someone other than the Corresponding Author declared above submitted this manuscript from his/her account in EVISE:

[Insert name below]

We understand that this author is the sole contact for the Editorial process (including EVISE and direct communications with the office). He/she is responsible for communicating with the other authors, including the Corresponding Author, about progress, submissions of revisions and final approval of proofs.

We the undersigned agree with all of the above.

Author's name (Fist, Last)	Signature	Date
1. __Green, Andrew__		__24/10/2019__